Norwegian University
of Life Sciences

Master's Thesis 2019 60 ECTS
Department of Medical Genetics, Oslo University Hospital

Target Prediction and Functional Validation of MicroRNA for Coagulation Factor V and TFPI in Liver Cancer

Katarina Baumgarten Skogstrøm
MSc Biotechnology
Faculty of Chemistry, Biotechnology and Food Science

Target Prediction and Functional Validation of MicroRNA for Coagulation Factor V and TFPI in Liver Cancer

Oslo University Hospital (OUS),
Department of Medical Genetics

and

Norwegian University of Life Sciences (NMBU),
Faculty of Chemistry, Biotechnology and Food Science

Acknowledgement

The work presented in this thesis was performed at the Department of Medical Genetics, Oslo University Hospital from September 2018 to May 2019. The thesis was a part of the master program in Biotechnology at the Norwegian University of Life Science (NMBU) at the Faculty of Chemistry, Biotechnology and Food Science (KBM).

I would like to thank my supervisor Dr. Philos Nina Iversen for allowing me to join the research group and letting me work on this exciting project. Your knowledge, guidance and support has been excellent, and I could not have done this without you. I would also like to thank both my co-supervisor Professor Simon Rayner and Ph.D. Yafei Xing for helping me with the bioinformatical part of this thesis. A special thanks goes to Marit Sletten for her excellent help and guidance in the laboratory. Finally, I would like to thank my internal supervisors at NMBU, Professors Ellen Sandberg and Thore Egeland.

Furthermore, I would like to thank my brother Ph.D. Jens Fredrik Skogstrøm and mother Dr. Barbara Baumgarten-Austrheim for reviewing the thesis several times and providing excellent commentary to improve the text. I would also like to thank friends and family for all the encouragement and support throughout this year.

Ås, May 2019

Katarina Baumgarten Skogstrøm

Abstract

Background: The connection between cancer and increased risk of thrombosis is well established and liver cancer (HCC) patients have been found to have an increased risk of thrombosis. microRNAs (miRNA) are post-transcriptional gene regulators and their dysregulation have been linked to both HCC progression and thrombosis. Coagulation factor V (FV encoded by *F5* gene) and Tissue Factor Pathway Inhibitor (TFPI encoded by *TFPI-1* gene) have both been linked to cancer progression, with their specific roles in liver cancer yet to be determined. The proteins have also been found to interact in plasma in both healthy and diseased individuals. Until now, two miRNAs have been identified as regulators of TFPI, while none have been identified for FV. Thus, this thesis aimed to identify novel miRNA regulators for FV and TFPI and assess their potential prognostic implications in liver cancer.

Methods: In silico selection of candidate miRNAs: miRNAs targeting *F5* 3'untranslated region (UTR) and *TFPI* 3'UTR were identified using computational analysis. miRNAs with negative correlation to *F5* expression in a breast cancer cohort (OsloII study) were also included in this study. *In vitro* analysis of miRNAs: Transient overexpression and inhibition of the respective miRNAs was achieved by transfection of miRNA mimics and inhibitors. Direct targeting of *F5* 3'UTR was determined by luciferase reporter assay in HEK293T cells. The effect of overexpression of the miRNAs on endogenous *F5* and *TFPI* mRNA levels were determined by qRT-PCR and on secreted FV and TFPIα protein levels by ELISA in HepG2 cells. Functional effects of overexpression of the miRNAs on apoptosis and viability were determined with an ELISA cell death detection kit and Wst-1 assay, respectively. Clinical significance of the miRNAs was assessed by analysing their expression levels correlated with outcome in liver cancer patients using Kaplan-Meier survival analysis. Expression analysis of miRNAs in tumour versus healthy liver tissue were performed in KM plotter.

Results: Computational analysis of *F5* 3'UTR identified binding sites for 12 miRNAs. Out of these, eight had additional bindings sites in *TFPI* 3'UTR. In addition, seven miRNAs negatively correlated with *F5* in breast cancer cohort (OsloII cohort) were identified with predicted binding sites in 3'UTR of both genes. In total, 19 miRNAs were selected for validation in this study. We found six miRNAs (miR-323a-3p, miR-568, miR-643, miR-651-3p, miR-1236-3p and miR-1278) that directly targeted the *F5* 3'UTR and significantly

downregulated *F5* mRNA and FV protein level in HepG2 cells. We also found one miRNA (miR-7-5p) that downregulated *TFPIα* mRNA and TFPIα protein level in HepG2 cells. All seven validated miRNAs impaired proliferation of HepG2 cells. Inhibition of miR-568 significantly increased the proliferation. Overexpression of miR-7-5p, miR-323a-3p and miR-1236-3p promoted apoptosis. High expression of miR-568, miR-643, miR-651-3p, miR-1236-3p and miR-1278 was associated with a significant increased estimated survival time in liver cancer patients. Conversely, low miR-7-5p and miR-323a-3p was associated with significantly increased survival time in liver cancer patients.

Conclusion: This study demonstrated that FV expression is directly regulated by six miRNAs in liver cancer. In addition, we also demonstrate that TFPIα expression is directly regulated by miR-7-5p in liver cancer. Future studies are necessary to further investigate the potential consequences of dysregulation of these miRNAs in relation to both the procoagulant state induced by HCC cells and liver cancer progression.

Sammendrag

Bakgrunn: Sammenhengen mellom kreft og en økt risiko for å utvikle tromboembolisk sykdom er veletablert og det er vist at leverkreftpasienter (HCC) har en økt risiko for å få tromboser. MicroRNA (miRNA) er post-transkripsjonelle genregulatorer og deres feilregulering har blitt knyttet til både progresjon av HCC og trombose. Koagulasjonsfaktor V (*F5* genet koder for FV) og Tissue Factor Pathway Inhibitor (*TFPI-1* genet koder for TFPI) har begge blitt knyttet til kreftprogresjon, mens deres spesifikke rolle ved leverkreft enda ikke har blitt fullstendig kartlagt. Proteinene har også blitt funnet å interagere i plasma hos både friske og syke individer. Inntil nå har bare to miRNA blitt identifisert som regulatorer av TFPIα, mens ingen har blitt funnet for FV. Dermed var målet for denne oppgaven å identifisere miRNA som regulerer FV og TFPI, og vurdere deres potensielle prognostiske betydning ved leverkreft.

Metode: *In silico* valg av miRNA-kandidater: miRNA som binder til *F5* 3'ikke translatert region (UTR) og *TFPI* 3'UTR ble identifisert ved bruk av beregningsanalyse. miRNA som var negativt korrelert med *F5* ekspresjon i en brystkreft kohort (OsloII) ble også inkludert i denne studien. *In vitro* analyse av miRNA: forbigående overekspresjon og inhibering av de respektive miRNAene ble oppnådd ved transfeksjon av miRNA etterligninger og inhibitorer. Direkte binding av *F5* 3'UTR ble bestemt vha luciferase reporter analyse i HEK293T celler. Effekten av overekspresjon av miRNA på endogene *F5* og *TFPI* mRNA-nivåer ble bestemt med qRT-PCR og nivået av utskilt FV og TFPIα protein ble målt vha ELISA i HepG2 celler. Den funksjonelle effekten av overekspresjon av miRNAene på apoptose og levedyktighet ble bestemt med, henholdsvis, ELISA celledøddeteksjonssett og WST-1 analyse. miRNAenes kliniske signifikans ble evaluert ved å analysere deres ekskresjonsnivå sammenlignet med utfall hos leverkreft-pasienter ved bruk av Kaplan-Meier overlevelsesanalyse. Ekspresjonsanalyse av miRNAene i tumor- versus friskt levervev ble utført i KM plotter.

Resultater: Beregningsanalyse av *F5* 3'UTR identifiserte 12 miRNA- bindingssteder . Åtte av disse hadde i tillegg bindingssteder på *TFPI* 3'UTR. I tillegg ble det på begge geners 3'UTR identifisert bindingssteder for syv miRNA som var negativ korrelert med *F5* i en brystkreftkohort (OsloII kohort). Totalt ble 19 miRNA valgt for videre validering i denne studien. Det ble funnet seks miRNA (miR-323a-3p, miR-568, miR-643, miR-651-3p, miR-1236-3p and miR-1278) som bandt til *F5* 3'UTR og nedregulerte *F5* mRNAet og FV

proteinnivået i HepG2 celler betydelig. I tillegg fant vi en miRNA (miR-7-5p) som nedregulerte *TFPIα* mRNA og TFPIα proteinnivået i HepG2 celler. Alle de syv validerte miRNAene hindret proliferasjon av HepG2 celler. Inhibering av miR-568 førte til en betydelig økning i proliferasjon. Overekspresjon av miR-7-5p, miR-323a-3p og miR-1236-3p fremmet apoptose i HepG2 celler. Høy miR-568, miR-643, miR-651-3p, miR-1236-3p og miR-1278 ekspresjon ble assosiert med økt estimert overlevelsestid hos pasienter med leverkreft, mens lav miR-7-5p og miR-323a-3p ekspresjon ble assosiert med det samme hos pasienter med leverkreft.

Konklusjon: Denne studien demonstrerte av FV ekspresjon ved leverkreft blir direkte regulert av seks miRNAer. I tillegg ble det vist at TFPIα-ekspresjon ved leverkreft blir direkte regulert av miR-7-5p. Fremtidige studier er nødvendig for videre kartlegging av potensielle konsekvenser av disse miRNAenes feilregulering, både i forhold til HCC-cellenes prokoagulative rolle og progresjonen av leverkreft.

Abbreviations

3'UTR	3'-Untranslated region
Ago2	Argonaute 2
Amp	Ampicillin
Amp	Ampicillin
ANOVA	analysis of variance
anti-miR	miRNA inhibitor
APC	activated protein C
ATIII	Anti-thrombin III
BCLC	Barcelona Clinic Liver Cancer
cDNA	complemenary DNA
CMV	Cytomegalovirus
CMV	cytomegalovirus
Ct	cycle threshold
DGCR8	DiGeorge syndrome critical region gene 8
DMEM	Dulbecco's modified eagle medium
DNA	deoxyribonucleic acid
DPBS	Dulbecco's phosphate-buffered saline
dsRNA	double-stranded RNA
DVT	Deep vein thrombosis
EGFR	Epithelial growth factor receptor
ELISA	Enzyme Linked Immunosorbent assay
EMT	Epithelial-mesenchymal transition
F3	*Coagulation Factor 3* encoding TF
F5	*Factor 5* encoding FV
FBS	foetal bovine sureum
FIX	Coagulation Factor IX
FIXa	activated FIX
FV	Coagulation Factor V
FVII	Coagulation Factor VII
FVIIa	activated FVII
FVIII	Coagulation Factor VIII
FVIIIa	activated FVIII
FVL	FV Leiden
FX	Coagulation Factor X
FXa	activated FX
FXI	Coagulation Factor XI
FXI	Coagulation Factor XI
GPI	Glycosylphosphatidylinositol
HCC	Hepatocellular carcinoma
hLuc	Firefly luciferase

hsa-mir-	human precursor miRNA
hsa-miR-	human mature miRNA
LB-A	Lysogeny broth with ampicillin
LIHC	Liver heptatocellular carcinoma
miRNA or miR	microRNA
MP	Microparticles
mRNA	messenger RNA
MSR	median survival rate
OS	Overall survival
PCR	polymerase chain reaction
PIK3CD	phosphoinositide 3-Kinase/Akt Pathway
PMM1	Phosphomannomuate 1
pre-miRNA	precursor miRNA
pri-miRNA	primary miRNA
PS	Protein S
PVT	Portal vein thrombosis
qRT-PCR	quantitative reverse transcriptase PCR
RISC	RNA Induced Silencing Complex
RNA	Ribonucleic acid
RQ	relative quantitiy
rTFPI	recombinant TFPI
SD	standard diviation
SOC	Super Optimal broth with Catabolite repression
ssRNA	single-strand RNA
SV40	Semian virus
TAE	Tris-acetate-EDTA
TAE	tris-acetate-EDTA
TF	Tissue Factor
TFPI	Tissue Factor Pathway Inhibitor
TRBP	Transactivating response RNA-binding Protein
VTE	Venous thromboembolism
vWF	von Willebrand Factor

Table of contents

1 Introduction

1.1 Cancer and coagulation

1.1.1 Cancer

Development of cancer is caused by a combination of mutations in the genome and environmental factors. The accumulation of gene mutations throughout life are caused by exposure to genotoxic agents as well as natural errors occurring during cell replications. The malignant phenotype of the cells is the result of a collaborative effect of thousands of mutations and it is the environmental context of the cells that determines whether these cells progress to initiate clinical cancers. Cancer cells exhibit a loss of growth control, forming a primary tumour and turning into a malignant tumour when the cells invade the cells around them. Malignant tumours may use the blood vessels and lymph system to spread and invade new tissues and thereby initiate metastasis. Metastasis, rather than the primary tumour, is the cause of 90% of the cancer deaths (Alberts *et al.*, 2015; Holly *et al.*, 2019)

1.1.1.1 Liver cancer

Primary liver cancer is the sixth most common cancer (new cases each year) and the second leading cause of cancer related deaths worldwide (World Cancer Research Fund, 2018)**.** Hepatocellular carcinoma (HCC) constitutes approximately 90% of all primary liver cancer cases. HCC is classified using the Barcelona Clinic Liver Cancer (BCLC) staging system. There are three main stages: Early (A), Intermediate (B) and Advanced (C) stage. Patients with an early stage diagnosis (~40-50% of the patients) can be treated by resection, transplantation or local ablation, which increases the median survival rate (MSR) from ~36 months to more than 60 months. Intermediate stage (B) HCC patients have retained liver function and benefit from treatment with chemoembolization with an estimated MSR of ~26 months. Patients diagnosed with advanced stage (C) HCC have generally had a very low survival rate of less than 8 months. However, in the last few years MSR for this group of patients has increased to ~11 months with the use of the multikinase inhibitor sorafenib. New drugs such as lenvatinib, regorafenib, cabozatinib and ramucirumab are in clinical trials and have demonstrated some improvement, though the MSR is still approximately 12 months. Overall, HCC is a highly therapy resistant cancer, making it very difficult to treat

with generally very poor prognosis (Llovet *et al.*, 1999; Llovet *et al.*, 2016; Llovet *et al.*, 2018).

1.1.2 Coagulation

Coagulation (haemostasis) is the process in which blood changes from a liquid to a gel, forming a blood clot to stop bleeding after an injury. The process is tightly regulated by several inhibitors to stop unwanted thrombus (clot) formation (Palta *et al.*, 2014). The coagulation process is regulated by a host of factors, which together end in the formation of the clot. The loss of some of these factors are the basis of several blood diseases. There have been several proposed models of the coagulation process, such as the waterfall/cascade models that emerged independently the same year (Davie & Ratnoff, 1964; Macfarlane, 1964; McMichael, 2012). The traditional version of these models proposed that the clot formation occurred as a step-wise process in which the factors (enzymes) activate each other ending with formation of thrombin and eventually fibrin. The factors were part of the intrinsic pathway, intrinsic as being part of the blood, and believed to be independent of the extrinsic, tissue factor (TF), pathway. Even though these models enhanced the knowledge on coagulation *in vitro*, they did not fully explain the process *in viv*o (McMichael, 2012). Mann *et al.* (1992) proposed an alternative model, the cell-based model of coagulation.

1.1.2.1 The Cell Based model

The Cell-based model is divided into three consecutive phases, an initiation phase, an amplification phase, and a propagation phase. Initiation of coagulation is caused by the exposure of TF to the blood. TF factor is mainly expressed by cells, such as adventitial cells, smooth muscle cells, and keratinocytes, located outside the vasculature and is only exposed to the blood flow by an injury to the endothelial barrier (Smith, 2009). In the case of an injury, TF is exposed to the blood flow and binds to activated factor VII (FVIIa), forming the TF-FVIIa-complex. The TF-FVIIa-complex activates Factor IX (FIX) and X (FX) to factors FIXa and FXa. FXa cleaves small amounts of prothrombin into thrombin. However, the TF-FVIIa-FXa is rapidly inhibited by tissue factor pathway inhibitor (TFPI) and free FXa and thrombin are inhibited by anti-thrombin III (ATIII), ending the initiation phase (Hoffman & Monroe, 2001; Hoffman, 2003; Lu *et al.*, 2004).

During amplification, thrombin acts as protease-activated receptors activating platelets, releasing the content of the α-granules, including factor V and VIII, to the surface of the platelets. Thrombin then cleaves FVIII from the von Willebrand factor (vWF) and activates FVIII, FV and FXI to FVIIIa, FVa and FXIa respectively (Hoffman, 2003; McMichael, 2012).

During the propagation phase, FVIIIa and FIXa assemble on the phospholipid surface of the platelets, creating the FVIIIa-FIXa "tenase" complex. Tenase activates FX into FXa, which then binds to the co-factor FVa on the platelet surface. The FXa-FVa "prothrombinase" complex cleaves prothrombin into thrombin at a high rate, generating a thrombin burst. Thrombin then binds and cleaves fibrinogen, creating fibrinopeptides A and B which polymerize and form protofibrils with surrounding fibrin molecules. These fibrin molecules then form the fibrin clot. FXIIIa, which is activated by thrombin, modifies the polymerized fibrin form cross links within the clot to stabilize it (Hoffman & Monroe, 2001; Hoffman, 2003; Smith, 2009).

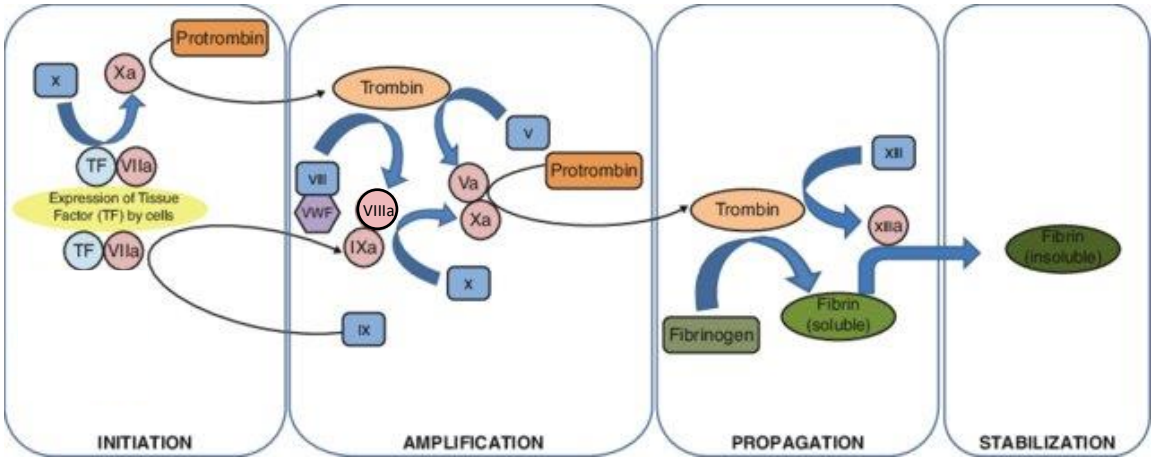

Figure 1: Representation of the cell-based model of blood coagulation with its four stages; initiation, amplification, propagation and stabilization. Illustration adapted with modifications from Bittar *et al.* (2015).

1.1.3 Cancer and thrombosis

The connection between cancer and thrombosis is well established. Cancer patients have an increased risk of thrombosis, in fact thrombotic events are the second leading cause of death after cancer itself (Khalil *et al.*, 2015). Further, cancer patients diagnosed with venous thromboembolism (VTE) have a 2.2-fold higher mortality rate compared to patients without VTE (Khorana *et al.*, 2007; Sorensen *et al.*, 2000). Moreover, thrombotic events may precede a clinical cancer diagnosis by weeks or even months (Falanga *et al.*, 2013;

Prandoni *et al.*, 2005). The diagnosis and subsequent treatment of thrombosis causes major complications in essential cancer treatments and may cause excessive bleeding during surgery. Around 25% of the patients require readmission for bleeding after surgery or recurrence of VTE (Donnellan & Khorana, 2017). Patients with cancer are six times more likely to develop VTE than their non-cancer counterpart and account for more than 20% of all new cases of VTE. Furthermore, the treatment of the cancer has been seen to increase the risk of thrombosis, in fact sorafenib, an antiangiogenic agent used in treatment of advanced HCC, increases the risk for arterial thrombotic events (Donnellan & Khorana, 2017; Khorana *et al.*, 2008).

1.1.4 Cancer progression and coagulation

Cancer progression has been closely linked to activation of coagulation factors. Tumour cells contribute to the hypercoagulable state by producing procoagulant factors. Haemostatic alterations have been found in 60-100% of patients with malignant tumours. These changes are in part comprised of elevated levels of blood coagulation proteins, such as FV, FVIII, FIX and FX, and increased concentrations of fibrin/fibrinogen degradation products. Further, the tumour cells actively release TF into the blood stream through TF-bearing microparticles (MPs). The MPs express phosphatidylserine on the surface, providing an anionic phospholipid surface on which to assemble the tenase and prothrombinase complexes, thereby increasing the coagulation (Ay *et al.*, 2017; Falanga *et al.*, 2013; Lima & Monteiro, 2013).

1.1.5 Liver cancer and coagulation

Patients diagnosed with HCC, as with other malignancies, have an increased risk of developing thrombotic complications as a result of the hypercoagubility caused by the tumour. Portal vein thrombosis (PVT) is the most common type of thrombosis in HCC patients and between 7.4% and 24% have been found with PVT within one year after HCC diagnosis. However, the risk of developing VTE as a result of HCC is only considered intermediate compared to other malignancies, like brain tumours and pancreatic cancer, with much higher incidence rates (47% and 19.2%, respectively) (Donnellan & Khorana, 2017; Zanetto *et al.*, 2018; Zhou *et al.*, 2011).

The liver is responsible for the synthesis of most of the coagulation factors (i.e. TF, FV, FVII etc.) and regulatory proteins of the haemostatic control system. A derangement caused

by development of HCC might therefore result in the state of hypercoagubility observed. An increased level of TF has been found in plasma of HCC patients and is significantly associated with invasion, angiogenesis, staging and survival (Lin *et al.*, 2016; Zanetto *et al.*, 2018). Similarly, increased concentration and polymerization of fibrinogen in HCC seems to be the main determinant of hypercoagubility and can also be used to distinguish between cirrhotic patients with and without malignancy. There is a lack of prospective studies that can elucidate which HCC patients carry an increased risk of developing thrombotic complications and given the high mortality rate associated with thrombosis this information is crucial (Zanetto *et al.*, 2018).

1.1.6 Coagulation factor V (FV)

1.1.6.1 Structure, activation and function of FV

Coagulation FV is a 330-kDa single-chain glycoprotein that is mainly produced by the liver and found in plasma and platelets. The 80-kb *factor 5* (*F5)* gene (coding for the FV protein) is located on chromosome 1, which gives rise to a 6.8-kb mRNA (Mann & Kalafatis, 2003). FV is a multidomain (A1-A2-B-A3-C1-C2) pro-cofactor, that is part of haemostasis as both a procoagulant and anticoagulant cofactor (Figure 2) (Mann & Kalafatis, 2003; Nicolaes & Dahlback, 2002). Activated FV (FVa) is a procoagulant cofactor that, together with FXa, forms the prothrombinase complex which cleaves prothrombin into thrombin. Prothrombinase has an approximately 300,000-fold higher rate of thrombin formation than FXa alone (Mann & Kalafatis, 2003; Nesheim *et al.*, 1979). FV is activated by a combination of proteases; thrombin, FXa, and plasmin. Thrombin is responsible for the most significant cleavage; the complete removal of the B-domain. FVa is left with one heavy chain (A1-A2) and one light chain (A3-C1-C2) which, with the use of Ca^{2+}, forms a non-covalent complex (Mann & Kalafatis, 2003; Nicolaes & Dahlback, 2002).

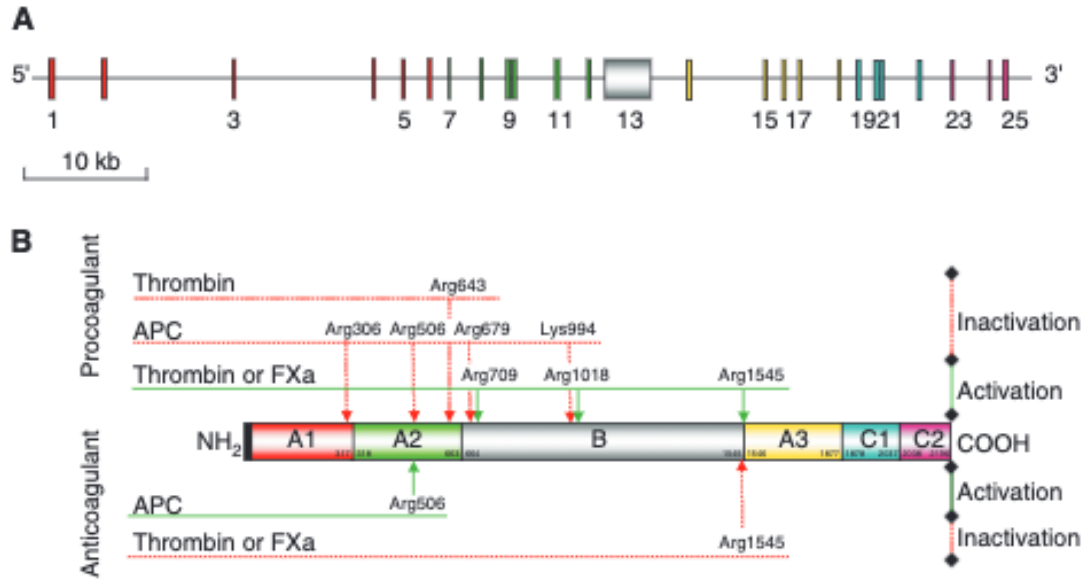

Figure 2: **Schematic illustration of the structure of the *F5* gene**: (A) The exons and introns of the *F5* gene, exons are illustrated in the coloured boxes and introns are the lines between the boxes. (B) The FV domains A1, A2, B, A3, C1, and C2 are coloured according to the exons they are translated form. Cleavage site wit amino acid number for procoagulant (top) and anticoagulant (bottom) functions of FV are indicated (green represents activation and red inactivation) (Asselta *et al.*, 2006).

FV is regulated by a negative feedback-loop. In the presence of thrombomodulin, thrombin cleaves protein C into activated protein C (APC). With the help of the B-domain, single-chain FV works as co-factor for APC, by activating and creating the APC/protein S complex (APC/S). The APC/S complex cleaves and inactivates FVIIIa and FVa, rapidly reducing the production of FXa and thrombin by inactivating the tenase and prothrombinase complexes (Dahlback, 2016; Mann & Kalafatis, 2003; Thorelli *et al.*, 1999).

1.1.6.2 The role of FV in disease

Considering FVs dual role in haemostasis; genetic or acquired defects and deficiencies may cause haemorrhagic or thrombotic incidents.

FV deficiency is a rare bleeding disorder, where lack of FV or dysfunctional FV causes the development of antibody inhibitors resulting in excessive bleeding due to a blocked blood clotting reaction (Knöbl & Lechner, 1998). In the liver, FV was found to be the best prognostic indicator of fulminant hepatic failure (FHF), with lower FV levels associated with lower survival rates (Bernuau *et al.*, 1986; Izumi *et al.*, 1996).

Factor V Leiden (FVL) thrombophilia is an inherited blood clotting disorder. The disease is caused by a guanine to adenine substitution which changes the translated amino acid from arginine (Arg506) to glutamine. Arg506 is one of the cleaving sites used by APC to inactivate FVa, and the mutation results in poor anti-coagulant response to APC and an increased risk of thrombosis (Martinelli *et al.*, 1996; Zoller *et al.*, 1996). The heterozygous variant is found in 3-8% of people of European ancestry, while 1 in 5000 are homozygous. People with FVL thrombophilia have a greater than average risk of developing deep vein thrombosis (DVT). However, the chance of DVT development is dependent on the person having one or two copies of the mutation (Genetics Home Research, 2019)

Beyond its role in coagulation, Liang *et al.* (2015) found that FV has a role in APC modulated anti-inflammatory cell signalling, using a sepsis model in mice. FV, cleaved at Arg506 by APC, is a cofactor together with protein S (PS) in APC modulated anti-inflammatory responses. FV-PS-APC complex destabilizes the TF-FVIIa-Xa complex leading to the inhibition of EPCR dependent PAR2 inflammatory signalling (Liang *et al.*, 2015).

Additional to its involvement in coagulation and inflammation, FV has alternative roles in malignant cells. A study done on FVL found that homozygous carriers had an increased risk of colorectal cancer (Vossen *et al.*, 2011). VanDeWater *et al.* (1985) found that FVa is bound to the plasma membrane together with calcium to generate the enzyme prothrombinase in tumour cells. Furthermore, in a study of the coagulation mechanisms, FV was found present in the perivascular and intercellular areas of colon cancer tumours (Witkowski *et al.*, 2016). A more recent study by Tinholt *et al.* (2014) found an association between certain *F5* SNPs and breast cancer. An association study performed on a breast cancer cohort and three breast cancer datasets further revealed an increased expression of *F5* in aggressive breast cancer subtypes. This was proposed as a possible marker of aggressive breast cancer, but also of favourable outcome for patients (Tinholt *et al.*, 2018).

1.1.6.3 The role of FV in liver cancer

As mentioned above, FV is synthesized in the liver and thus highly expressed there. An expression profile plot was created using the web-application GEPIA2 to study the gene expression of *F5* across all tumour samples and paired normal samples (Figure 3) (Tang *et al.*, 2017). As expected, *F5* expression was much higher in liver tissue (LIHC) compared

to most of the other tissues. Further, a significant difference in expression in normal liver tissue versus tumour tissue was apparent. The increased *F5* expression was also considerable in pancreas-, prostate- and stomach cancer. When the three stages of HCC (Figure 4) were compared to normal liver tissue, *F5* was also higher expressed in the more aggressive stages.

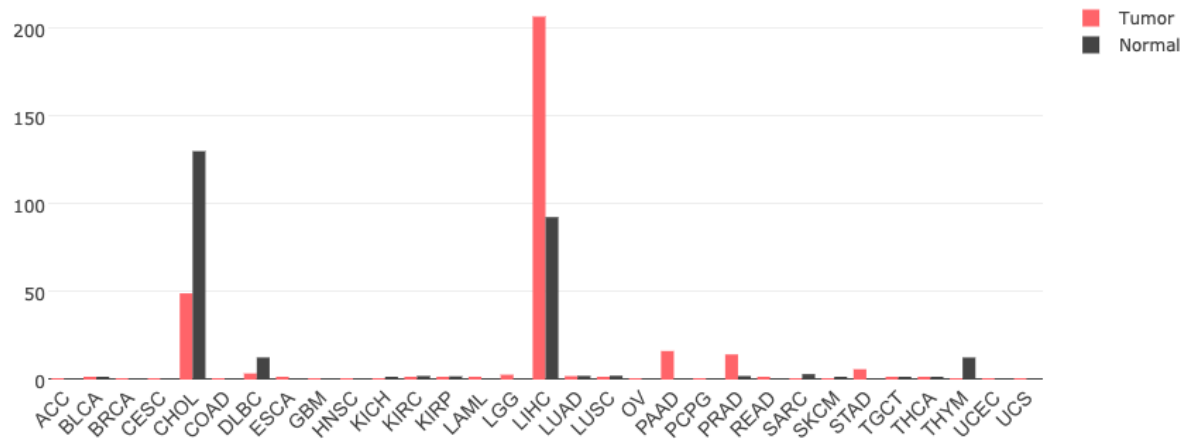

Figure 3: The Bars represent the median *F5* expression in certain tumour types (red) with corresponding normal tissue (black). Derived from TCGA data using the GEPIA2 web application (Skogstrøm (unpublished), 2019; (Tang *et al.*, 2017).

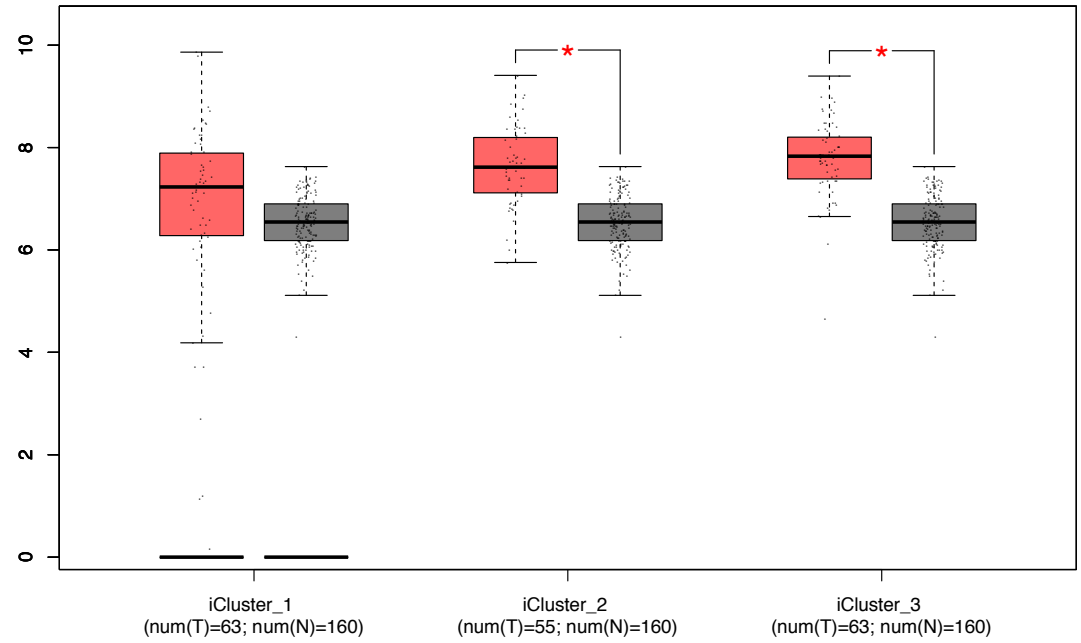

Figure 4: Median *F5* expression in normal liver, n = 160, (black) and liver hepatocellular carcinoma (LIHC) cells (red) divided into the three stages (considered significant if: *P<0.05). Stage A = cluster_1 (n = 63),

Stage B = cluster_2 (n = 55) and stage C = cluster_3 (n = 63). Derived from TCGA data using the GEPIA2 web application (Skogstrøm (unpublished), 2019; (Tang *et al.*, 2017).

A general search of "*F5"* or "coagulation FV" and "HCC" or "liver cancer", yielded no results in either PubMed or Web of Knowledge. Nevertheless, a master thesis written by Cathrine McCoig in 2018 in our group studied the functional role of FV in liver cancer. McCoig (2018) found that knock-down of *F5* expression in the liver cancer cell lines HepG2 and Huh7 promoted apoptosis and reduced migration (unpublished results), hinting at a possible oncogenic function of overexpressed FV in liver cancer. However, these *in vitro* findings contradict clinical analysis. High *F5* expression has previously been associated with aggressive types of breast cancer, but also with positive outcome (Tinholt *et al.*, 2018). Figure 4 shows the same trend, with higher *F5* expression in more aggressive types of LIHC. In addition, high expression of *F5* in liver cancer patients have a higher survival rate than those with low expression (Figure 5). Thus, the true role of *F5* in HCC has yet to be determined.

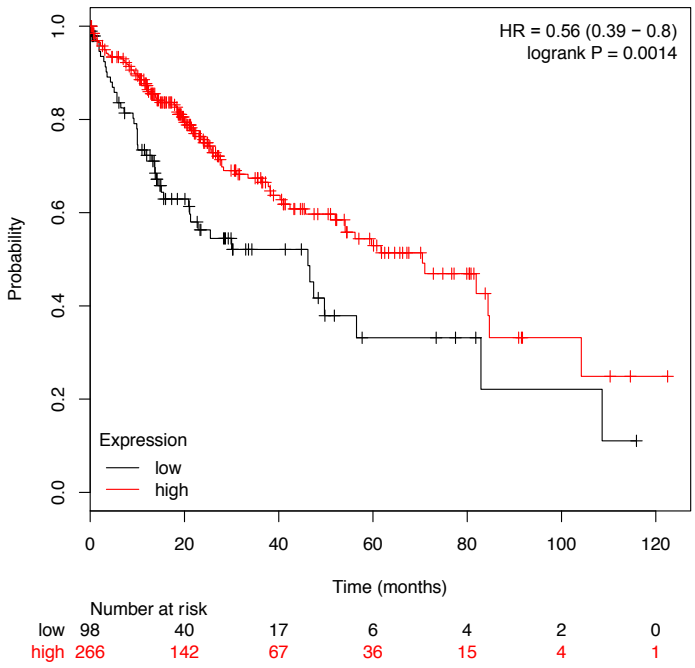

Figure 5: Kaplan-Meier survival plot with high and low expression of *F5*. Created with KMPlot.com on RNA-sequencing data (Skogstrøm, 2019 (unpublished); (©KMPlotter.com).

1.1.7 Tissue factor pathway inhibitor (TFPI)

The human tissue factor pathway inhibitor (*TFPI*) spans 91kb, is located at chromosome 2 and is transcribed into 10 exons containing three Kunitz-type inhibitory domains (K1-3), a positively charged C-terminal and Glycosylphosphatidylinositol (GPI) anchor. Alternative

splicing of the pre-mRNA gives rise to three alternative isoforms; TFPIα, TFPIβ and TFPIδ (Broze & Girard, 2013). Though the latter isoform is listed at NCBI Gene Bank (AB209866.1), it has yet to been found to translate into a functional protein and will therefore not be discussed further (Maroney *et al.*, 2010). TFPIα and TFPIβ are the two major isoforms. Common for both isoforms are the K1 and K2 domains and the N-terminal. In addition, TFPIα contains the K3 domain and the highly basic C-terminal, while TFPIβ contains the GDP-anchor (Wood *et al.*, 2014).

Endothelial cells and megakaryocytes are the main producers of TFPI, but smaller amounts are also produced by other cell types such as monocytes and smooth muscle cells (Wood *et al.*, 2014). Because TFPIβ contains the GPI-anchor, it is found bound to the endothelium (Girard *et al.*, 2012), and often in association with caveolae which enhances the anti-TF activity (Lupu *et al.*, 1997; Lupu *et al.*, 2005). A large quantity of TFPIα produced is secreted and circulates in the blood stream, while only a small part is found anchored to the membrane surface. To bind to the surface, TFPIα uses its K3 domain to bind PS located on the membrane surface and increasing the inhibitory ability of TFPIα (Wood *et al.*, 2014).

The main inhibitory function of TFPIα and β is FXa dependent TF-FVIIa inhibition. The K1 and K2 domain bind and inhibit FVIIa and FXa, respectively. Immediately after FX activation, TFPI most likely inhibits both FXa and TF-FVII simultaneously by binding to the TF-FVIIa-FXa ternary complex (Baugh *et al.*, 1998; Wood *et al.*, 2014). Further, the K2 domain binding to the active site of FXa is possibly the rate-limiting step (Warn-Cramer *et al.*, 1988).

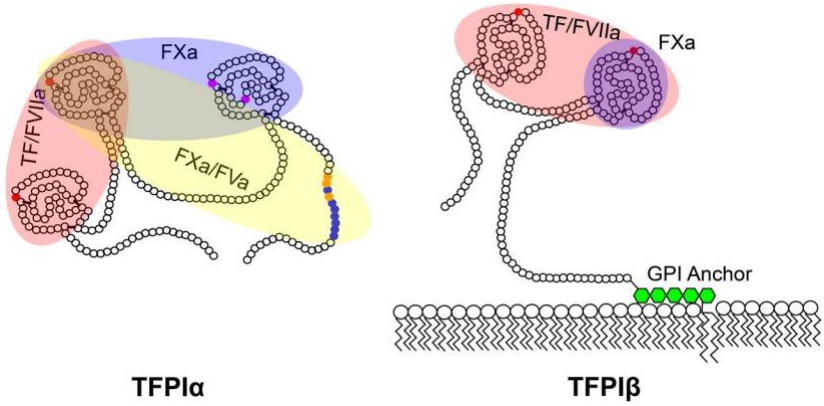

Figure 6: **Structure of the TFPI protein**. TFPIα (left) and TFPIβ (right). Illustration from Wood *et al.* (2014)

1.1.8 TFPI and Cancer

Several studies indicate that TFPI plays a role in cancer development. Lindahl *et al.* (1989) was first to report that TFPI activity increased in parallel with the progression of gastro-intestinal cancer, while anti-thrombin and protein C decreased. A similar effect was also observed in pancreatic patients (Lindahl *et al.*, 1992). Iversen *et al.* (1998) found that patient with solid tumours had an increased level of plasma TFPI. Further, TFPI expression was found in cancer tissues and cell lines, such as breast, colon, liver and pancreas cell lines (Broze & Miletich, 1987; Kurer, 2007; Sierko *et al.*, 2010). Injection of full length TFPI was found to reduce lung metastasis (Amirkhosravi *et al.*, 2002) and injection of recombinant TFPI (rTFPI) inhibited both primary and metastatic tumour growth in mice (Hembrough *et al.*, 2003). A study by Hembrough *et al.* (2004), showed that C-terminal TFPI peptide inhibited angiogenesis both *in vitro* in endothelial cells and *in vivo* in mice. Full length rTFPI was also found to inhibit migration of human gastric cancer cells (Di *et al.*, 2010). Furthermore, Stavik *et al.* (2010) reported that overexpression of TFPIα and TFPIβ led to inhibition of proliferation and induced apoptosis in breast cancer cells. Overexpression also led to changes in the expression of mRNA and miRNAs involved in immunological response and cancer cell growth, these changes might have been affected through the epidermal growth factor receptor (EGFR) pathway (Stavik *et al.*, 2012). Correspondingly, down-regulation of TFPI in breast cancer cells increased self-sufficient growth and inhibited apoptosis (Stavik *et al.*, 2011).

1.1.9 TFPI and Liver cancer

As mentioned, TFPI is produced by several cell types, including liver cells. Figure 7 illustrates the expression of *TFPI* in several malignancies in cancer and normal tissue. *TFPI* expression was increased in liver cancer compared to normal liver tissue and this was also the case for kidney cancers. In contrast, the expression level was reduced considerably in other malignancies, and lung cancer with the largest reduction. When the three stages of HCC (Figure 8) were compared to normal liver tissue, *TFPI* was also higher expressed in the most aggressive subtype, Stage C HCC. As illustrated in Figure 9, an increased expression of *TFPI* did not significantly alter the overall survival rate for patients with HCC.

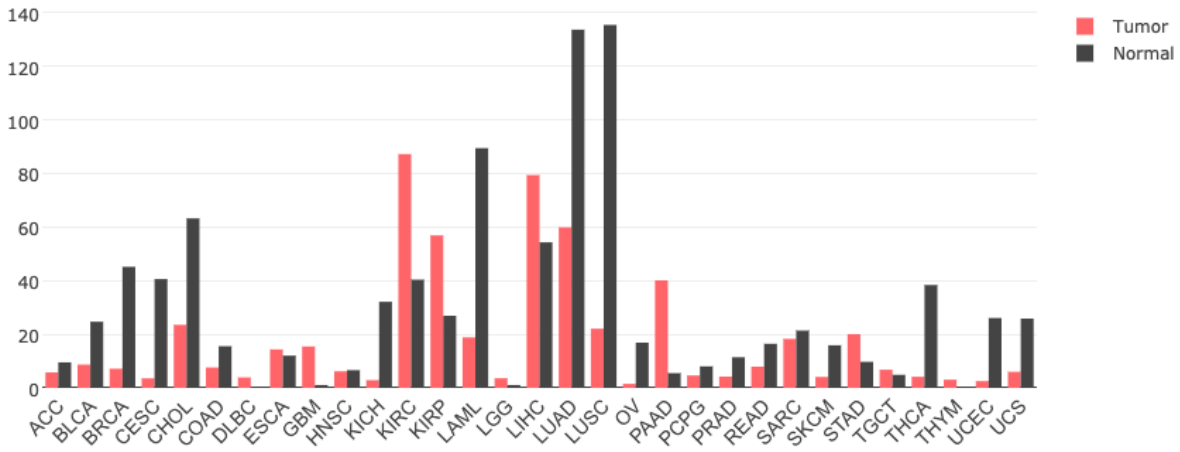

Figure 7: The Bars represent the median *TFPI* expression in certain tumour types (red) with corresponding normal tissue (black). Derived from TCGA data using the GEPIA2 web application (Skogstrøm (unpublished), 2019; (Tang *et al.*, 2017).

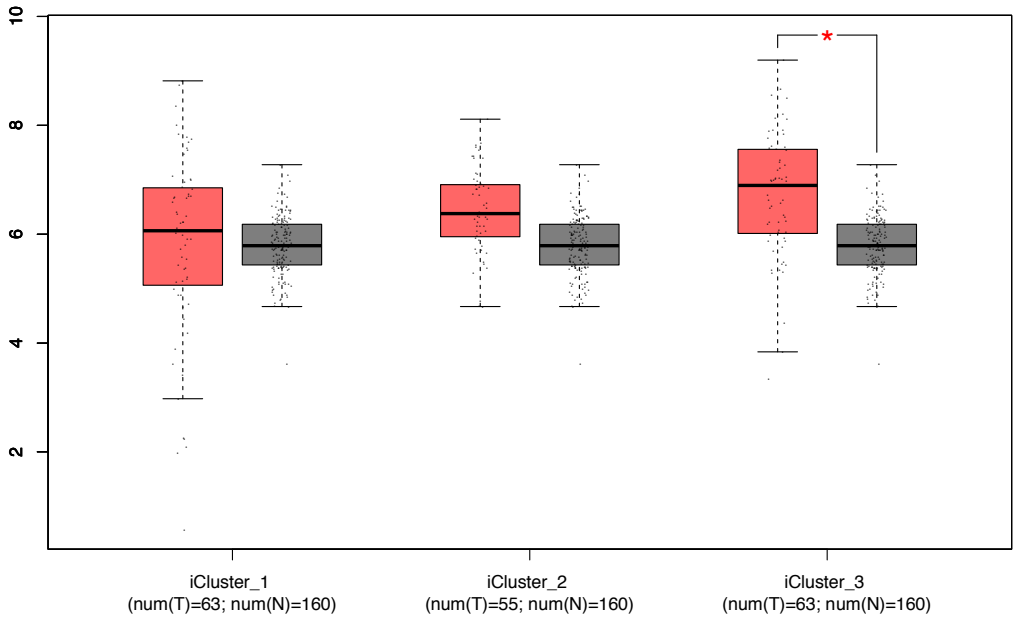

Figure 8: *TFPI* expression in normal liver, n = 160, (black) and liver hepatocellular carcinoma (LIHC) cells divided into the three stages(red). Stage A = cluster_1 (n = 63), Stage B = cluster_2 (n = 55) and stage C = cluster_3 (n = 63). Derived from TCGA data using the GEPIA2 web application (Skogstrøm (unpublished), 2019; (Tang *et al.*, 2017).

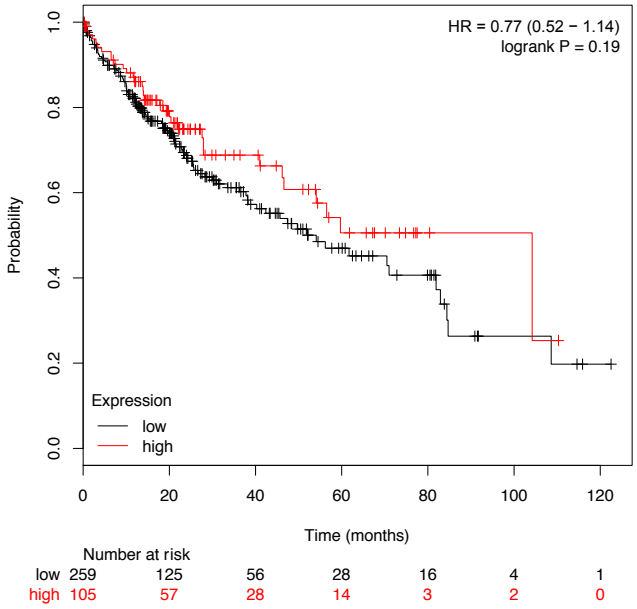

Figure 9: Kaplan-Meier survival plot with high and low expression of *TFPI*. Created with KMPlotter on RNA-sequencing data (Skogstrøm, 2019 (unpublished); (©KMPlotter.com).

1.1.9.1 FV and TFPI interaction

FV and TFPIα has been found to interact in several ways through the TFPIα C-terminus. TFPIα has a prothrombotic inhibitory function that is distinct from the TFPIβ isoform and facilitated by binding FVa. The B-domain of FV has a basic and an acidic part, that is responsible for inhibiting binding of FXa. Proteolysis by FXa removes part of the B-domain. If the acidic part remains, the basic TFPIα C-terminal can bind to this area (Figure 6, area in TFPIα marked with yellow). This binding, combined with the interaction between FXa and K2-domain, allows TFPIα to inhibit prothrombinase and thus the production of thrombin (Wood *et al.*, 2014).

Duckers *et al.* (2008) proposed that TFPIα modulated bleeding in FV-deficient patients. They found that patients deficient in FV were also deficient in TFPIα. This dual deficiency allows for small amount of thrombin formation, protecting individuals from bleeding.

Interaction between FV and TFPIα contributes to the east Texas bleeding disorder. The disorder is caused by a FV mutation, resulting in alternative splicing of the mRNA that removes part of the FV B domain. This "FV-short" isoform retains the acidic region of the B-domain which, as mentioned earlier, binds the TFPIα basic C-terminus. The interaction can result in a ~10-20-fold increase in circulating TFPIα which will cause a moderate to severe bleeding disorder. Healthy individuals have been shown to have very low concentrations of FV-short and TFPIα was shown to preferentially bind FV-short over full-length FV. Thus, FV-short might be the primary form of plasma FV that interacts with TFPIα (Dahlback *et al.*, 2013; Kuang *et al.*, 2001; Vincent *et al.*, 2013).

1.2 Regulation of gene-expression

In healthy cells, gene expression is tightly controlled by several mechanisms, including transcription factors, post-transcriptional control, epigenetic regulators and stimuli (Alberts *et al.*, 2015).

An emerging major kind of regulators are the small-noncoding RNAs that carry out RNA interference (RNAi). There are three types of RNAi; small interfering RNAs (siRNAs), microRNAs (miRNAs) and piwi-interacting RNAs (piRNAs). All three types of RNAs generally locate their target mRNA by RNA-RNA base-pairing and cause a reduction of

gene expression. In this thesis, the focus will be on miRNAs ability to target and regulate *F5* and *TFPI* gene expression in HCC (Alberts *et al.*, 2015).

1.2.1 microRNA (miRNA)

miRNAs are small single-stranded non-coding RNAs of approximately 22 nucleotides, and are either derived from their own promotor (50%), or from within introns or exons of coding or non-coding transcription units (Saini *et al.*, 2007). miRNAs are the most studied kind of non-coding RNAs and are encoded in genomes of most eukaryotes. They were last estimated to be able to modulate up to 60% of all protein coding genes at the translational level. They have a ubiquitous role in gene regulation and are involved in many physiological processes, including differentiation, proliferation, apoptosis and development. As a result, dysregulation of miRNAs has been related to various forms of pathological disorders including cancer and VTE (Catalanotto *et al.*, 2016).

miRNAs were first discovered in 1993 by Victor Ambros and colleagues. They discovered that the gene *lin-4* did not code for a protein, it produced a pair of small RNAs (~22 and ~66 nucleotides) (Lee *et al.*, 1993). The Ruvkan laboratory then discovered that lin-14 was post-transcriptionally regulated and that the lin-14 levels were inversely proportional to the level of let-4 RNA (Wightman *et al.*, 1993). It took seven years before the next miRNA, let-7, was discovered and found to repress expression of *lin-14, lin-41, lin-28, lin-42* and *daf-12* during development (Reinhart *et al.*, 2000). Homologs of let-7 were identified in several vertebrate species, including humans. This led to a world-wide cloning effort of small miRNAs.

1.2.1.1 miRNA biogenesis

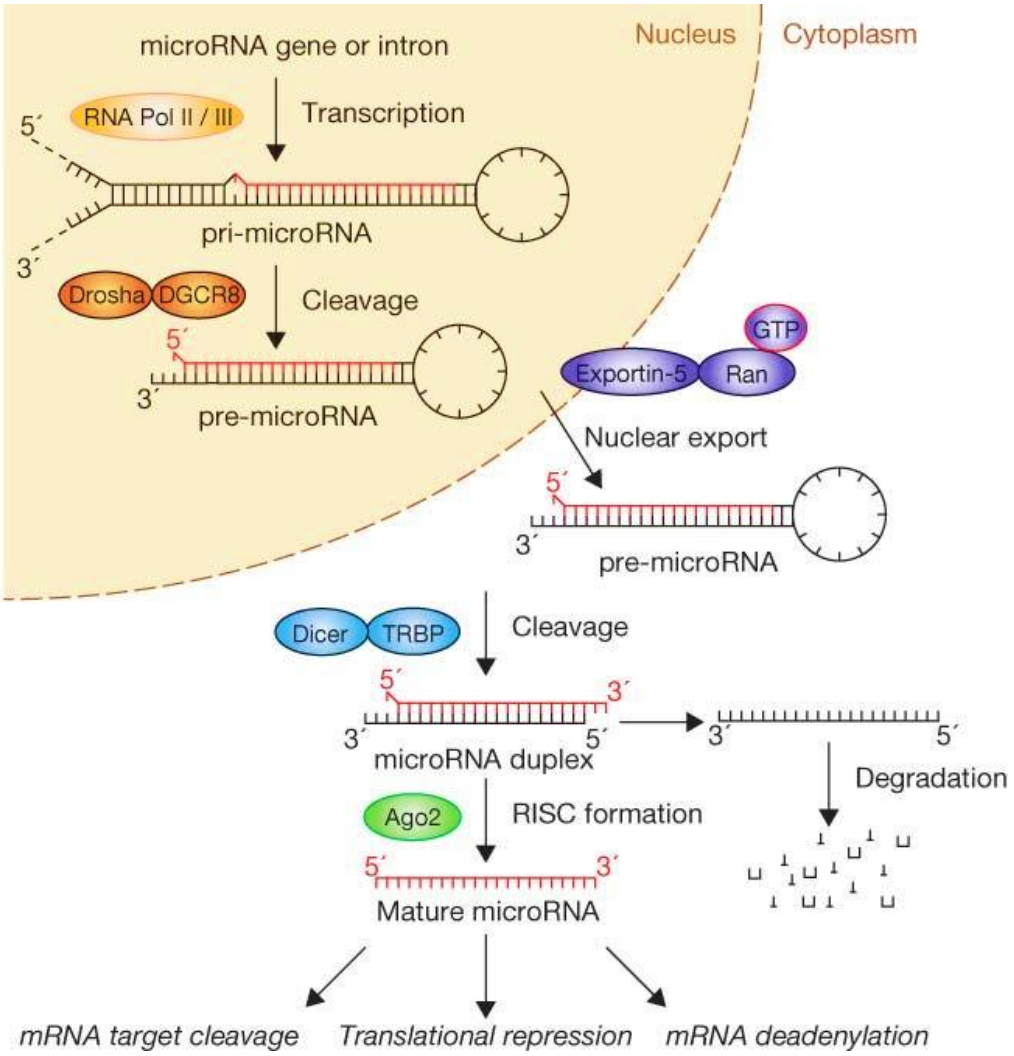

Figure 10: **The canonical miRNA biogenesis pathway** (Winter *et al.*, 2009).

The miRNA biogenesis is split into the canonical and alternative pathway. In the canonical pathway (Figure 10), RNA Polymerase II or III transcribes the hundreds of nucleotide long primary transcripts (pri-miRNA), which are capped with 7-methylguanosine and polyadenylated (Borchert *et al.*, 2006; Cai *et al.*, 2004; Lee *et al.*, 2004). The nuclear RNAse III-type protein Drosha together with its cofactor: the DiGeorge syndrome critical region gene 8 (DGCR8) form a complex called the microprocessor, which cleaves the pri-miRNA into a ~70 nucleotide precursor miRNA (pre-miRNA) with an imperfect stem-loop structure (Gregory *et al.*, 2004; Han *et al.*, 2004; Lee *et al.*, 2003). Exportin-5, a RAN-GTP dependent nucleo/cytoplasmic cargo transporter, exports the pre-miRNA from the nucleus to the cytoplasm (Bohnsack *et al.*, 2004; Lund *et al.*, 2004; Yi *et al.*, 2003).

The RNA Induced Silencing Complex is the effector machine of the miRNA pathways, it contains a single-stranded miRNA which guides the complex to the target mRNA. RISC loading complex (RLC) is responsible for the pre-miRNA processing and RISC assembly in the cytoplasm. RLC is a multiprotein complex, made up of four proteins; the type-III RNase Dicer, the double-stranded RNA-binding (dsRNA) domain proteins TRBP (Transactivating response RNA-Binding Protein) and PACT (protein activator of PKR) and the core component of RISC Argonaute-2 (Ago2) (Chendrimada *et al.*, 2005; Gregory *et al.*, 2005; Haase *et al.*, 2005; Lee *et al.*, 2006; MacRae *et al.*, 2008). Dicer cleaves off the loop in the pre-miRNA and generates a roughly 22-nucleotide miRNA duplex with two nucleotides protruding as overhangs at each 3'end (Ketting *et al.*, 2001). TRBP and PACT are not essential for dicer mediated cleavage, but they facilitate it and TRBP aids by stabilizing Dicer (Chendrimada *et al.*, 2005; Haase *et al.*, 2005; Lee *et al.*, 2006).

Following Dicer-mediated cleavage, Dicer, TRBP and PACT dissociate from the dsRNA duplex (Schwarz *et al.*, 2003). The duplex is unwound by a helicase and the strand with the least thermodynamic stable base pair at its 5'end in the duplex is incorporated into the miRNA-Ago2 protein complex called RISC and functions as the guide strand. The remaining strand is degraded (Khvorova *et al.*, 2003; Schwarz *et al.*, 2003). The mature miRNA strands are annotated -3p or -5p depending on which arm of the pre-miRNA hairpin it hails from. Ago2 is the mediator of the RISC effects on mRNA targets, mediating mRNA degradation, destabilization and translational inhibition (Meister *et al.*, 2004; Pillai *et al.*, 2004).

An alternative biogenesis pathway bypasses the Drosha mediated processing of pri-miRNA to pre-miRNA. Mirtrons are intron-derived miRNAs released from their host transcripts after intron splicing. If the intron has the appropriate size to form a hairpin resembling a pre-miRNA, it bypasses the microprocessor and is exported from the nucleus. In the cytoplasm, Mirtrons are processed into mature miRNAs in the same manner as described in the canonical pathway (Okamura *et al.*, 2007; Ruby *et al.*, 2007).

1.2.1.2 miRNA and mRNA interaction

Once incorporated into the RISC complex, the mature miRNA strand functions as a guide strand leading the complex to its target. The translational inhibition or mRNA degradation is performed by the Ago2 protein in the RISC complex. miRNA predominantly bind to

their target via a seed region (Figure 11). The seed region is the sequence from the 2nd to the 8th nucleotide in the 5'end of the miRNA. They mainly target the 3' untranslated region (3'UTR) of messenger RNAs (mRNAs), nevertheless, targeting inside the coding region or the 5'UTR has also been reported. The short length of the seed region allows a single miRNA to simultaneously inhibit the expression of hundreds of different mRNAs or a single mRNA can be targeted by multiple miRNAs (Bartel, 2009; Lewis *et al.*, 2005).

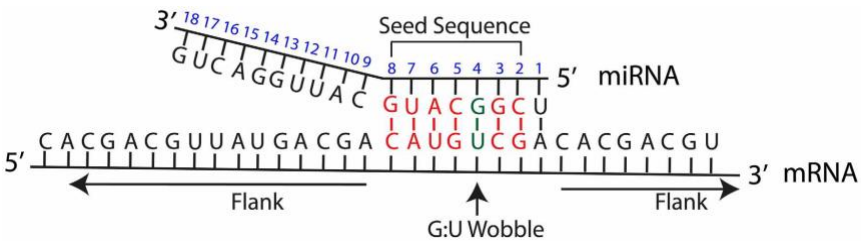

Figure 11: A schematic overview of the miRNA and mRNA target interaction (Peterson *et al.*, 2014).

MiRNA inhibitors, also known as anti-miRs, inhibit their specific miRNA from hybridizing with them and are commonly employed in loss of function studies. They are commonly designed with complementary sequences to the miRNA they inhibit and bind to the miRNA by complementary base-pairing (Stenvang *et al.*, 2012).

1.3 miRNAs involved in haemostasis and HCC

As presented earlier in this introduction, thrombosis and cancer are closely linked and dysregulation of miRNAs involved in both may be the linking factor. miRNAs can target multiple mRNAs and can therefore have targets important for both cancer and thrombosis without being the same mRNA. Only a handful of the factors involved in haemostasis have been identified as targets of miRNAs. These targets, summarized in Table 1, include fibrinogen, TF, TFPI, AT, PS, PAI-1 and FXI. In contrast, the number of miRNAs involved in HCC, either as oncogenes or tumour suppressors, was considerable larger with several thousand published reports (Otsuka *et al.*, 2017). Nevertheless, several of the miRNAs involved in haemostasis are also involved in HCC, such as, miR-18a, -19b, -29b, -126, -145, -181a, -223, -494 (Table 1). Some of their regulatory functions in both thrombosis and HCC are presented below.

Table 1: Summary of miRNAs targeting haemostatic factors and targets involved in HCC tumorigenesis.

miRNA	Haemostatic factor target	HCC Target	Reference
miR-18a	Fibrinogen (indirect), AT	KLF4	(Brock *et al.*, 2011; Liu *et al.*, 2017; Teruel *et al.*, 2011a)
miR-19a/b	TF, AT	Cyclin D1	(Yu *et al.*, 2013; Zhang *et al.*, 2011; Zhang *et al.*, 2015)
miR-20a	TF	-	(Teruel *et al.*, 2011b)
miR-27a/b	TFPI	-	(Ali *et al.*, 2016; Arroyo *et al.*, 2017)
miR-29a/b*/c	Fibrinogen	*MMP-2	(Fang *et al.*, 2011; Fort *et al.*, 2010)
miR-30c	PAI-1	-	(Marchand *et al.*, 2012; Patel *et al.*, 2011)
miR-106b	TF	-	(Chuang *et al.*, 2012)
miR-126	TF	LRP6, PIK3R2	(Du *et al.*, 2014; Witkowski *et al.*, 2016)
miR-145-5p	TF, FXI	IRS1, IRS2, IGF-signalling	(Law *et al.*, 2012; Sahu *et al.*, 2017; Sennblad *et al.*, 2017)
miR-181a-5p	FXI	PTEN	(Chang *et al.*, 2017; Salloum-Asfar *et al.*, 2014)
miR-223	TF, FXIII-A	Rab-1	(Dong *et al.*, 2017; Elgheznawy *et al.*, 2015; Li, S. F. *et al.*, 2014)
miR-301a	PAI-1	-	(Patel *et al.*, 2011)
miR-409-3p	Fibrinogen	-	(Fort *et al.*, 2010)
miR-421	PAI-1	-	(Marchand *et al.*, 2012)
miR-494	TFPI, PS	TET1	(Ali *et al.*, 2016; Chuang *et al.*, 2015; Tay *et al.*, 2013)

TFPI was found to be a direct target of miR-27a/b and miR-494, and the expression of these miRNAs were also upregulated by estrogens. Thus, decreased TFPI levels in the endothelium by estrogens was suggested to be, in part, mediated by overexpression of these miRNAs. In addition, miR-27a/b was shown to be downregulated by testosterone in endothelial cells, suggesting a role of testosterone in regulating miR-27a/b-TFPIα as well (Ali *et al.*, 2016; Arroyo *et al.*, 2017). Furthermore, Tay *et al.* (2013) showed that estrogen increased miR-494 expression in hepatocytes, and that miR-494 was a direct regulator of Protein S. They suggested that miR-494 had a role in estrogen-mediated downregulation of Protein S expression. In addition, miR-494 was overexpressed in human HCC tissues and was involved in cellular transformation by regulating the G1/S cell cycle transition by targeting mutation suppressors in colorectal cancer (Lim *et al.*, 2014). The miRNA could also trigger gene silencing of multiple invasion-suppressor miRNAs by inhibiting genomic DNA demethylation by direct targeting of TET1, thereby leading to tumour vascular invasion (Chuang *et al.*, 2015).

TF is the target of several miRNAs, such as, miR-126, miR-145-5p, miR-223, and miR-19a/b, in addition to their role in HCC. Direct injection of miR-145-5p into mice impaired expression of TF and reduced thrombosis (Sahu *et al.*, 2017). miR-145-5p also regulated FXI protein by direct targeting of the *F11* gene (Sennblad *et al.*, 2017). miR-145 was also a strong tumour suppressor. Its expression could induce G2-M cell cycle arrest and apoptosis by targeting multiple components of oncogenic insulin-like growth factor (IGF) signalling, including insulin receptor substrate- (IRS1-) 1, IRS2, and insulin-like growth factor 1 receptor signalling pathway (Law *et al.*, 2012). miR-126 was also shown to be a direct regulator of TF. Diabetic patients with low levels of miR-126 had high levels of TF which may contribute to their increased risk of thromboembolism (Witkowski *et al.*, 2016). In cancer tissue, Du *et al.* (2014) reported that miR-126-3p contributed to metastasis and angiogenesis in HCC due to degradation of LRP6 and PIK3R2. TF is also directly targeted by miR-223 and exogenous expression of miR-223 in vascular endothelial cells was demonstrated to block tumour necrosis factor α (TNF-α) procoagulant activity of TF (Li, S. F. *et al.*, 2014). Dong *et al.* (2017) showed that miR-223 suppressed cell growth and promoted apoptosis in HCC cell lines by targeting Ras-related protein Rab-1. Additionally, downregulation of miR-223 after resection was correlated with poor prognosis and associated with an increased Stathmin-1 expression (Imura *et al.*, 2017). Thus, its over-expression may have an anti-tumour effect by inactivating the mTOR pathway caused by the suppression of Rab-1 (Dong *et al.*, 2017). Moreover, upregulation of miR-19b was correlated with good prognosis after resection in resected patients in advanced HCC (Hung *et al.*, 2015).

Salloum-Asfar *et al.* (2014) found FXI to be directly regulated by miR-181a-5p and their levels inversely correlated in healthy liver tissue. They suggested that low miR-181a-5p may be a causative factor leading to high FXI levels and thromboembolic disease in human liver (Salloum-Asfar *et al.*, 2014). In HCC patients, miR-181a-5p deregulation in serum was correlated with worse disease control after sorafenib therapy (Nishida *et al.*, 2017). miR-181a was found to be upregulated in HCC tissues and levels were higher in metastatic HCC tissues than non-metastatic. miR-181a-5p regulates the proliferation and invasion of HCC cells by targeting PTEN, the reduction of which activated the PI3K/Akt pathway (Chang *et al.*, 2017).

Fibrinogen is another important factor in blood clot formation and its production in the liver is dependent on the coordinated transcription of all three fibrinogen genes (Fuller & Zhang, 2001; Tay *et al.*, 2016). These genes are targeted by several miRNAs, such as miR-29b (Fort *et al.*, 2010) and miR-18a (Brock *et al.*, 2011), with additional roles in HCC progression. miR-29b exerts its anti-angiogenesis function by suppressing matrix metalloproteinase-2 (MMP-2) expression (Fang *et al.*, 2011). miR-18a enhances the production of fibrinogen in human hepatocytes (Brock *et al.*, 2011). In addition, miR-18a is involved in the Wnt/β-catenin pathway and found upregulated in HCC tissue. This upregulation promotes the proliferation and migration of HCC cell lines by inhibiting KLF4, a factor that negatively regulates β-catenin expression (Liu *et al.*, 2017).

As illustrated in Table 1, only a few miRNAs regulating some of the coagulation factors have been identified and the gap in knowledge of miRNAs involved in thrombosis is still large. No research into miRNA regulation of FV has yet been published and further research into regulation of TFPI is still needed. This thesis aims to fill a part of this gap by identifying novel miRNA regulators of FV and TFPI.

2 Aim

The link between cancer and increased risk of thrombosis is well established. Thus, studying the regulation of coagulation factors associated with cancer may provide a better understanding of this regulation. This can in turn contribute to the discovery of new individualized treatments for patients with cancer and cancer related thrombosis. Furthermore, miRNAs are post-transcriptional gene regulators and their dysregulation have been linked to both cancer progression and thrombosis. Coagulation FV and TFPI have both been linked to cancer progression, with their specific roles in liver cancer yet to be determined. The proteins have also been found to interact in both normal and disease state. Until now, two miRNAs have been identified as regulators of TFPI, while none have been identified for FV. This thesis aimed to identify novel miRNA regulating FV and TFPI, and to study their functional effect on liver cancer progression.

The specific aims of this study were as follows:

1. *In Silico* prediction of miRNA candidates that target *F5* 3'UTR and *TFPIα/β* 3'UTR
2. Validate the regulatory mechanism of miRNA on *F5* and *TFPI:*
    a. Study the miRNAs ability to target *F5* 3'UTR using a luciferase reporter system
    b. Study the miRNAs ability to downregulate *F5* and *TFPI* mRNA expression in HepG2 cells.
    c. Study the miRNAs ability to downregulate *F5* and *TFPIα* protein expression in HepG2 cells.
    d. Study the effect of inhibition of the miRNAs on *F5* and *TFPI* mRNA and protein expression in HepG2 cells
3. Study the effect of overexpression of miRNAs on apoptosis and proliferation in HepG2 cells.
4. Clinical significance of validated miRNAs in liver cancer (or HCC)

3 Materials and Methods

A complete list of software, instruments, solutions, kits, primers, miRNAs and disposables used in this thesis are listed in Appendices B, C, D and E.

3.1 In Silico analysis

Some of the most frequently used bioinformatical programs for miRNA prediction and data analysis have been listed and explained in this section. The tools used for miRNA prediction were TargetScan 7.2 (Agarwal *et al.*, 2015), miRAW (Pla *et al.*, 2018), DIANA-microT-CDS (Paraskevopoulou *et al.*, 2013; Reczko *et al.*, 2012), Exiqon miRSearch 3.0 (Lewis *et al.*, 2005), and miRDB (Wong & Wang, 2015). For data handling and analysis, a combination of Excel, RStudio and Anaconda Spyder were used. Survival analysis comparing overall survival to high and low levels of miRNA expression in liver cancer patients was performed using the web application Kaplan-Meier Plotter (©KMPlotter.com; Nagy *et al.*, 2018).

3.1.1 miRNA prediction tools and selection

Five different prediction tools were used to predict miRNA binding sites within the 3'-UTR region of *F5* and *TFPI*. The prediction tools were based on different algorithms and were using different rules as a basis for their prediction, some of these are summarized below and in Table 2.

The primary rule of most prediction software is the seed match. Seed match refers to the Watson-Crick pairing between miRNA seed region and the target site on the mRNA. The seed region is defined as the 2-8th nucleotide at the 5'end of the miRNA (Lewis *et al.*, 2003; Peterson *et al.*, 2014). To supplement the prediction additional rules are applied, such as, conservation, free energy, site accessibility, target-site abundance, 3'complementary site and extended seed region (Peterson *et al.*, 2014). Conservation is referred to as the maintenance of a sequence across species, which means that the sequence is preferentially selected for because it has an important function. Some prediction algorithms consider the conservation of regions in the 3'UTR, 5'UTR, the miRNA or a combination of all three, in its predictions (Lewis *et al.*, 2003). In general, there is a higher conservation of the seed region than the non-seed region of the miRNA. Nevertheless, some miRNA-mRNA target interactions additionally have conserved regions in the 3'end of the miRNA. These are

called 3'compensatory sites which refers to base pair matching with, for example, miRNA nucleotides 12-17 to compensate for mismatches within the seed region (Friedman & Jones, 2009). An extended seed region (2-10th nucleotide) can also be applied to make up for mismatches within the normal seed region and reduces the stringency of the algorithm slightly (Peterson *et al.*, 2014; Pla *et al.*, 2018). Free energy can be used as measure of the stability of a biological system. By predicting how the miRNA and the mRNA hybridize, regions of high and low free energy can be inferred, and overall free energy can be used as an indicator of how stable the bond is. If the bond is predicted as stable, the mRNA is considered more likely to be a true target of the miRNA (Peterson *et al.*, 2014; Yue *et al.*, 2009). Site accessibility takes into account the secondary structure the mRNA assumes after transcription and measures the ease with which the miRNA can hybridize to the target site (Long *et al.*, 2007). Target-site abundance determines the number of predicted miRNA target sites occurring within a 3'UTR sequence (Garcia *et al.*, 2011). Finally, some of the algorithms have used a machine learning approach, either as a supplement or as the main feature, to develop the model used to predict the miRNA target. The machine learning approach creates a model based on training data and often uses more features in their final model, after testing their predictive power on positive and negative datasets (Peterson *et al.*, 2014).

Table 2: Summary of the rules applied by the miRNA target prediction tools used in this thesis.

	Prediction tool				
Features:	**TargetScan 7.2**	**miRAW**	**Exiqon miRSearch**	**DIANA-microT-CDS**	**miRDB**
Seed Match	**X**	**X**	**X**	**X**	**X**
Conservation	**X/-**		**X**	**X**	**X**
Free energy	**X**			**X**	**X**
Site accessibility		**X**		**X**	**X**
Target-site abundance	**X**			**X**	
Machine learning		**X**		**X**	**X**
3'compensatory site		**X**			**X**
Extended seed region		**X**		**X**	
Coding sequence				**X**	

miRNAs found by two or more tools and with a Context++ score (by TargetScan only) lower than -0.02 were selected for this study. The programming language Python (Anaconda Spyder) was used to compare the predicted miRNA results from each tool with

each other and with the full list of human miRNAs found in miRBase, version 22 (downloaded 12.09.2018) (Griffiths-Jones, 2004; Griffiths-Jones *et al.*, 2006; Kozomara & Griffiths-Jones, 2011; Kozomara & Griffiths-Jones, 2014). To integrate and process results a Python script was written and used. The script used a Boolean operator of True and False, predicted miRNAs were marked as True, while those not on the list of predicted miRNAs were marked with False. The number of times a miRNA was marked as True, from zero to five, was counted and this result was used in the final selection of candidate miRNAs. For the selected miRNAs, miRNA mimics were designed and synthesized by Dharmacon (Appendix C, Table S7).

In addition, from the OsloII cohort previously studied by our group, miRNAs that were negatively correlated with *F5* expression were analysed to see if any of them were predicted to target *F5*- or *TFPI* 3'UTR using the same method as above for selection.

3.2 Plasmid techniques

3.2.1 Plasmid

To assess the miRNAs ability to bind to the 3'UTR of the *F5* mRNA transcript, a miTarget™ miRNA 3'UTR Target clone from GeneCopoeia™ was used as reporter plasmid. The target clone HmiT005058-MT06 consists of the vector pEZX-MT06, illustrated in Figure 12, with the *F5* 3'UTR sequence inserted downstream of the secreted hLuc gene into the area called "miR Target". In mammalian cells a chimeric mRNA consisting of the hLuc and the *F5* 3'UTR target is transcribed from the SV40 promotor. In addition, the vector contained a Renilla luciferase gene is constitutively expressed from the *Cytomegalovirus (CMV)* promotor. The plasmid further contained an Ampicillin (Amp^R) gene which enabled easy selection during transformation and amplification of the plasmid in bacteria.

If the transfected miRNA binds to the 3'UTR, translation of firefly luciferase (transcribed from the hLuc gene) is inhibited, resulting in a lower luminescence measurement than if the miRNA is unable to bind. Translation of the Renilla luciferase is unaffected by the miRNA and its luminescence can therefore be used for normalization. This enables the comparison of samples. To see if the miRNA has bound to the 3'UTR, each sample transfected with a miRNA is normalized against a negative control miRNA (Negative

control #2, Dharmacon). The negative control is set equal to 100%; if a miRNA has bound it will result in a value <100% (Figure 13).

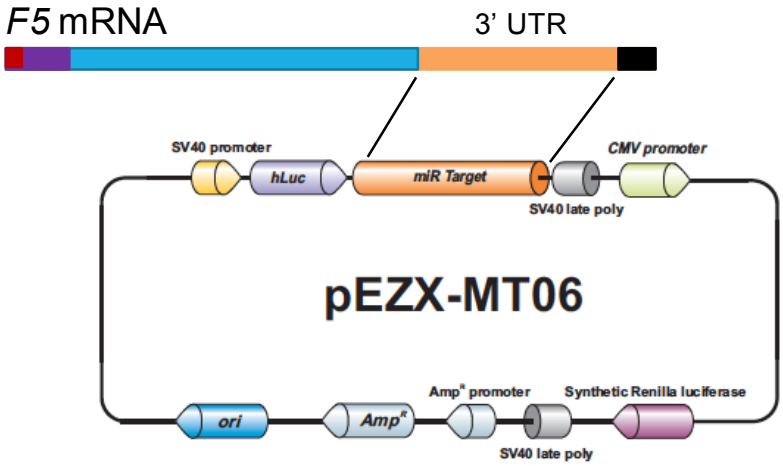

Figure 12: pEZX-MT06 with *F5*-3'UTR (HmiT005058-MT06) inserted into the are marked "miR Target", produced by GeneCopoeia™.

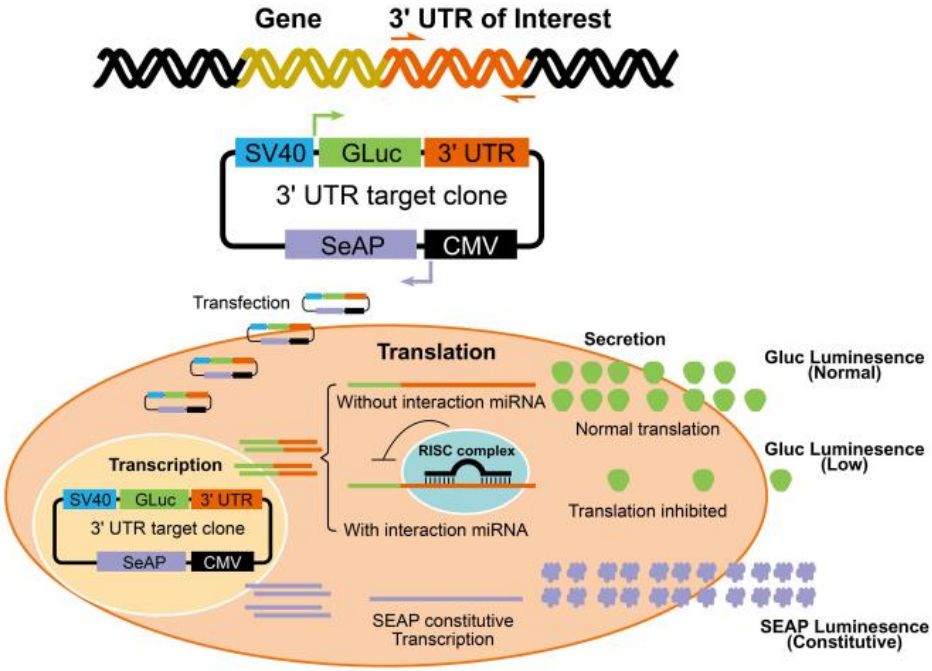

Figure 13: **Illustration of the dual-luciferase assay function**. The miRNA and plasmid are co-transfected into cells. The plasmid is then transcribed, and the 3'UTR sequence and the Firefly luciferase are transcribed together, while the Renilla Luciferase is transcribed separately. If the miRNA is able to bind the firefly luciferase translation is reduced and the resulting luminescence also low. Meanwhile, the Renilla luciferase translation and resulting luminescence is unaffected by miRNA. Firefly luminescence can therefore be normalized against the Renilla luminescence. Illustration created by GeneCopoeia™.

3.2.2 Transformation of *Escherichia coli*

Transformation of plasmids and colony growth for amplification of the plasmid HmiT005058-MT06 was performed following the manufacturer's procedure for "TOPO® Cloning Reaction and Transformation" with some modification in volume.

For each sample, 10 µl TOP10 Chemically Competent *Escherichia coli* were gently mixed with one micro litre plasmid DNA. After incubation for 25 minutes on ice, the sample was heat-shocked for 30 seconds at 42°C and put back on ice. 100 µl of Super Optimal broth with Catabolite repression (SOC) was added and the cells incubated at 37°C and 200 rpm for 1 hour. After incubation, the cell culture was spread on selective lysogeny broth agar plates containing 50 µg/ml Ampicillin (LB-A) and left over-night at 37°C. The following day, single colonies were picked and incubated in 4 ml LB-A medium preculture for 8h with shaking, then transferred to 100 ml LB-A medium at 37°C over-night with shaking.

3.2.3 Maxi-prep for isolation of plasmid DNA

The Maxiprep was performed on the overnight culture with transformed *E. coli* to isolate the plasmid DNA from the bacteria. This was performed using the ZymoPure™ II Plasmid Maxiprep Kit produced by Zymo Research and following the kits' protocol. Briefly, the transformed *E. coli* were pelleted to remove the LB media, then lysed. Using the centrifugation protocol, the lysed bacterial cell sample was cleared using a filter syringe, removing cell debris. The plasmid was bound to the filter in a spin column and washed several times to remove all contaminants, leaving only the plasmid to be eluted. Finally, the sample was run through a new column to reduce the level of endotoxins and the plasmid was ready to be used. Plasmid concentration and purity was measured using the NanoDrop® ND-1000 (see section 3.4.1).

3.2.4 Agarose gel electrophoresis

To see if the plasmid amplification had worked, the plasmid was run on a 1% agarose gel containing GelRed®. Supercoiled plasmid DNA will migrate further than the size of the plasmids indicates compared to the ladder of known sizes. If any of the plasmids are nicked or cleaved these will appear as separate bands of a larger size in the agarose gel. Agarose was mixed with 1X Tris-acetate-EDTA (TAE) for a 1% agarose gel. Each plasmid (1 µg) maxiprep mixed with loading dye was applied to the agarose gel together with the

GeneRuler DNA Ladder Mix (1 KB). The agarose gel was submerged in 1X TAE before sample application and an electrical current of 80 volt was applied for ~1.5 hours. The plasmid DNA was visualized with ImageQuant LAS 4000.

3.3 Cell methods

3.3.1 Cell lines

In this thesis, human hepatoma derived cell line (HepG2) and human embryonic kidney 293 cell line (HEK293T) were used (Table 3 and Figure 14). The HEK293T cell line was used as a host to study miRNAs binding to *FV*-3'UTR. The HepG2 cell line was selected because it had high endogen expression of *F5* and *TFPI* and was therefore used to study the regulatory effect of miRNAs on *F5* and *TFPI* mRNA expression and FV and TFPI protein levels.

Table 3: HepG2 and HEK293T cell line characteristics, including ATCC catalogue number, tissue, derivation, morphology, growth properties and mutations.

	HepG2	**HEK293T**
ATCC Catalogue No.:	HB8065	CRL-3216
Organism:	Homo Sapiens	Homo Sapiens
Tissue:	Liver	Embryonic Kidney
Derivation:	Derived from a hepatocellular carcinoma of a 15-year-old Caucasian male	fetus
Morphology:	Epithelial (hepatocyte)	Epithelial
Growth Properties:	Adherent	Adherent
Growth Media and Serum	Dulbecco's Modified Eagle Medium (DMEM) supplemented with 10% Fetal Bovine Serum (FBS)	Dulbecco's Modified Eagle Medium (DMEM) supplemented with 10% Fetal Bovine Serum (FBS)
Mutation:		SV40 large T antigen
P53 status:	Wild type	Wild type

3.3.1.1 Cultivation of cell lines

The HEK293T and HepG2 cell lines (Figure 14) were cultured in Nunc™ Cell culture treated EasYFlasks™ (T25, T75 and T125). Dulbecco's Modified Eagle Medium (DMEM) with 10% foetal bovine serum (FBS) was used for passaging and growth of the cells. FBS

provided extra growth factors, which were necessary for cell growth. Further, the serum neutralized Trypsin, which was toxic to the cells, but used to dissociate the cell-flask and cell-cell adhesion during passaging. The cell lines were incubated at 37°C with 5% CO_2 in a Steri-cycle CO_2 humidified incubator.

To start a new cell culture, a vial containing ~1 million cryopreserved cells was gently thawed and added to 9 ml of medium. Cryopreserved cells are stored in a medium containing dimethyl sulfoxide (DMSO), a cryoprotective agent which, due to its ability to dissolve the cell membrane, is harmful to the cell viability. To remove the DMSO, the cells were pelleted by centrifugation for 7 minutes at 1500 rpm. The medium was then removed, before the cells were resuspended in fresh medium and transferred to a T25 culture flask.

Passage of the cell lines was performed by removing the old medium, washing the cells gently with Dulbecco's phosphate-buffered saline (DPBS), then detaching the cells using 1 mL of trypsin. Finally, the cells were suspended in fresh medium and passaged in accordance to its confluency and were kept in culture for a maximum of 6 weeks. Confluency was determined visually using a Nikon eclipse Ts2-FL microscope, and kept under ~90% to avoid over-growth.

A B

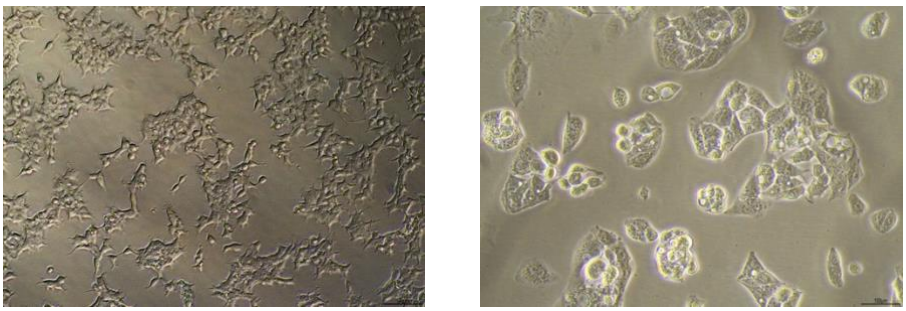

Figure 14: (A) Human Embryonic kidney cells (HEK293T) and (B) Human hepatoma (HepG2) cells during culturing.

3.3.1.2 Cell quantification

NucleoCounter® NC-100™ was used for cell quantification, following the manufacturers protocol. Briefly, 100 µl cell suspension was mixed 100 µl Reagent A (lysis buffer) and 100 µl Reagent B (stabilizer) and loaded into a NucleoCassette™. The NucleoCassette™

contains propidium iodide (PI), a fluorescent dye, which stains the cell nuclei by binding to the DNA. Green light excites the PI-DNA intercalation and red light emitted is registered by a CCD camera, and the amount of light is then automatically converted to the cell number per ml.

3.3.2 Reverse-transfection

Transfection is the process in which foreign material, such as plasmids or miRNA, is introduced into the cell cytoplasm. In reverse transfection cells in suspension are combined with the transfection-mixture simultaneously, in contrast to forward transfection were cells are seeded the day before transfection.

Two transfection reagents, Lipofectamine® 3000 and Lipofectamine® RNAiMAX, were used in this thesis. In general, lipofectamine reagents are cationic lipids (liposomes) consisting of a positively charged head group and one or two hydrocarbon chains. The positive charge mediates interaction between the lipid and the negatively charged phosphate backbone of the nucleic acids. The positive surface charge provided by the liposomes allows the nucleic acids to enter the cell through the cell membrane by endocytosis. Inside the cell, DNA diffuses through the cytoplasm and enters the nucleus for transcription, while RNA and proteins stay in the cytoplasm (Figure 15). Lipofectamine® 3000 is well suited for co-transfection of plasmid DNA and miRNAs and was used for transfection of plasmid and miRNA into HEK293T cells. Lipofectamine® RNAiMAX is optimized for short RNAs, such as miRNA and siRNA, and was used to transfect miRNA into HepG2 cells (ThermoFisher-Scientific).

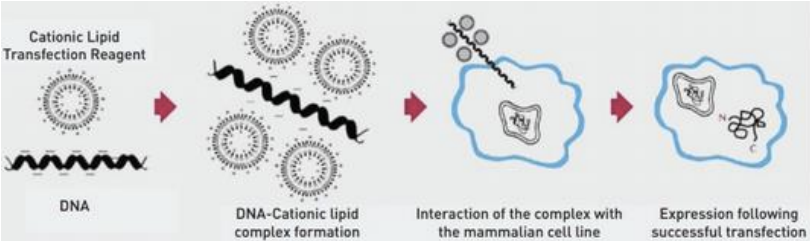

Figure 15: A schematic overview of the mechanism of cationic lipid mediated transfection of nucleic acids into a eukaryotic cell (ThermoFisher-Scientific).

3.3.2.1 3'UTR target validation of candidate miRNAs in HEK293T cells

The miRNAs selected for this study were all predicted to target the 3'UTR of *F5* and this was validated, using a dual luciferase assay. Reporter plasmid *F5-3'UTR*-pEZX-MT06 (see section 3.2.1 and Figure 12) co-transfected together with the miRIDIAN miRNA mimic, hsa-miR-134a-3p, -323a-3p, -510-3p, -532-5p, -543, -548c-3p, -568, -643, -651-3p, -1236-3p, -1278,-1291 and miRNA negative control, were reverse co-transfected into HEK293T cells with six parallels. In each experiment a plasmid coding for green fluorescent protein (GFP) was added as positive control of transfection.

A transfection mixture of miRNA, plasmid, P3000™, Lipofectamine 3000 and Opti-MEM was prepared according to Table 4 and incubated for 15 minutes at room temperature. A DMEM cell suspension of 4 x 10^5 cells/ml of HEK293T was prepared. To each well, 100 µl of cell suspension (4 x 10^4 cells) and 10 µl of transfection mixture was added. The plate was incubated for 48 hours. The experiment was repeated twice, with six parallels for each combination of reporter plasmid and miRNA.

Table 4: Details of transfection reagents, cells number and amounts used in reverse co-transfection of miRNA and plasmid into HEK293T cells. All concentrations and volumes are shown for one well.

Reagents:	96-well plate
Opti-MEM	10 µl
miRNA	30 nM
Plasmid	0.05 µg
Lipofectamine 3000	0.3 µl
P3000	0.1 µl
No. HEK 293T cells	4.0 x 10^4
DMEM 10% FBS	100 µl
Total volume:	110 µl

3.3.2.2 Reverse-transfection of miRNA into HepG2 cells for analysis of effect of miRNA on *F5* and *TFPI* mRNA expression

To analyse the regulatory ability the miRNAs have on the *F5*- and *TFPI* mRNA expression, protein synthesis and apoptosis, each miRNA, found to bind to the *F5*-3'UTR, was transfected into HepG2 cells. The miRIDIAN miRNA mimics transfected were: hsa-miR-7-5p (only 48h), -145-5p (only 48h), -323a-3p, -510-3p, -532-5p, -548c-3p, -568, -643, -651-3p, -1236-3p, -1278 and -1291. For each sample, one miRNA and Lipofectamine® RNAiMAX were diluted in Opti-MEM, mixed following Table 5 and incubated for 15

minutes. A HepG2 cell suspension with $3x10^5$ cells/ml for 24h experiment and $2x10^5$ cells/ml for 48h experiment was prepared. In a 24-well plate, 500 µl of the cell suspension was distributed into each well, before 100µl of the transfection mixture was added. The plates were incubated for 24- and 48 hours. Because there was only effect of miRNAs after 48 hours, only the 48-hour experiment was repeated three times with three parallels each.

3.3.2.3 Reverse-transfection of miRNA Inhibitors into HepG2 cells

miRNA inhibitors are designed to bind to the miRNA present in the cells and reverse the effect the miRNA have on the mRNA of interest. They are specific to one miRNA each. miRIDIAN miRNA mimics has-miR-323a-5p, -568, -1278 and Negative Control #2 miRNA and their respective inhibitors were reverse transfected into HepG2 cells according to Table 5. The experiment was performed in both 24-well plates and 12-well plate. The samples from the 24-well plates were harvested for mRNA analysis. The samples from the 12-well plates were harvested for apoptosis and total protein analysis. The experiment was set up in parallels of three and repeated three times.

3.3.2.4 Reverse-transfection of miRNA and miRNA inhibitors for analysis of cell viability

miRNAs were reverse-transfected into HepG2 cells to analyse the effect they had on cell viability. The miRIDIAN miRNA mimics and inhibitors transfected were; hsa-miR-7-5p, -145-5p, -323a-3p, -568, -643, -651-3p, -1236-3p, -1278 and -1291, and anti-miR-323a-3p, -568 and -1278. For each sample, one miRNA and Lipofectamine® RNAiMAX were diluted in Opti-MEM, mixed following Table 5 and incubated for 15 minutes. In a 96-well plate, 84 µl of the cell suspension (1.6×10^4 cells/ml) was distributed into each well, before 16 µl of the transfection mixture was added. The plates were incubated for 48 hours. The experiment was set up in parallels of three and repeated three times.

Table 5: Details of transfection reagents, cells number and amounts used in reverse co-transfection of miRNA into HepG2 cells. All concentrations and volumes are shown for one well for both 24- and 12 well plates.

Reagents:	96-well plate	24-well plate	12-well plate
Opti-MEM	16	100 µl	200 µl
miRNA	30 nM	30 nM	30 nM
miRNA inhibitor (anti-miR)	50 nM	50 nM	50 nM
Lipofectamine RNAiMAX	0.25 µl	1.5 µl	3.0 µl
No. HepG2 cells	1.6×10^4	1.0×10^5	2.0×10^5
DMEM 10% FBS	84 µl	500 µl	1000 µl
After 24h additional DMEM 10%FBS	100 µl		
Total volume:	200 µl	600 µl	1200 µl

3.3.3 Harvest of cells for further analysis

3.3.3.1 Harvest of HEK293T cells for luciferase assay

HEK293T cells co-transfected with miRNAs and plasmid (described in section 3.3.2.1) were harvested after 48h. The medium was removed, and the cells washed gently with DPBS and lysed with either passive lysis buffer (PLB) from the Dual-Luciferase® Reporter Assay from Promega, or with 1X Lysis Buffer from the Luc-Pair™ Duo-Luciferase Assay Kit 2.0. The harvested cells where stored at -80°C until further analysis.

3.3.3.2 Harvest of cells for mRNA analysis

HepG2 cells transfected with miRNA or miRNA inhibitors in 24-well plates were harvested after 48 hours for mRNA analysis. The medium was removed and stored for FV and TFPI protein analysis. The cells were washed once with cold DPBS, before 1X Monarch DNA/RNA Protection reagent was added. All samples were stored at -20°C until further analysis. Monarch DNA/RNA Protection reagent was part of the Monarch® Total RNA Miniprep Kit. The reagent preserves the nucleic acid integrity during storage.

3.3.3.3 Harvest cells for protein analysis

HepG2 cells transfected with miRNA or miRNA inhibitors in 12-well plates were harvested after 48 hours for total protein and apoptosis in cell lysis, and FV and TFPI protein analysis by ELISA in the medium from the cells. The medium was removed and stored for protein analysis, and the cells were washed three times with cold DPBS. Further, 150 µl of RIPA buffer with 1X Halt™ Protease and Phosphatase inhibitor cocktail was added. The cells were then suspended using a cell scraper, transferred to Eppendorf tubes and incubated on

ice for 30 min. The cell lysates were centrifuged at 1500 rpm (200g) for 10 min before 1:5 dilutions of the supernatants were prepared for the apoptosis analysis using the Cell Death Detection ELISA^{PLUS} (further described in section 3.5.3.3). The remaining cell lysate was stored at -20°C for total protein analysis.

3.4 mRNA analysis

3.4.1 RNA/DNA quantification

RNA and DNA were quantified using the NanoDrop® ND-1000, following the manufacturers procedure. Briefly, 1.5 µl of sample was loaded onto the spectrometer and wavelength absorption at 260, 280, and 230 nm was measured, and the ratios 260/280, and 230/260 was calculated. A 260/280 ratio of ~1.8 was considered pure DNA and ~2.0 pure RNA. The 230/260 ratio of 2.0-2.2 was considered free from contaminants.

3.4.2 Isolation and quantification of RNA

Total RNA from HepG2 cells, transfected with miRNA or miRNA inhibitors, was isolated using Monarch® Total RNA Miniprep Kit. HepG2 cells kept in 1X Monarch® DNA/RNA Protection reagent after harvest, were lysed and genomic DNA was removed from the samples following the manufacturers protocol. The RNA was then treated with DNase to remove any traces of genomic DNA. The samples were eluted in nuclease free water and quantified as described in section 3.4.1.

3.4.3 cDNA synthesis

Isolated RNA was synthesized into complementary DNA (cDNA) by reverse transcription in preparation to quantify *F5*- and *TFPI* mRNA in the cells after miRNA treatment. The cDNA synthesis was performed using the High Capacity cDNA Reverse Transcription Kit® and following the manufacturers protocol. Each sample was diluted in nuclease free water to ensure equal input amount of RNA in each run (400-1000ng). The reaction was setup for each sample as listed in

Table 6, before it was run on the 2720 Thermal Cycler using the program described in Table 7.

Table 6: High Capacity cDNA Reverse Transcription Kit mixture for one reaction

	Volume (µl)
10X RT buffer	4.0
25X dNTP Mix	1.6
10X RT Random Primers	4.0
Multiscribe™ Reverse Transcriptase	2.0
Nuclease-free water	8.4
RNA (1 ng/µl – 25 ng/µl)	20
Total	40

Table 7: Thermal cycler protocol optimized for cDNA synthesis using the High Capacity cDNA Reverse Transcription Kit

	Step 1	Step 2	Step 3	Step 4
Temperature (°C)	25	37	85	4
Time (minutes)	10	120	5	∞

3.4.4 Relative quantification of *F5*- and *TFPI* mRNA by qRT-PCR

Quantitative reverse transcriptase polymerase chain reaction (qRT-PCR) was used to determine the relative amount of *F5*- and *TFPI* mRNA in HepG2 cells transfected with either miRNA or miRNA inhibitors. Using a fluorescent reporter, qRT-PCR detects each PCR cycle as it occurs enabling quantification of the initial concentration of nucleic acids in the sample. In this thesis, TaqMan® probes specific for *F5, TFPI* and *PMM1* were used as fluorescent reporters. The *PMM1* gene was used as the endogenous control as it was mostly unaffected by the miRNA treatment (See Appendix A for test of endogen control genes). Endogenous control genes are genes whose expression should not differ between samples or be affected by the treatment. They are used to correct for reverse transcriptase efficiency and variations in cDNA input.

The TaqMan® assay contains a probe which anneal to the target sequence between two synthetic primers. The probes are single-stranded DNA sequences, specific for the gene of interest, flanked by a fluorescent reporter dye on the 5'-end and a non-fluorescent quencher (NFQ) on the 3'-end. While the probe is intact, the quencher is close enough to the reporter to absorb the fluorescence emitted. For each PCR cycle, the primers and probe anneal to the sequence, and the DNA polymerase extends the strand from the primer in the 3' to 5' direction. DNA polymerase has a 5'-3' exonuclease ability which ensures that when the

probe is reached it is cleaved from its 5'-end releasing the reporter (Figure 16). Away from the quencher the emitted light from the reporter is no longer quenched and can now be detected. The light intensity is proportional to the amount of target cDNA in the sample.

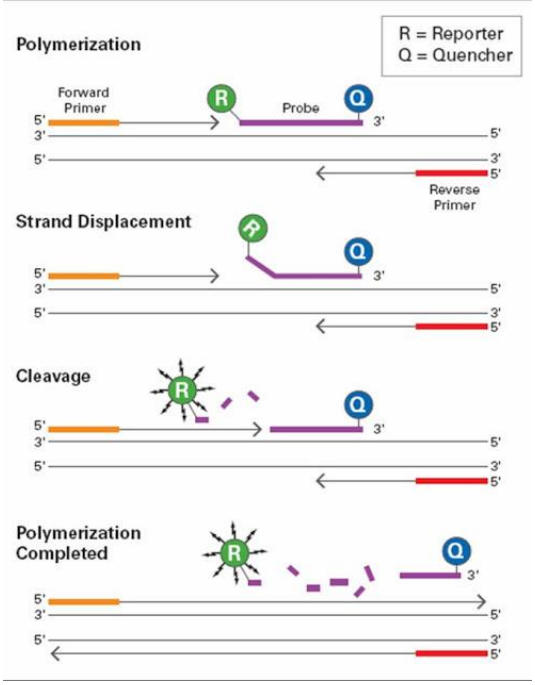

Figure 16: Illustration of how the TaqMan probe works.

Figure 17 illustrates the amplification plot made during qRT-PCR. For each cycle the number of target template increases logarithmically, and the fluorescent light (signal) detected is proportional to this. During the baseline phase the increase and amount of signal is low and overshadowed by background noise. In the exponential phase the signal increases exponentially above the baseline until it reaches the plateau were the signal ceases to increase. A threshold is set automatically in the exponential phase and the cycle in which the signal reaches the threshold is called the Ct-value (cycle-threshold).

The mRNA expression of the target gene was calculated using the $\Delta\Delta C_T$ or Livak method (eq. 1-3). Relative quantity (RQ) is the relative amount of mRNA in the treated sample compared to the calibrator (negative control miRNA). RQ levels <1 indicates downregulation and >1 indicates upregulation, where the calibrator has a RQ equal to one. To use this method, the difference in amplification efficiency between the endogen control gene and the target gene must be <0.1 in slope. This has been previously tested.

$$\Delta C_T = C_{T\,(Target\ gene)} - C_{T\,(Refernce\ gene)} \quad (1)$$

$$\Delta\Delta C_T = \Delta C_{T\,(Target\ sample)} - \Delta C_{T\,(Control\ sample)} \quad (2)$$

$$RQ = 2^{-\Delta\Delta C_T} \quad (3)$$

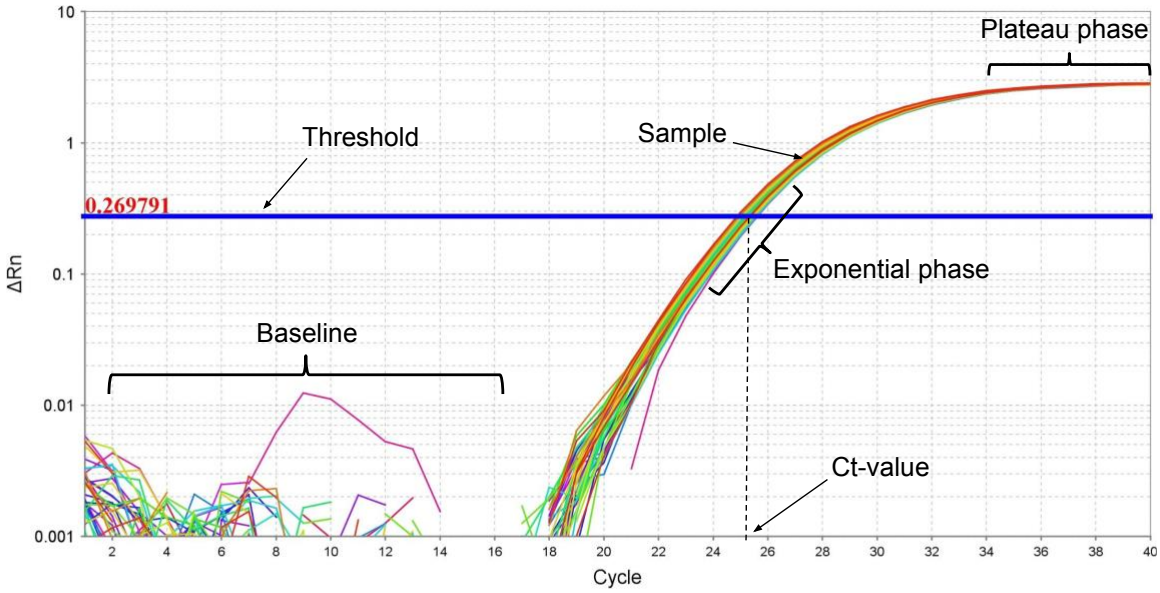

Figure 17**: qRT-PCR amplification plot**. A qRT-PCR amplification plot showing the baseline phase, exponential (log) phase and plateau phase. The threshold is indicated with the blue line and the Ct-value indicated with the black dotted line.

Three Taq-Man assays were used in the thesis, of these two were designed using Primer Express software (TFPIα/β and PMM1) while *F5* was ordered from ThermoFisher (Appendix C, Table S6). A reaction mixture containing cDNA (diluted 1:5 to avoid the inhibitory effects of reverse transcriptase) and the master mix (see Table 8A) was set up in a 96-well plate, before it was transferred in triplicate to a 384-well plate. A non-template control of nuclease free water instead of cDNA was included to ensure that there was no DNA contamination. The plate was run on Applied Biosystems™ QuantStudio™ 12K Flex Real-Time System, using the cycling parameters listed in Table 8B.

Table 8: (A) TaqMan® reaction mix used for qRT-PCR of *F5*, *TFPI* and *PMM1*. Volumes listed are for one reaction. (B) Cycling parameters for one qRT-PCR reaction within one well on the 384-plate.

A)

Reagent	Volume
2X TaqMan® Gene Expression Master Mix	5.0 µl
cDNA	5.0 µl
TaqMan Assay Gene Expression (20x)	0.5 µl
Total	10.5 µl

B)

	Step 1	Step 2	Step 3	
Cycle			1	2
Temperature (°C)	50	95	95	60
Time	2 min	10 min	15 sec	1 min

3.5 Protein techniques

3.5.1 Luciferase measurement

A dual-luciferase assay was used to identify which of the candidate miRNAs that could bind to the 3'UTR of *F5* mRNA. The assays were performed using the Dual-Luciferase® Reporter Assay and the Luc-Pair™ Duo-Luciferase Assay Kit 2.0, following the protocol provided for each kit by the manufacturers. Both kits use the same principle of detection, by first measuring the amount of firefly luciferase in the sample and then the renilla. Firefly substrate (D-Luciferin) was added first, and the resulting luminescence was measured. Further, a reagent containing both the renilla substrate (Coelenterazine) and a component which stops the firefly reaction was added and the luminescence was measured again. For each sample, 5 µl of lysed HEK293T cell co-transfected with the reporter plasmid (section 3.2.1) and miRNA was transferred to a white half-area, µclear® 96-well plate. Both the application of the reagents and the measurement of the luminescence was performed using the BioTek® Synergy H1 luminometer with auto-injection system.

3.5.2 Total protein measurement

Total protein quantification was performed on cell lysates from transfected cells to determine the total concentration of protein in the sample. The quantification was performed using the Pierce™ BCA Protein Assay Kit. The assay is a combination of two colorimetric methods. First, proteins in an alkaline medium reduces Cu^{2+} to Cu^{1+} forming a light blue colour; this is known as the biuret reaction. Then, two Bicinchronic acid (BCA) molecules chelate with one cuprous ion (Cu^{1+}) creating an intense purple coloured reaction product. The density of the purple colour, measured at 570nm, is proportional to the amount of protein in the sample.

Briefly, a standard dilution series containing five concentrations of Albumin, 2 µg/ml to 0 µg/ml, was prepared. Cell lysates were spun down at 3500 rpm (200*g*) for 10 minutes to remove cell debris. 5 µl of samples, standards, and blank (1X Halt RIPA buffer) was added in triplicate to a 96-well plate before adding 200 µl BCA working reagent (1:50 ration of reagent A + B). The plate was incubated for 30 min. at 37°C before absorbance at 570nm was measured using the VersaMax™ Microplate Reader. Protein concentration in the sample was calculated using the SoftMax Pro 6.4 software with a quadratic fit standard curve.

3.5.3 Enzyme-Linked Immunosorbent Assay (ELISA)

Enzyme-Linked Immunosorbent Assay (ELISA) is a sensitive immunological method for the detection and quantification of specific antigens, such as proteins. The antigen of interest is "sandwiched" between an immobilized antibody and a secondary enzyme-linked antibody that enables colorimetric detection (Figure 18). In this thesis Abcam Factor V Human ELISA Kit, ASSERACHROM® Total TFPI and the Cell Death Detection ELISA^{PLUS} kit were used.

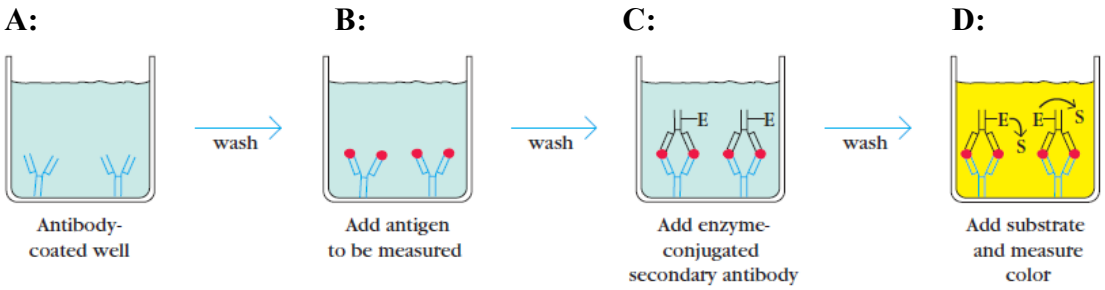

Figure 18: **Diagram of the sandwich ELISA assay illustrating the main steps.** A) The antibody attached to the well surface. B) Antigen from sample attaches to the antibody. C) Secondary antibody with an enzyme attaches to the antigen. D) Substrate is added and cleaved by the enzyme, resulting in a coloured product. The density of the colour is in accordance with the protein concentration in the sample.

3.5.3.1 Quantification of FV protein using ELISA

The FV Human ELISA Kit was used to determine FV protein level in the culture of medium after treatment with miRNAs. The assay was performed following the manufacturers protocol. Briefly, a FV standard dilution series was made with concentrations ranging from 120 ng/ml to 0 ng/ml. Samples and duplicates of standard were added to wells pre-coated with FV specific antibodies. Subsequently, Biotinylated Factor V Antibody was added followed by addition of Streptavidin-Peroxidase Conjugate. Each well was washed with wash buffer between each addition to remove unbound sample, antibody and conjugates. Chromogen substrate containing TMB was added. The TMB was catalysed by the Streptavidin-Peroxidase enzyme reaction and produced a blue colour that changed into a yellow colour by adding the acidic stop solution. The density of the yellow colour was measured using the VersaMax™ Microplate Reader at 450nm with correction for optical noise at 570 nm and the SoftMax® Pro 6.4 software was used to plot the standard curve and calculate the initial concentration in the samples.

3.5.3.2 Quantification of TFPIα protein using ELISA

The Asserachorm® Total TFPI kit was used to determine the level of TFPIα in the sample medium after miRNA treatment (see section 3.3.2 and 3.3.3). The assay was performed following the manufacturers protocol. Briefly, a TFPI standard dilution series was prepared with concentrations ranging from 180 ng/ml to 0 ng/ml. Samples and mouse anti-TFPI monoclonal antibody-peroxidase conjugate were added simultaneously to wells pre-coated with monoclonal TFPI antibody and incubated for two hours before unbound sample and antibodies were washed out. For colour development, Ortho-Phenylenediamine and Urea peroxidase was added, and the reaction was stopped using the acid 3M H_2SO_4. The

resulting colour was measured at 490 nm using the VersaMax™ Microplate Reader and standard curve and concentration was calculated by the SoftMax® Pro 6.4 software.

3.5.3.3 Relative quantification of apoptosis using ELISA

The effect of miRNA treatment on apoptosis in the HepG2 cell line was measured with the Cell Death Detection ELISA^{PLUS} Kit. During apoptosis, DNA fragmentation and release of nucleosomes into the cytoplasm is an early event (Salgame *et al.*, 1997). The kit is based on the detection and quantification of these nucleosomes in the cytoplasm as a measure of the relative level of apoptosis in the sample (Salgame *et al.*, 1997). The sample is deposited in a Streptavidin coated microplate-well together with anti-histone-biotin and anti-DNA-peroxidase (POD). The biotin in the anti-histone-biotin binds to the Streptavidin, while the histones in the nucleosomes bind to the anti-histone. In addition, anti-DNA binds to the DNA in the nucleosomes, thus, creating an anti-histone-nucleosome-anti-DNA sandwich bound to the surface by the streptavidin-biotin complex (Figure 19). Unbound components are removed in a washing step. The number of nucleosomes is quantified through the POD, bound to the anti-DNA, by adding the ABTS substrate creating a green colour.

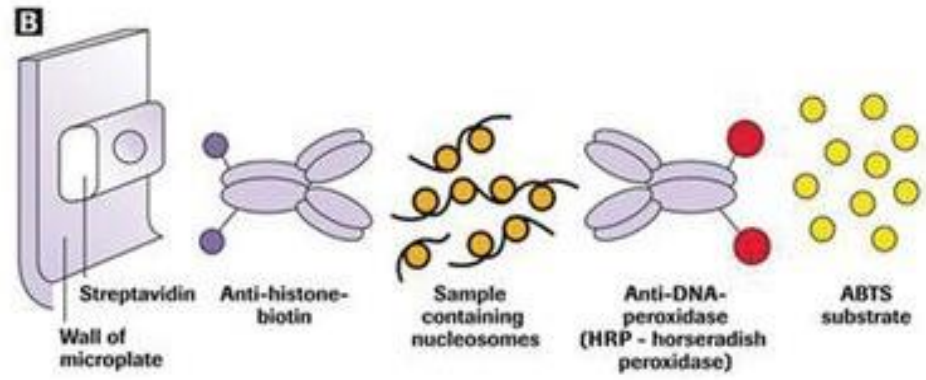

Figure 19: Schematic illustration of the Cell Death Detection ELISA^{PLUS} illustration by Roche

In this thesis, apoptosis was measured in fresh protein lysates harvested 48h after transfection of miRNAs or their inhibitors into HepG2 cells (see section 3.3.3.3). The assay was performed according to the manufacturers protocol. In short, 20 µl of the samples (diluted 1:5) was deposited into each well, before adding 80 µl immunoreagent (containing the antibodies). Further, following a two-hour incubation with shaking, the plate was washed and 100 µl ABTS solution was added. The plate was then incubated for 20 min

with shaking, before absorbance at 405 nm (with 490 nm as reference) was measured using the VersaMax™ Microplate Reader and the SoftMax Pro 6.4 software.

3.5.4 Measuring cell proliferation

The effect of the miRNAs on cell proliferation (cell growth) in HepG2 cell lines as studied using the cell proliferation reagent WST-1. Tetrazolium salt (WST-1) is cleaved into the soluble formazan dye complex by complex cellular mechanisms that are largely dependent on the glycolic production of NAD(P)H in viable cells. Thus, the amount of formazan dye produced correlates directly with the number of viable cells in the culture.

In short, 48 hours after transfecting HepG2 cells with the miRNAs (as described in section 3.3.2.4) 20 µl WST-1 reagent was added to the wells and incubated for 30 min at 37°C with 5% CO_2. The absorbance was measured at 450 nm with 750 nm as reference, using the VersaMax™ Microplate Reader and the SoftMax Pro 6.4 software.

3.6 Statistical analysis

Comparison between treatment and control were performed using the unpaired t-test. If more than three treatments were tested, then an analysis of variance (ANOVA) followed by Dunnett's post-hoc test was performed. A p-value lower than 0.05 was considered significant. All tests were performed using R and Microsoft Excel.

ANOVA and Dunnett's test were used to reduce the likelihood of falsely rejecting null-hypotheses, known as the multiple comparisons problem. This likelihood is reduced by first testing if there is a difference between any of the groups. If there is, then a post-hoc test is performed, in this thesis Dunnett's test was used. The Dunnett test tests if there is a significant difference between each treatment and control and adjusts the p-value according to the number of hypothesis that are tested.

Estimation of the effect high and low expression of the miRNAs have on patient survival time was calculated using the Kaplan-Meier estimator and plotted with a Kaplan-Meier survival curve. The estimator is based on non-parametric statistics and commonly used to estimate the survival function from life time data.

4 Results

4.1 In Silico miRNA target prediction

Five miRNA prediction tools, described in section 3.1.1, were used to predict miRNA binding to the two genes of interest, *F5* and *TFPIα/β*. The miRNAs were selected based on the consensus of two or more programs, a TargetScan Context++ score <-0.15 and its presence in the first part of the latest miRBase release. The five tools showed different results both in number of predictions and which miRNA they predicted to target *F5*- or *TFPIα/β*-3'UTR. TargetScan had the highest number of predictions with 647 (FV) and 690 (TFPI) miRNA, followed by DIANA-microT-CDS with 30 (FV) and 142 (TFPI), miRAW with 63 (FV) and 78 (TFPI), miRDB with 53 (FV) and 91 (TFPI) and finally Exiqon miRSearch with 18 (FV) and 22 (TFPI). Twelve miRNAs were selected, of these, four targeted only *F5*, while eight targeted both *F5* and *TFPI* (Table 9 and Figure 20). In addition, the selected miRNAs were almost all conserved over a minimum of three species, where the seed-regions matched almost perfectly.

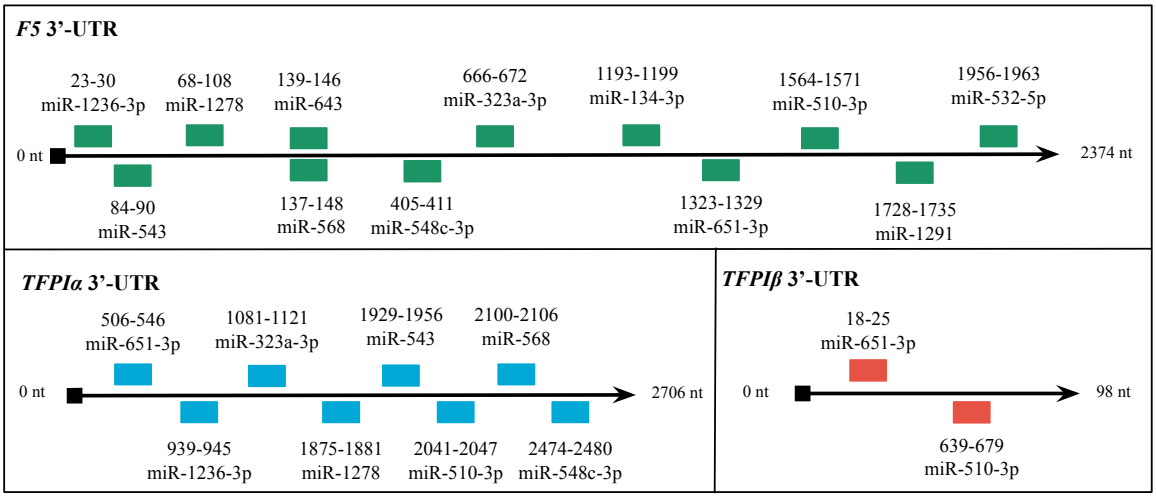

Figure 20: Predicted miRNA binding on the mRNA 3'-UTR of *F5, TFPIα/β*. Some of the miRNA had several predicted binding sites, however, only the binding sites with the highest Context++ score (TargetScan) or miRAW score for the miRNAs are presented.

Table 9: Overview of miRNA selected for further study in this thesis

(a) miRNA predicted for F5 only

miRNA Mature	Context++ score	Position on gene	Program[$]	miRNA mature sequence 5'-3'
hsa-miR-134-3p	-0.24	1193-1199	F5: 1, 3	CCUGUGGGCCACCUAGUCACCAA
hsa-miR-532-5p	-0.22 -0.08	1956-1963 1474-1481	F5: 1, 2	CAUGCCUUGAGUGUAGGACCGU
hsa-miR-643	-0.62	139-146 109-147 (miRAW)	F5: 1, 2, 3, 5	ACUUGUAUGCUAGCUCAGGUAG
hsa-miR-1291	-0.03 -0.22	1728-1735 840-846	F5: 1, 3	UGGCCCUGACUGAAGACCAGCAGU

(b) miRNA predicted for F5 and TFPI-α/β

miRNA Mature	Context ++ score	position on gene	Program[$]	miRNA mature sequence 5'-3'
hsa-miR-323a-3p	-0,02 (F5) -0,01 (F5)	666-672 (F5) 155-161 (F5) 52-92 (miRAW F5) (miRAW TFPI): 1081-1021 1015-1055 656-696	F5: 1, 2 TFPI-α: 2	CACAUUACACGGUCGACCUCU
hsa-miR-510-3p	-0,12 (TFPI-α) -0,04 (TFPI-α) -0,03 (F5) -0,03 (F5)	2041-2047 (TFPI-α) 1781-1787 (TFPI-α) 707-714 (F5) 1564-1571 (F5) 639-679 (miRAW TFPI-β)	F5: 1 TFPI-α: 1, 4, 5 TFPI-β: 2, 4, 5	AUUGAAACCUCUAAGAGUGGA
hsa-miR-543	-0,12 (TFPI-α) -0,04 (F5) -0,02 (F5) -0,01 (F5)	1929-1936 (TFPI-α) 84-90 (F5) 1688-1694 (F5) 1131-1137 (F5) 53-93 (miRAW F5)	F5: 1, 2 TFPI-α: 1, 2, 4, 5 TFPI-β: 4, 5	AAACAUUCGCGGUGCACUUCUU
hsa-miR-548c-3p	-0,02 (F5) -0,02 (F5) -0,01 (TFPI-α)	405-411 (F5) 497-503 (F5) 2474-2480 (TFPI-α)	F5: 1, 4, 5 TFPI-α: 1, 4 TFPI-β: 4	CAAAAAUCUCAAUUACUUUUGC
hsa-miR-568	-0,46 (F5) -0,09 (TFPI-α)	137-148 (F5) 2100-2106 (TFPI-α) 107-147 (miRAW F5)	F5: 1, 2, 3, 5 TFPI-α: 1	AUGUAUAAAUGUAUACACAC
hsa-miR-651-3p	-0,48 (TFPI-β) -0,05 (F5)	18-25 (TFPI-β) 506-546 (TFPI-α) 1323-1329 (F5) 81-121 (miRAW F5)	TFPI-β: 1, 2, 4 ,5 TFPI-α: 2, 4, 5 F5: 1, 2	AAAGGAAAGUGUAUCCUAAAAG
hsa-miR-1236-3p	-0,41 (F5) -0,03 (F5) -0,01 (F5) -0,04 (TFPI-α) -0,01 (TFPI-α)	23-30 (F5) 2002-2009 (F5) 430-436 (F5) 939-945 (TFPI-α) 919-925 (TFPI-α)	F5: 1, 3, 5 TFPI-α: 1	CCUCUUCCCCUUGUCUCUCCAG
hsa-miR-1278	-0,26 (TFPI-α) -0,16 (TFPI-α)	1875-1881 (TFPI-α) 552-558 (TFPI-α) 68-108 (miRAW F5)	F5: 2 TFPI-α: 1, 2, 4, 5 TFPI-β: 4, 5	UAGUACUGUGCAUAUCAUCUAU

$- Programs used: 1. TargetScan, 2. miRAW, 3. miRSearch, 4. DIANA-CDS-microT and 5. miRDB

4.2 miRNAs effect on FV expression

4.2.1 *In vitro*: miRNA targeting of the *F5* 3'UTR mRNA

To study the miRNAs, selected by the prediction tools described in section 4.1, ability to bind to the 3'UTR of *F5* mRNA, 12 miRIDIAN miRNA mimics from Dharmacon were each reverse co-transfected into HEK293T cells together with a luciferase reporter plasmid containing the *F5* 3'UTR sequence. The luciferase activity was measured 48 hours after transfection. Seven miRNAs previously used in a pilot study performed by our group and found to be negatively correlated with *F5* in breast cancer cohort (OsloII), were also tested to see if any of them could target *F5* 3'UTR mRNA.

Of the twelve first selected miRNA mimics (Figure 21A), ten reduced the luciferase activity by 19-39% ($P<0.01$). The remaining two miRNAs, miR-134a-3p and miR-543, had no significant effect on the luciferase activity. Of the addition miRNAs that were tested (Figure 21B), only miR-7-5p and miR-145-5p caused a significant reduction in activity of 32-24% ($P < 0.01$).

For the next validation steps with mRNA analysis, only the 12 (out of 19) miRNAs that significantly reduced the luciferase activity were selected: miR-7-5p, -145-5p, -323a-3p, -510-3p, -532-5p, -548c-3p, -568, -643, -651-3p, -1236-3p, -1278 and -1291.

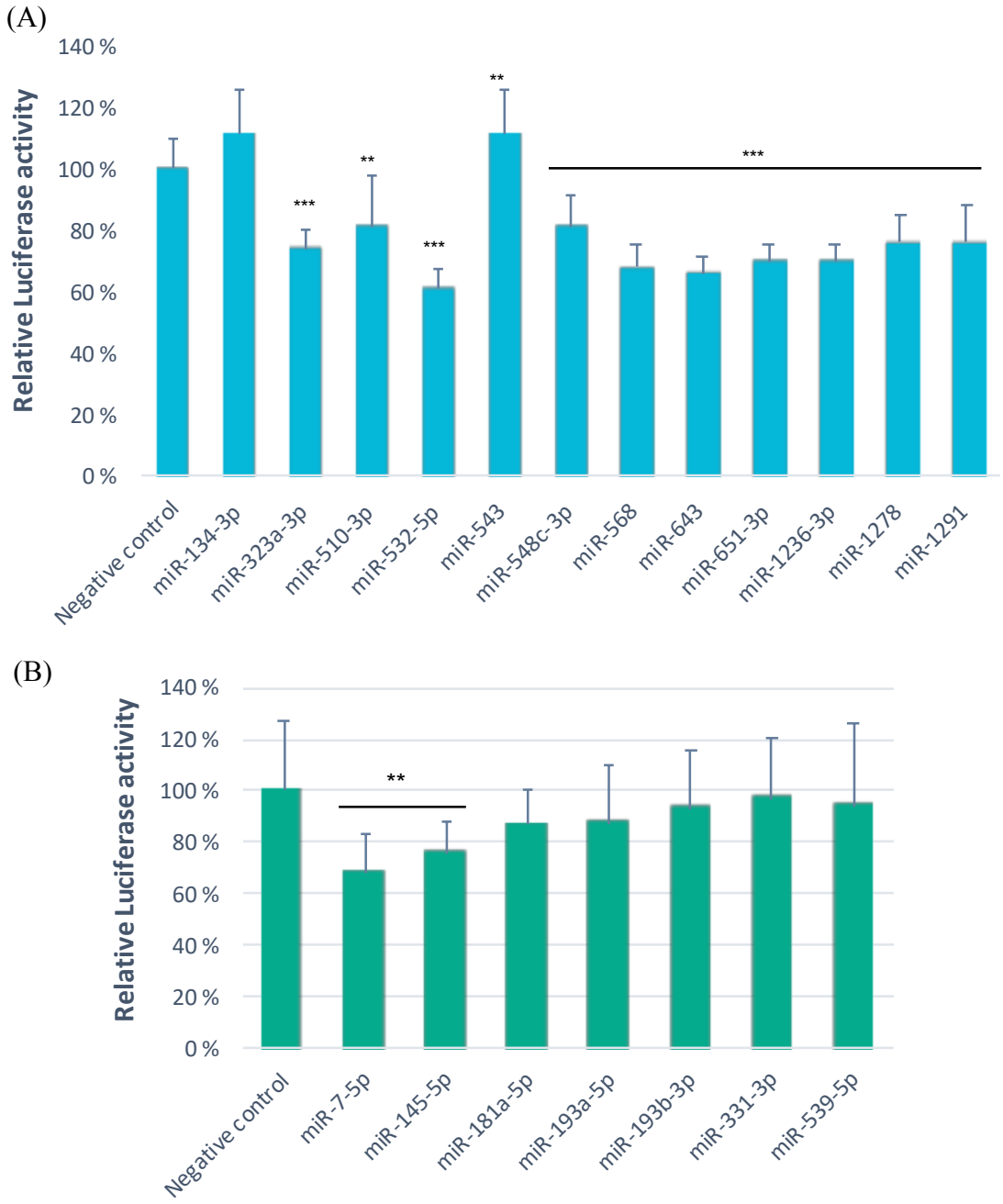

Figure 21: ***F5* 3'UTR mRNA targeted by miRNAs.** HEK293T cells were transfected with a luciferase reporter plasmid with *F5* 3'UTR (HmiT005058-MT06) and miRIDIAN microRNA mimics (A) hsa-miR-134a-3p, -323a-3p, -510-3p, -532-5p, -543, -548c-3p, -568, -643, -651-3p, -1236-3p, -1278 and -1291. (B) hsa-miR-7-5p, -145-5p, -181a-5p, -193a-5p, -193b-3p, -331-3p, -539-5p. miRIDIAN microRNA mimic Negative Control #2 was used as the control. Firefly luciferase activity was normalized to renilla activity. The results are represented as mean ± SD, of five replicates from two independent experiments (n = 10). The normalized data were expressed as changes relative to the data of the cells transfected with the negative control mimic and set to one (1.0). ANOVA followed by a Dunnett's test was performed on miRNA vs. control (*P < 0.05, **P<0.01, ***P<0.001).

4.2.2 The miRNAs effect on *F5* mRNA expression in HepG2 cells

To study the effect the miRNAs had on the *F5* mRNA, the 12 miRNAs that was found to target the *F5* 3'UTR (section 4.2.1) were reverse transfected into HepG2 cells. *F5* is highly expressed in HepG2 cells which made these cells a good model to study the effect of miRNAs on *F5* expression. The miRNAs effect on *F5* mRNA was tested at 24h and 48h after transfection, and optimal incubation time was deemed to be 48h (Figure 22).

Nine out of twelve miRNAs downregulated *F5* mRNA expression up to 36% compared to the negative control miRNA ($P<0.01$). In contrast, miR-532-5p caused a 45% upregulation of *F5* mRNA expression ($P<0.001$).

For the next validation step, FV protein analysis, nine of the twelve miRNAs were selected: miR-7-5p, -145-5p, -323a-3p, -568, -643, -651-3p, -1236-3p, -1278 and -1291.

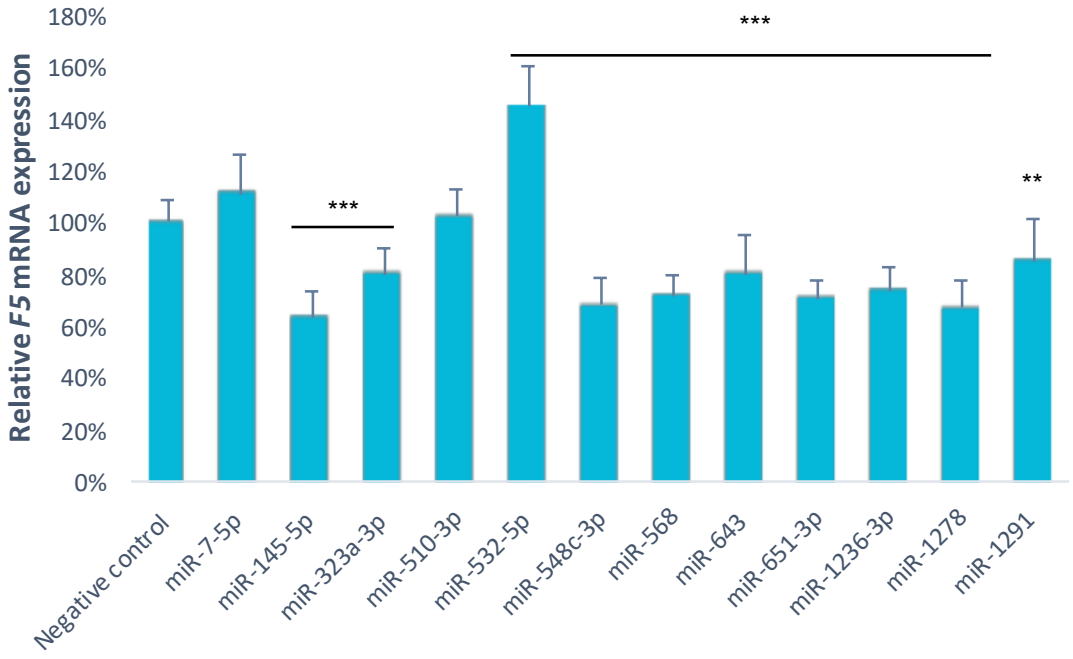

Figure 22: **Effect of miRNAs on the *F5* mRNA expression in HepG2 cells.** HepG2 cells were reverse transfected with 30nM miRIDIAN microRNA mimics and harvested (A) 24h and (B) 48h after transfection. The *F5* mRNA was analysed by qRT-PCR. Results are presented as mean ± SD of three replicates from 3-6 independent experiments ((A) n = 6 and (B) n = 9-18). The data is presented as changes in mRNA in relation to the cells transfected with the negative control miRNA and set to 1.0. ***P<0.001, **P<0.01, ANOVA and Post-hoc Dunnett's test was calculated on miRNA vs. control.

4.2.3 miRNAs effect on FV protein levels

FV ELISA was used to study the effect the miRNAs had on the FV protein levels. Eight miRNAs that downregulated the *F5* mRNA were selected to test their effect on FV protein synthesis. The protein levels were measured in the medium since FV is secreted into the medium, and results were related to total protein in the samples (Figure 23). Five of the miRNAs, miR-323a-3p, -568, -643, -651-3p, -1236-3p and -1291, downregulated FV protein synthesis ($P<0.01$). Notably, miR-323a-3p decreased FV protein level by 52% compared to the control. Furthermore, miR-1278 reduced FV protein level but its effect was not significant after correcting for multiple testing.

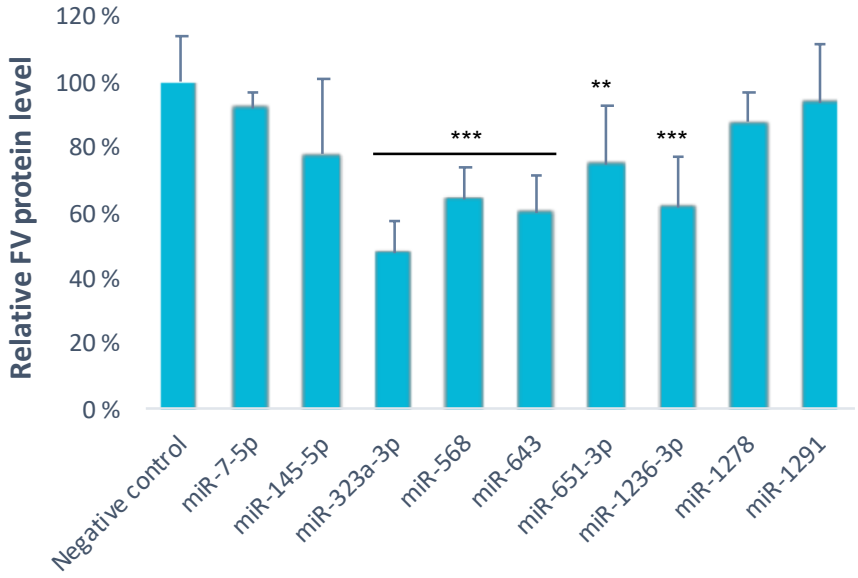

Figure 23: **Effect of miRNAs on synthesis of FV protein.** HepG2 cells were transfected with 30nM miRIDIAN miRNA mimics and harvested after 48h. Total protein (mg) was measured from protein lysates and FV (ng) was measured in the medium. Results given in mean ± SD (n = 3-9), where mean is the relative change compared to the negative control (set to 1.0), after correcting for total protein in the sample. ANOVA followed by post-hoc Dunnett's test was performed on miRNA vs. negative control: ***P<0.001, **P<0.01.

4.2.4 Effect of miRNA inhibitors on *F5* mRNA and protein expression

To further investigate the target specificity of the miRNAs, miR-323a-3p, -568 and -1278, on *F5* mRNA expression levels were assessed by transfecting HepG2 cells with miRNA mimics and miRNA hairpin inhibitors (anti-miRs), only miR-568 and anti-miR-568 were co-transfected. Due to time constraints, these miRNAs were selected for further study based on the initial results at mRNA level.

F5 mRNA levels were determined by qRT-PCR and secreted FV levels by ELISA (Figure 24). *F5* mRNA expression and protein synthesis were both significantly downregulated following transfection of all three miRNAs. As shown in Figure 24A/B, miR-323a-3p reduced the *F5* mRNA level by 18% and the protein level by 52%. The inhibitor, anti-miR-323a-3p, reversed the miRNAs downregulatory effect. Figure 24C/D revealed that miR-568 downregulated *F5* mRNA and protein expression by 25% and 36%, respectively ($P<0.001$). Co-transfection of miR-568 and anti-miR-568 negated the miRNAs downregulatory ability and increased the mRNA and protein expression slightly. Finally, as illustrated in Figure 24E/F, miR-1278 downregulated *F5* mRNA expression by 30% ($P<0.001$), however protein synthesis was only reduced by 13% ($P<0.05$). Inhibition of miR-1278 activity by anti-miR-1278 resulted in a slight increase in *F5* mRNA expression but had no effect on FV protein synthesis.

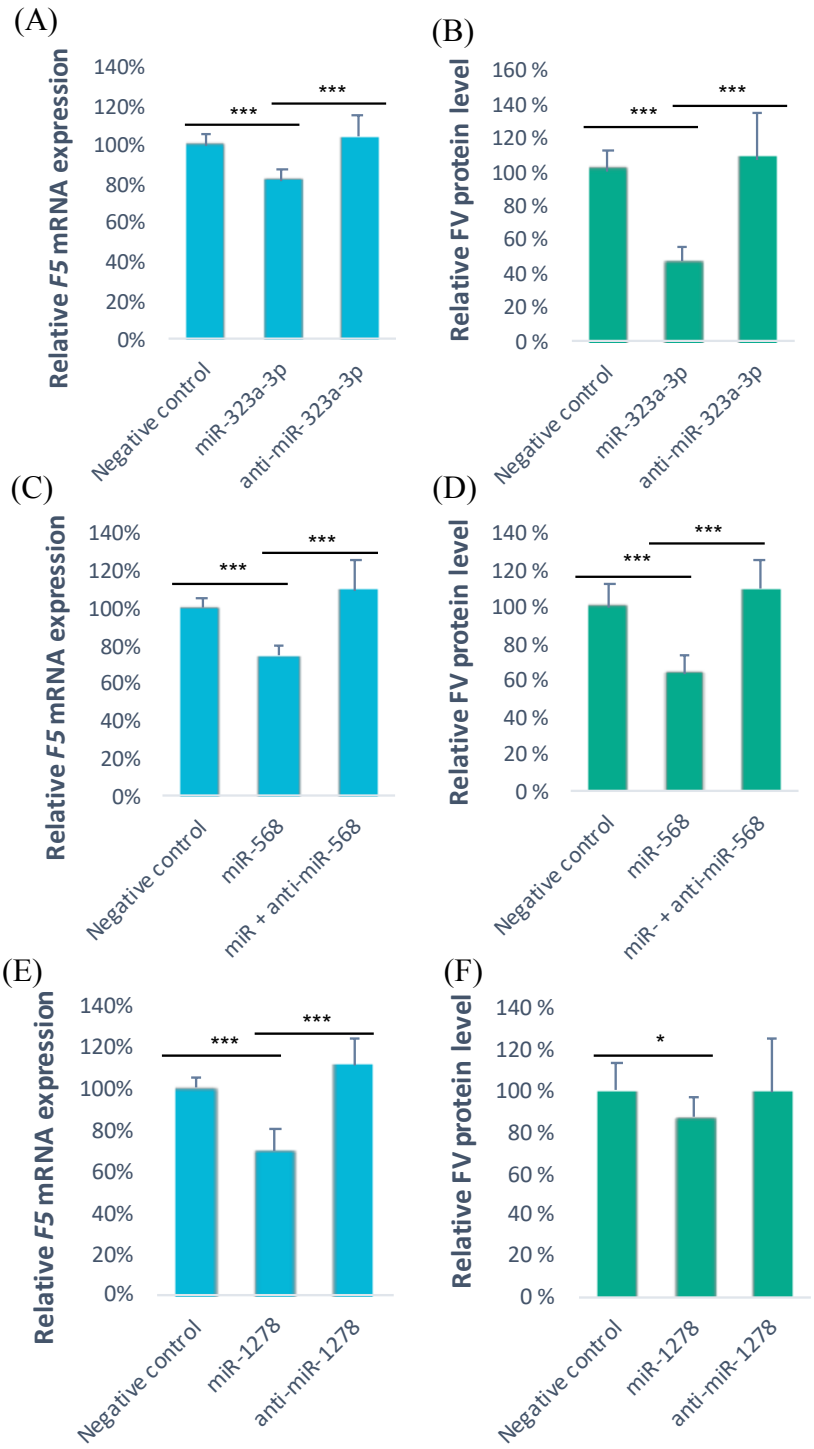

Figure 24: **Effect of miRNA inhibitor (anti-miR) on *F5* mRNA expression and protein synthesis.** HepG2 cells were transfected with 30nM has-miR-323a-3p, -568, - 1278 or negative control, and 50nM miRIDIAN hairpin inhibitors (anti-miR) -323a-3p, -568, -1278, or negative control. Protein lysate, total RNA and extracellular media was obtained 48h after transfection. All results are represented as mean ± SD in relation to the miR and anti-miR negative control (n = 9). (A) miR-323a-3p and anti-miR-323a-3p effect on *F5* mRNA, (B) miR-323a-3p and anti-miR-323a-3p effect on FV protein. (C) miR-568 and anti-miR-568 effect on *F5* mRNA and (D) miR-568 and anti-miR-568 effect on FV protein. (E) miR-1278 and anti-miR-1278 effect on *F5* mRNA and (F) miR-1278 and anti-miR-1278 effect on FV protein. Studentized T-test was performed on miRNA vs. anti-miR, miRNA vs. negative control and anti-miR vs. anti-miR negative control: ***P<0.001, **P<0.01, *P<0.05.

4.3 The miRNAs effect on TFPI expression

4.3.1 The miRNAs effect on mRNA expression of *TFPI* in HepG2 cells

To assess whether the twelve miRNAs found to target the *F5* 3'UTR mRNA (section 4.2.1) also targeted *TFPI* mRNA expression, HepG2 cells were reverse-transfected with the miRNAs. *TFPI* mRNA levels were analysed by qRT-PCR 24- and 48-hours after transfection. The optimal incubation time was found to be 48h and results are presented in Figure 25. Eight out of the twelve miRNAs transfected, downregulated the *TFPI* mRNA expression by 23-85% ($P<0.05$). In contrast, miR-532-5p and -568 resulted in an upregulation of mRNA by 40% and 21% ($P<0.05$), respectively. For the next. validation step, TFPI protein analysis, seven of the miRNAs with regulatory effect on TFPI mRNA were selected: miR-7-5p, -145-5p, -323a-3p, -651-3p, -1236-3p, -1278 and -1291.

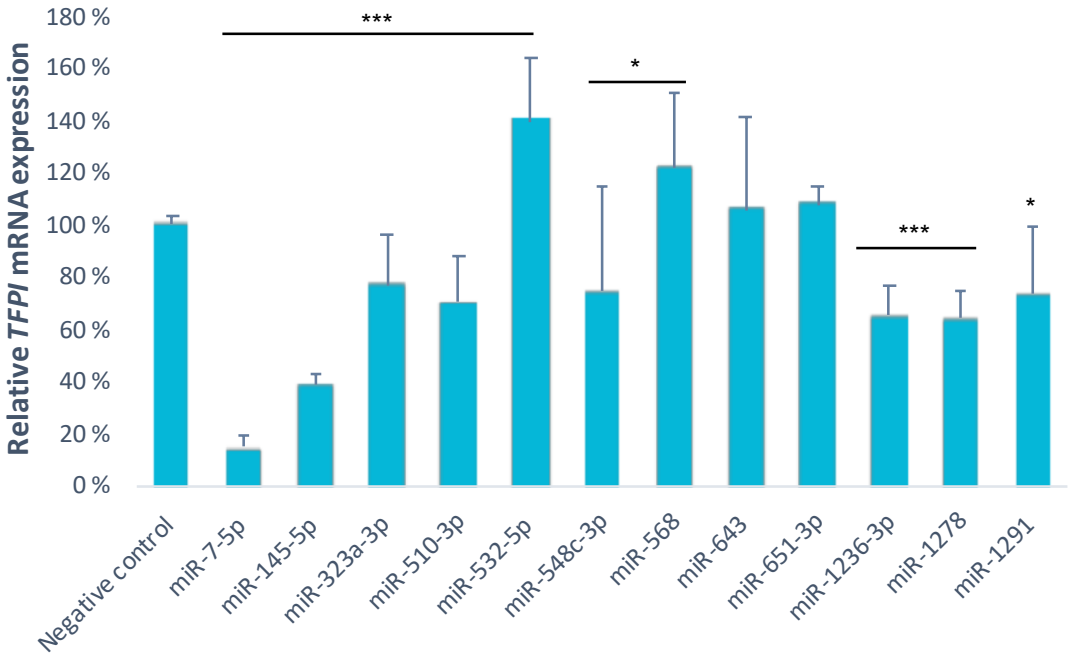

Figure 25: **Effect of miRNAs on the *TFPI* mRNA in HepG2 cells.** HepG2 cells were reverse transfected with 30nM miRIDIAN microRNA mimics and harvested (A) 24h and (B) 48h after transfection. The *TFPI* mRNA was analysed by qRT-PCR. Results are presented as mean ± SD of three replicates from 3-6 independent experiments ((A) n = 3, (B) n = 9-18). The data is presented as changes in mRNA in relation to the cells transfected with the negative control miRNA and set to 1.0. ***P<0.001, **P<0.01, *P<0,05, ANOVA and Post-hoc Dunnett's test was calculated on miRNA vs. control.

4.3.2 miRNAs effect on TFPIα protein synthesis

TFPI ELISA was used to study the effect the miRNAs had on TFPIα protein synthesis. The eight selected miRNAs that downregulated *TFPI* mRNA expression (section 4.3.1) were tested to assess their effect on TFPIα protein synthesis. Secreted TFPIα level was measured in the medium and related to the total protein in the cell lysates (Figure 26). Interestingly, only miR-7-5p had an effect on the TFPIα protein synthesis, downregulating the synthesis by 53% (P<0.001).

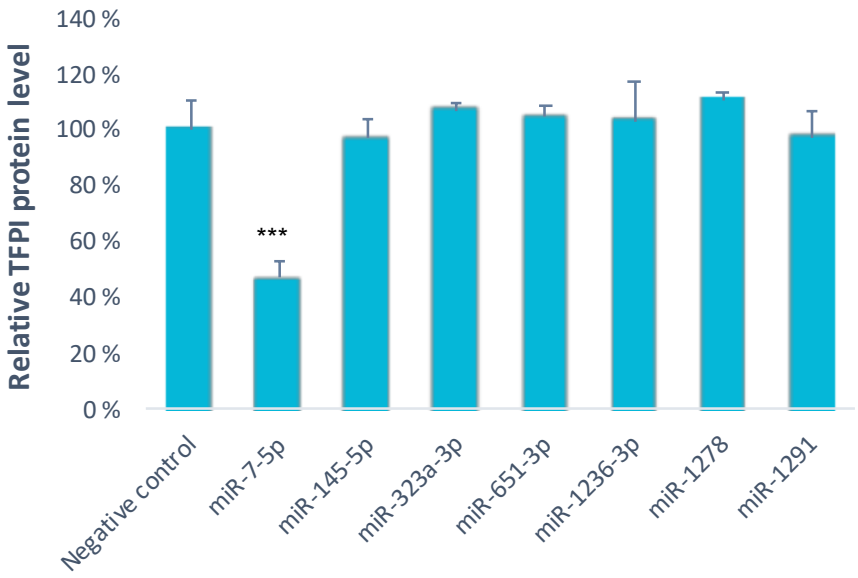

Figure 26: **Effect of miRNAs on TFPIα protein level.** HepG2 cells were transfected with 30nM miRIDIAN miRNA mimics and harvested after 48h. Total protein (mg) was measured from protein lysates and TFPIα (ng) was measured in the medium. Results given in mean ± SD (n = 3), where mean is the relative change compared to the negative control (set to 1.0), after correcting for total protein in the sample. ANOVA followed by post-hoc Dunnett's test was performed on miRNA vs. negative control: ***P<0.001.

4.3.3 Effect of miRNA inhibitors on *TFPI* mRNA and TFPIα protein expression

To further investigate the specificity of the miRNAs, hsa-miR-323a-3p, and -1278, on *TFPI* mRNA and protein expression levels were assessed by transfecting HepG2 cells miRNA mimics and miRNA hairpin inhibitors (anti-miRs). Due to time constraints, these miRNAs were selected for further study based on the initial results at mRNA level.

TFPI mRNA levels were determined by qRT-PCR and secreted TFPIα levels by ELISA (Figure 27). miR-323a-3p downregulated *TFPI* mRNA expression by 19% (mean = 0.81, $P<0.001$). The inhibitor, anti-miR-323a-3p, reversed the miRNAs downregulatory effect, and increased the *TFPI* mRNA expression by 18% (mean = 1.18, $P<0.001$) (Figure 27A). The downregulation of *TFPI* mRNA expression did not have effect on the TFPIα protein level, though, the anti-miR-323a-3p still increased the protein synthesis slightly (mean = 1.09, $P>0.05$) (Figure 27B). miR-1278 downregulated *TFPI* mRNA expression by 36% (mean = 0.64, $P<0.001$) and inhibition of its activity by anti-miR-1278 resulted in an increase in *TFPI* mRNA expression by 17% (mean = 1.17, $P<0.05$) (Figure 27C). There was no effect of either up- or downregulation of TFPIα protein level (Figure 27D).

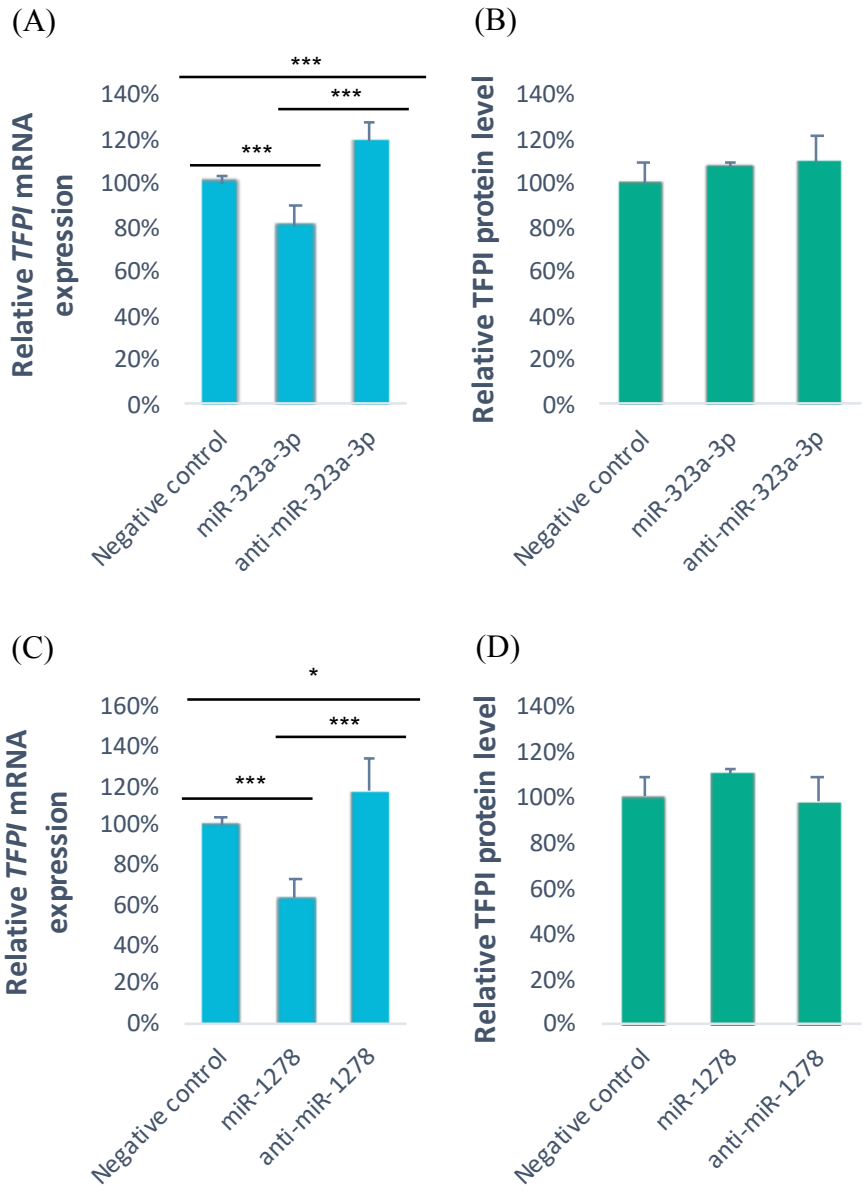

Figure 27: **Effect of miRNA inhibitor (anti-miR) on *TFPI* mRNA expression and TFPIα protein level.** HepG2 cells were transfected with 30nM has-miR-323a-3p, - 1278 or negative control, and 50nM miRIDIAN hairpin inhibitors (anti-miR) -323a-3p, -1278, or anti-miR-negative control. Protein lysate, total RNA and extracellular media was obtained 48h after transfection. All results are represented as mean ± SD in relation to the miR and anti-miR negative control (n = 9). (A) miR-323a-3p and anti-miR-323a-3p effect on *TFPI* mRNA, (B) miR-323a-3p and anti-miR-323a-3p effect on TFPIα protein. (C) miR-1278 and anti-miR-1278 effect on *TFPI* mRNA and (D) miR-1278 and anti-miR-1278 effect on TFPIα protein. Student T-test was performed on miRNA vs. anti-miR, miRNA vs. negative control and anti-miR vs. anti-miR negative control: ***P<0.001, **P<0.01, *P<0.05.

4.3.4 Summary of miRNAs effect on *F5* 3'UTR, and *F5* and *TFPI* mRNA and protein expression

In summary, twelve miRNAs were predicted by up to five prediction tools to target the *F5* 3'UTR mRNA and eight of these to also target *TFPI* 3'UTR mRNA. The effect of these was then validated on three levels, direct targeting of *F5* 3'UTR mRNA sequence, and targeting of endogen *F5* and *TFPI* mRNA and protein expression the HepG2 cell line. Only the miRNAs with effect on a validation step was selected for further validation. The results from each validation step is presented in Table 10.

Five miRNAs, miR-323a-3p, -568, -643, -651-3p, -1236-3p and -1278, targeted *F5* 3'UTR mRNA and downregulated *F5* mRNA and protein expression. None of these were predicted by DIANA-microT-CDS, and miRAW was the only one that predicted miR-1278 to target *F5*. Only has-miR-7-5p downregulated the *TFPI* mRNA and protein expression as predicted by all tools except TargetScan.

Table 10: **Summary of the prediction and target validation results:** prediction, *F5* 3'UTR, mRNA expression and protein synthesis of FV and TFPI. miRNA predicted by; (1) TargetScan, (2) miRAW, (3) miRSearch, (4) DIANA-CDS-microT and (5) miRDB. Results of validation steps marked by: "Yes" significant change or "No" not-significant. miRNAs not included in a validation step is marked with negative sign "- ". miRNAs that caused significant downregulation of either *F5* or *TFPI* on all levels are written in red.

	Predicted by		**FV**			**TFPIα**	
miRNA	*F5*	*TFPI*	3'UTR	mRNA	Protein	mRNA	Protein
hsa-miR-7-5p	1	2, 3, 4, 5	Yes	No	No	Yes	Yes
hsa-miR-134-3p	1, 3	-	No	-	-	-	-
hsa-miR-145-5p	1	-	Yes	Yes	No	Yes	No
hsa-miR-323a-3p	1, 2	2	Yes	Yes	Yes	Yes	No
hsa-miR-510-3p	1	1, 2, 4, 5	Yes	No	No	Yes	-
hsa-miR-532-5p	1, 2	-	Yes	Yes	No	Yes	-
hsa-miR-543	1, 2	1, 2, 4, 5	No	-	-	-	-
hsa-miR-548c-3p	1, 4, 5	1, 4	Yes	Yes	No	Yes	-
hsa-miR-568	1, 2, 3, 5	1	Yes	Yes	Yes	Yes	-
hsa-miR-643	1, 2, 3, 5	-	Yes	Yes	Yes	No	-
hsa-miR-651-3p	1, 2	1, 4, 5	Yes	Yes	Yes	No	No
hsa-miR-1236-3p	1, 3, 5	1	Yes	Yes	Yes	Yes	No
hsa-miR-1278	2	1, 2, 4, 5	Yes	Yes	Yes	Yes	No
hsa-miR-1291	1, 3	-	Yes	Yes	No	Yes	No

4.4 miRNAs effect on cell growth and survival

4.4.1 Apoptosis

To study if the miRNAs affected cell death in the HepG2 cells, the cells where transfected with miRNA and cell lysate was harvested after 48 hours. All miRNAs and anti-miRs tested on protein level were included in this analysis to study their effect on apoptosis, independent of their regulatory effect on *F5* and *TFPI*. The assay used quantified the number of nucleosomes released into the cytoplasm from the cell lysates (Figure 28). The results indicate an 20-36% increase in apoptosis, compared to the negative control, caused by hsa-miR-7-5p, -145-5p, -323a-3p, -1236-3p and -1291 ($P<0.1$). However, this was only significant using a T-test and not after correcting for multiple testing due to large variations within each group.

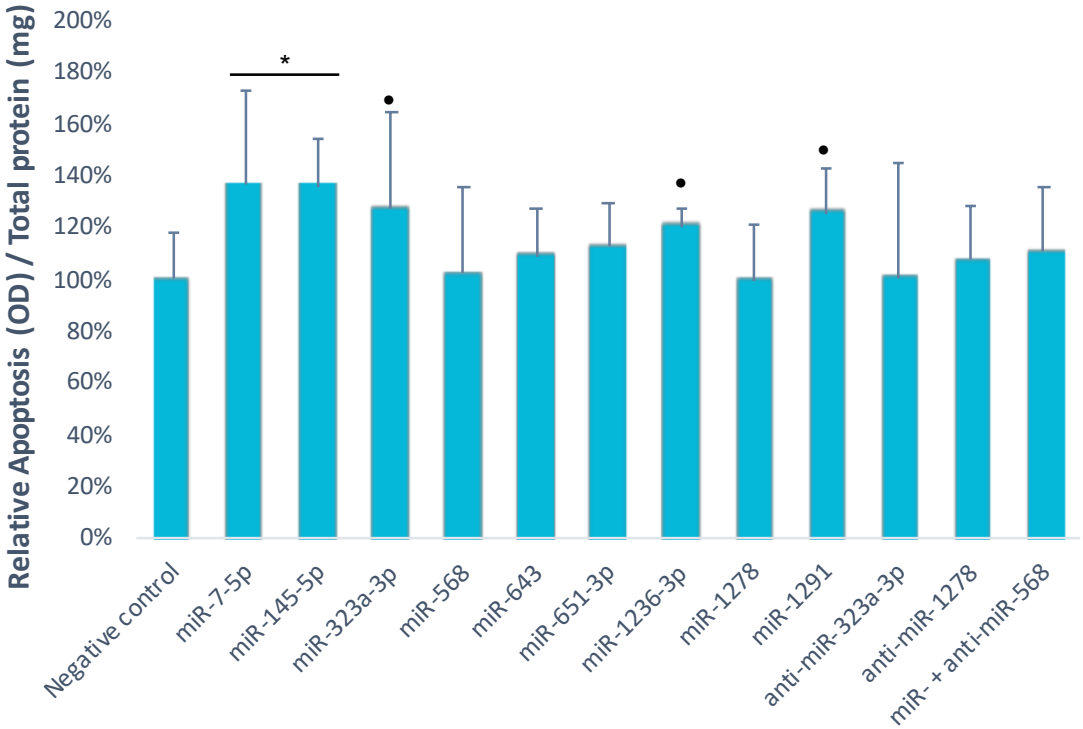

Figure 28**: Effect of miRNAs on apoptosis in HepG2 cells**. HepG2 cells were transfected with 30nM miRIDIAN miRNA mimics or hairpin inhibitor miRNA (anti-miR) and harvested after 48h. Total protein (mg) and apoptosis (OD) was measured from protein lysates. Results given in mean ± SD (n = 3-9), where mean is the relative change compared to the miR or anti-miR negative control (set to 100%), after correcting for total protein in the sample. Studentized T-test was performed on miRNA vs. negative control and anti-miR vs. anti-miR negative control: *$P<0.05$, •$P<0.1$.

4.4.2 Viability

It was interesting to see whether the miRNAs or anti-miRs would have any effect on the proliferation of the HepG2 cells. All miRNAs and anti-miRs tested on protein level were included in this analysis to study their effect on cell proliferation, independent of their regulatory effect on *F5* and *TFPI*. The results indicate that most of the miRNAs have a large effect on the cell viability (Figure 29). miR-7-5p, -145-5p, -323a-3p, -568, -643, -651-3p, -1236-3p, -1278 all reduced the cells proliferation by over 49% ($P<0.001$), while miR-1291 and anti-miR-323a-3p had no significant effect. Anti-miR-1278 increased the cell proliferation by 20% ($P>0.05$) and the combination of anti-miR-568 and miR-568 increased the cell proliferation by 83% ($P<0.001$).

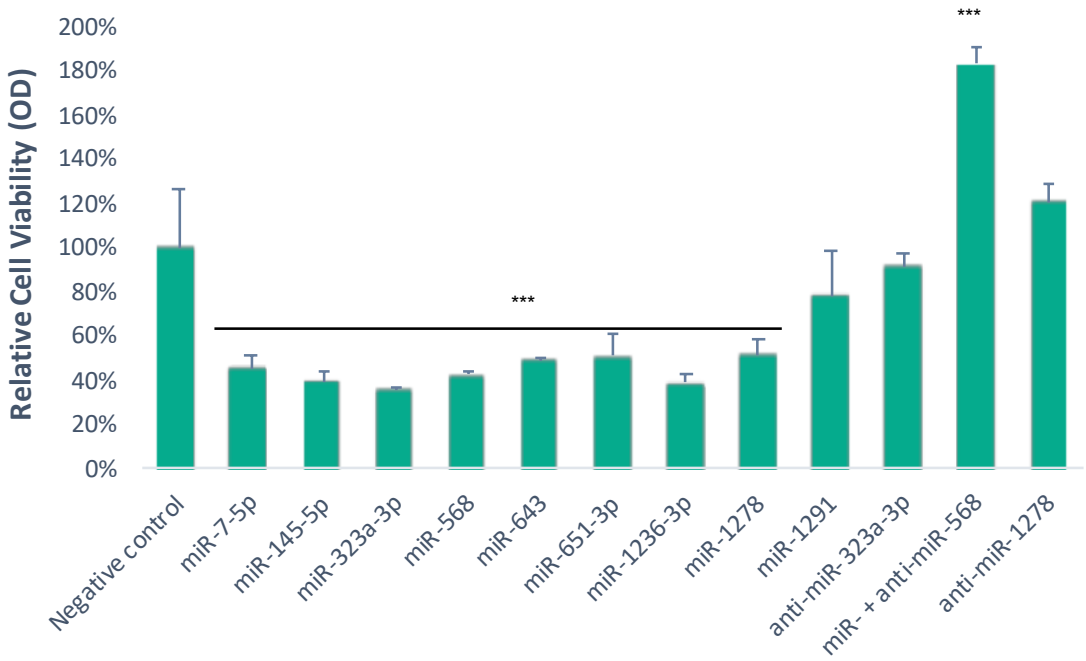

Figure 29: **Effect of miRNAs on cell viability in HepG2 cells.** HepG2 cells were transfected with 30nM miRIDIAN miRNA mimics or hairpin inhibitor miRNA (anti-miR). Cell viability was measured by absorbance 48h after transfection. Results given in mean ± SD (n = 3), where mean is the relative change compared to the miR or anti-miR negative control (set to 100%). ANOVA followed by post-hoc Dunnett's test was performed on miRNA vs. negative control: ***P<0.001.

4.5 Clinical significance of miRNAs expression

4.5.1 Survival rates according to high and low expression of the miRNAs

To investigate the clinical significance of the miRNAs that was found to downregulate FV and TFPI protein synthesis, a survival analysis on patients with high or low expression of the miRNAs was performed. In addition, an expression analysis of miRNA in normal liver tissue and tumour tissue was performed. The analysis was done using the online tool Kaplan-Meier Plotter on liver cancer data from the TCGA database.

The miRNAs effect on median overall survival (OS) in high expression cohorts could be divided into two groups, tumour suppressor and oncogene activity. Patients with high expression of miRNAs; miR-7-5p and miR-323a-3p, had a ~50% shorter median survival time than the low expression cohorts (Table 11 and Figure 30A-B). In contrast, high expression of miRNAs, miR-568, -643, 651-3p, -1236-3p and -1278, were associated with a 2-fold longer survival time (Table 11 and Figure 30C-G).

Comparison of miRNA expression in tumour and normal tissue was only found for miR-7-5p, -323a-3p, -643 and -651-3p. Common for all the miRNAs was that the median expression in tumour was lower than in normal liver tissue, though the difference was only significant (at 10% level) and visible for miR-7-5p and -323a-3p.

Table 11: **Clinical analysis** of overall survival in high and low miRNA expression cohorts in HCC patients and median expression of miRNAs in normal and tumour tissue. Derived from TCGA data using the KMPlotter web-tool.

miRNA	Median survival Low expression (months)	Median survival High expression (months)	P-value High- vs. Low expression	Median expression Normal tissue	Median expression Tumour	P-value Normal vs. Tumour
miR-7-5p	71.03	36.27	0.002	17	13	0.09
miR-323a-3p	108.6	52	0.079	4	1	0.0002
miR-568	27.57	82.87	<0.0001	-	-	-
miR-643	46.2	84.4	0.0041	0	0	0.04
miR-651-3p	42.37	71.03	0.076	4	2	0.45
miR-1236-3p	27.57	82.87	<0.001	-	-	-
miR-1278	25.67	82.87	<0.001	-	-	-

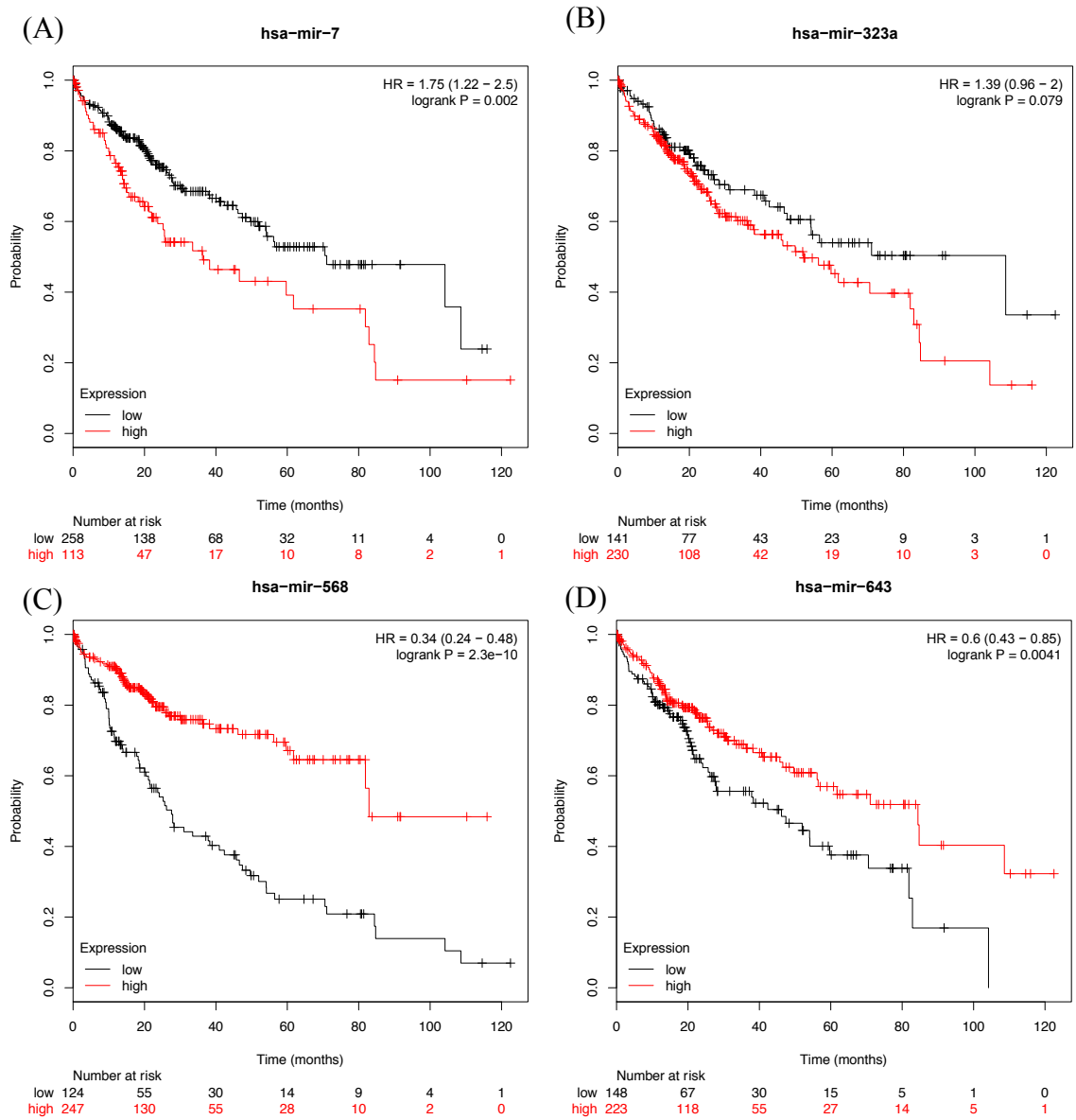
(A)
hsa−mir−7
HR = 1.75 (1.22 − 2.5)
logrank P = 0.002
Probability
Expression
low
high
Time (months)
Number at risk
low 258 138 68 32 11 4 0
high 113 47 17 10 8 2 1
(B)
hsa−mir−323a
HR = 1.39 (0.96 − 2)
logrank P = 0.079
Probability
Expression
low
high
Time (months)
Number at risk
low 141 77 43 23 9 3 1
high 230 108 42 19 10 3 0
(C)
hsa−mir−568
HR = 0.34 (0.24 − 0.48)
logrank P = 2.3e−10
Probability
Expression
low
high
Time (months)
Number at risk
low 124 55 30 14 9 4 1
high 247 130 55 28 10 2 0
(D)
hsa−mir−643
HR = 0.6 (0.43 − 0.85)
logrank P = 0.0041
Probability
Expression
low
high
Time (months)
Number at risk
low 148 67 30 15 5 1 0
high 223 118 55 27 14 5 1

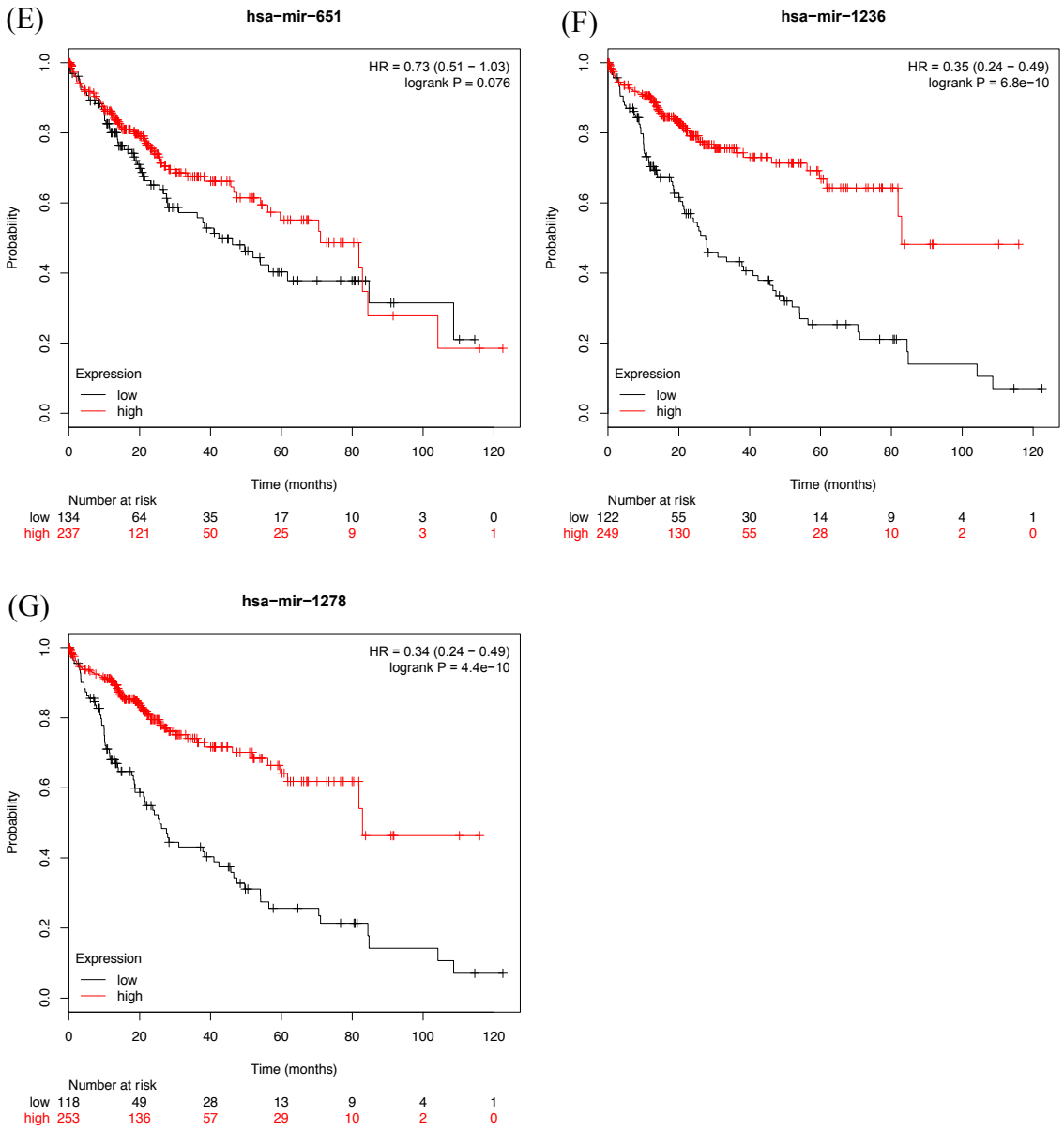

Figure 30: **Kaplan-Meier survival curves presenting overall survival rates in HCC patients with high and low expression levels of miRNAs**: (A) miR-7, (B) miR-323a-3p, (C) miR-568, (D) miR-643, (E) miR-651, (F) miR-1236, (G) miR-1278. Created with the web-tool Kaplan-Meier Plotter (©KMPlotter.com).

5 Discussion

As discussed in the introduction to this thesis, the connection between cancer and increased risk of thrombosis is well established. Thrombosis is the second leading cause of death after the cancer itself (Khalil *et al.*, 2015). Cancer progression has been linked with deregulation of coagulation factors (Falanga *et al.*, 2009). Indeed, tumour cells have been reported to directly activate the haemostatic system by producing procoagulants and microparticles (Falanga *et al.*, 2009). Thus, studying the regulation of coagulation factors associated with cancer may provide important insights. This can in turn contribute to the discovery of new individualized treatments for patients with cancer and cancer related thrombosis.

MiRNAs are post-transcriptional gene regulators, responsible for the regulation of hundreds of genes involved in physiological processes within the cell. Their dysregulation has been linked to both cancer progression and thrombosis (Catalanotto *et al.*, 2016). This motivated the topic of this thesis: The regulation of coagulation *F5* and *TFPI* by miRNAs in liver cancer cells. FV and TFPI are both important factors within the coagulation cascade and have been linked to cancer (HCC) progression. However, their specific roles in liver cancer have yet to be determined. FV has been found expressed in different tumour tissues such as colon- and breast cancer (Tinholt *et al.*, 2018; Wojtukiewicz *et al.*, 1989). Furthermore, high *F5* expression in breast cancer was associated with aggressive types of breast cancer, but also with favourable outcome for patients (Tinholt *et al.*, 2018).

Expression data derived from TCGA showed that both *F5* and *TFPI* were upregulated in liver cancer. High *F5* expression was also associated with increased median overall survival, while high *TFPI* expression also showed favourable outcome, although not significant, in liver cancer (see introduction sections 1.1.6.3 and 1.1.9).

Only a few miRNAs regulating some of the coagulation factors have been identified and the gap in knowledge of miRNAs involved in thrombosis is still large. No research into miRNA regulation of FV has yet been published and further research into regulation of TFPI is still needed. This thesis aims to fill a part of this gap by identifying novel miRNA regulators of FV and TFPI.

5.1 In Silico miRNA target prediction

The *in silico* results were the starting point of this thesis. Using a combination of five miRNA target prediction algorithms, twelve miRNAs were selected as candidate miRNAs to be validated *in vitro*. All twelve miRNAs were predicted to target the *F5* 3'UTR sequence, while eight of the miRNAs were additionally predicted to target the *TFPI* 3'UTR sequence.

Bearing in mind that approximately 70% of all *in silico* predictions by individual algorithms are thought to be false positives (Baek *et al.*, 2008; Tay *et al.*, 2018), we sought to reduce this percentage by applying a combination of miRNA target prediction algorithms. Next, from the list of predicted miRNAs, the final candidate miRNAs were selected based on several additional criteria. The candidate miRNAs were then validated three times, targeting of the 3'UTR, mRNA and protein level.

For *F5,* this strategy to select miRNA candidates worked better than expected. For miRNAs predicted to target *F5* 3'UTR; 83% were confirmed to target the 3'UTR, while 66% of the twelve were able to regulate endogen *F5* mRNA expression and finally 50% were confirmed as true regulators of *F5* expression by reducing the FV protein level, which was a strong indication that these miRNAs may be true positive predictions. Thus, for miRNAs predicted to regulate *F5* our strategy may have reduced the percentage of false positive predictions from 70% to 50%.

Of the miRNAs predicted to target *TFPI* 3'UTR, 75% were able to downregulate endogen *TFPI* mRNA expression, however, none of the initial miRNAs were able to regulate TFPI at protein level. Hence, for TFPI the percentage of false positives increased to 100%. There are several possible explanations for this result: Only the miRNAs that could target the *F5* 3'UTR were verified at mRNA and protein level for TFPI, this left one miRNA predicted to bind to TFPI out of the analysis. Furthermore, on protein level we only analysed protein level of TFPIα and some of the miRNAs were predicted as regulators of TFPIβ. Thus, further analysis is still needed to verify the miRNAs predicted to target TFPIα and TFPIβ.

In summary, this *in silico* method of finding miRNAs able to regulate our genes of interest (*F5* and *TFPI)* served as a good preliminary screen to narrow down the pool of possible candidates. Since we find that the percentage of false positives remains high, our findings

show that the predictions need to be validated *in vitro* before concluding on the regulatory ability of predicted miRNAs.

5.2 In Vitro *target validation of miRNAs for* F5 *and* TFPI

This thesis is the first to identify miRNAs that target and downregulate *F5* in liver cancer, in addition to presenting a novel miRNA which downregulates *TFPIα*. None of these miRNAs have previously been connected to haemostatic factors, and only some of the miRNAs have been reported in liver cancer. In this section the general results and their limitations are discussed, while the miRNAs confirmed to regulate at the protein level will be discussed in the following section.

In this thesis, three to four verification steps were taken to identify the final miRNAs with regulatory ability. The three steps were: (1) miRNA targeting of *F5* 3'UTR mRNA, (2) downregulation by miRNA of *F5* or *TFPI* mRNA expression, (3) downregulation by miRNAs of FV or TFPI protein synthesis, and (4) specificity of some of the miRNAs for FV and TFPI by use of miRNA inhibitors.

5.2.1 3'UTR

In the first verification step, the targeting ability of each miRNA were tested. We confirmed that ten out of the twelve candidate miRNAs directly targeted the 3'UTR of *F5*. Two additional miRNAs, previously studied in our group, were also confirmed to target *F5* 3'UTR. In total, we confirmed that twelve miRNAs could directly target *F5* 3'UTR.

Verification of miRNAs targeting ability of the 3'UTR was performed using a dual luciferase reporter system. The system provided a simple and efficient method to observe the binding/targeting ability for the selected miRNAs. It is simple in the way that if the miRNAs bind to the 3'UTR of the target gene, in our case *F5*, then the amount of firefly luciferase protein synthesised by the cell is reduced. This output is then related to the renilla luciferase which is unaffected by the miRNAs and each sample can then be directly compared to each other. It is efficient because there is very little post-harvest treatment; substrate is added directly to the harvested cells in the wells and measured.

The predicted binding sites for the miRNAs have not been validated in this thesis and may be of interest for further studies. These may be validated by removing the predicted binding site with the 3'UTR in the reporter plasmid.

5.2.2 mRNA

In the second verification step, we confirmed the ability of the miRNAs to regulate *F5* and *TFPI* mRNA expression in HepG2 cells. We found that *F5*- and *TFPI* mRNA expression were down- or upregulated by ten miRNAs, with seven of the miRNAs regulating both genes.

These were very promising findings, however, analysis on the selected endogen control gene PMM1 revealed that some of the miRNAs affected its expression. In fact, miR-532-5p downregulated *PMM1* expression, this resulted in a higher Ct value due for the endogen control. Calculating the relative *F5* and *TFPI* expression based on the increased Ct value as reference compared to the negative control which did not affect the endogen control, resulted in the high expression of *F5* and *TFPI* mRNA reported. Conversely, miR-145-5p upregulated *PMM1*, thereby decreasing the Ct value, which resulted in falsely reporting that miR-145-5p downregulates *F5* and *TFPI* mRNA. These results highlight the importance of selecting the correct endogen control beforehand. However, because miRNAs affect several different mRNAs each, finding one common endogen control that is not targeted by at least one of the twelve miRNAs is very difficult. In fact, all three controls tested were regulated by at least one of the miRNAs. Ideally, each miRNA should have been tested with its own endogen control. This test was not preformed early enough to affect the results presented in this thesis, but it might be a good strategy for future experiments to reduce false positive rates.

Luckily eight of the miRNAs did not have a regulatory effect on PMM1 and could therefore be considered as true positive results. However, downregulation of mRNA alone does not affect the cell significantly, and therefore the third verification step was needed; verification of regulatory effect of the miRNAs on FV- and TFPI protein level.

5.2.3 Protein

In the third validation step, the miRNAs effect on FV and TFPI protein expression were analysed. In total, six miRNAs were confirmed to downregulate FV protein expression,

while only one miRNA, miR-7-5p, downregulated TFPIα protein expression in HepG2 cells. Even though mRNA analysis was promising, none of these last included miRNAs were found to regulate both genes at the protein level. Thus, we were not able to identify miRNAs co-regulating both TFPI and mRNA.

Because we measured TFPI protein level in the medium, only TFPIα was measured at protein level as TFPIβ would have been attached to the cell surface and not present in the medium. Several of the miRNAs were predicted to also target TFPIβ, this effect is of interest to measure in future studies and may reveal miRNAs that co-regulate both genes.

When we increased the incubation time after transfection of miRNAs into HepG2 cells from 24h to 48h, the results were clearer on mRNA level, which indicated that the miRNA need time to affect the mRNA level within a cell. Thus, it may be of interest to analyse the effect of incubating the cells for 72h and see if this increases their effect on protein level.

Our results show that validating target specificity at 3'UTR or mRNA level does not actually reveal their true effect on these genes when expressed endogenously. Hence, validating miRNAs regulatory ability at protein level is crucial.

5.3 Functional effect of the validated miRNAs on F5 and TFPI

5.3.1 miR-7-5p is a novel regulator of TFPIα in HCC

In this study, the prediction algorithms miRAW, miRSearch, Diana-microT-CDS and miRDB predicted that miR-7-5p could target the 3'UTR of *TFPI*. It was confirmed that miR-7-5p inhibits endogenous *TFPIα* expression at both the mRNA and protein levels in HCC, while the direct targeting ability to 3'UTR has yet to be confirmed. Moreover, overexpression of miR-7-5p promoted apoptosis and inhibited proliferation in HepG2 cells.

Interestingly, endogenous expression of miR-7-5p was lower in liver tumours compared to healthy liver cells, which is in contrast to the high expression of *TFPI* in HCC. This finding further supports the assertion that miR-7-5p downregulates the expression of TFPI. In line with our findings, Ma *et al.* (2013) reported miR-7-5p to be downregulated in HCC cells and that its overexpression suppressed hepatoma cell viability and proliferation.

Although TFPIα has previously been given a tumour suppressor role in other types of malignancy, such as breast cancer (Stavik *et al.*, 2010), high expression of TFPI did not change overall survival of HCC patients significantly. In addition, expression of TFPI in liver and kidney cancer was upregulated which contrasts with other malignancies were TFPI was downregulated. Indeed, the upregulation of TFPI observed liver cancer may suggest a different role in regard to cancer development. Nevertheless, survival analysis of low miR-7-5p was in concert with the previously proposed tumour suppressor role of TFPI; low miR-7-5p expression was associated with higher survival rates compared to high expression.

MiR-7-5p has previously been reported as a tumour suppressor in HCC. Fang *et al.* (2012) was first to show that overexpression of miR-7-5p had a tumour suppressor effect in HCC both *in vivo* and *in vitro*, by inhibiting growth and metastasis by targeting the phosphoinositide 3-Kinase/Akt Pathway (PIK3CD). Ma *et al.* (2013) found that miR-7-5p upregulated Cullin 5 (*CUL5*) expression, which inhibited G1/S transition in the cell cycle. Similarly, Zhang *et al.* (2014) reported that miR-7-5p targeted the oncogene *CCNE1* expression, causing cell cycle arrest at G1. Moreover, Wang, F. R. *et al.* (2016) showed that overexpression of miR-7-5p reduced the migration and invasiveness of two HCC cell lines.

Overexpression of TFPIα has been shown to alter the expression of several mRNA and miRNA, and cause alterations in the EGFR pathway in breast cancer cells (Stavik *et al.*, 2012). The EGFR pathway is located upstream of the PIK3CD pathway, thus downregulation of TFPIα by miR-7-5p may have caused some of the tumour suppressor effect reported by Fang *et al.* (2012).

In summary, this thesis demonstrates that TFPIα is targeted by miR-7-5p, thus providing further evidence for miRNA-mediated suppression of *TFPIα* mRNA and protein levels. Overall, the evidence provided indicated a strong tumour suppressor role of miR-7-5p in HCC cells through, at least in part, the suppression of TFPIα.

5.3.2 miR-323a-3p is a regulator of *F5* expression in HCC

In this study, the prediction algorithms TargetScan and miRAW predicted that miR-323a-3p could target the 3'UTR of *F5*. The luciferase reporter system was first used to confirm

that miR-323a-3p directly targets the 3'UTR of *F5*. Next, we confirmed that miR-323a-3p inhibits endogenous *F5* expression at both the mRNA and protein levels. Furthermore, overexpression of miR-323a-3p promoted apoptosis and reduced proliferation, while inhibition of the miRNA removed its effect in HepG2 cells. When *F5* was knocked down, the apoptosis in HepG2 cells was also increased (McCoig, 2018(unpublished)).

Interestingly, miR-323a-3p was downregulated in HCC cells compared to normal liver tissue, while *F5* has been shown to be upregulated in liver tumours. Indeed, low miR-323a-3p expression cohorts were associated with good prognosis compared to high expression. Consistent with this finding, high *F5* expression was associated with increased overall survival in liver cancer patients. Thus, reduced miR-323a-3p in tumour may, at least partially, explain the high *F5* observed in tumours and *F5's* positive effect on survival in liver cancer, because, at low levels miR-323a-3p cannot downregulate the *F5* expression.

Although no literature on liver cancer was attainable, there were some articles of miR-323a-3p in other cancers. Li, J. F. *et al.* (2017) found that miR-323a-3p had a tumour suppressor function in bladder cancer by targeting MET and SMAD3. Their downregulation repressed epithelial-mesenchymal transition (EMT) progression. Chen *et al.* (2018) reported that overexpression of miR-323a-3p suppressed glycolysis and inhibited tumour growth by targeting lactate dehydrogenase in Osteosarcoma cell lines. Indeed, miR-323a-3p was downregulated in both Osteosarcoma cells and cell lines, further indicating a tumour suppressor role (Chen *et al.*, 2018).

In summary, the clinical analysis of high miR-323a-3p expression and poorer survival in liver cancer suggests an oncogene function, as its upregulation would have downregulated *F5*. However, as previous *in vitro* analysis of *F5*, performed in our group, indicated an oncogene functional role in liver cancer (unpublished data), the *in vitro* functional analysis in this study suggests that miR-323a-3p has a tumour suppressor role in HCC by targeting and downregulating *F5* expression. Thus, the functional role in HCC of both miR-323a-3p and *F5* is still in need of further studies.

5.3.3 miR-568 is a regulator of *F5* expression in HCC

In this study, the prediction algorithms TargetScan, miRAW, miRSearch and miRDB predicted that miR-568 could target the 3'UTR of *F5*. The luciferase reporter system was

first used to confirm that miR-568 directly targets the 3'UTR of *F5*. Next, we confirmed that miR-568 inhibits endogen *F5* expression at both the mRNA and protein levels, while inhibition of miR-568 removed its effect on *F5* expression in HepG2 cells. Interestingly, overexpression of miR-568 impeded cell proliferation, while inhibition promoted proliferation drastically. This functional effect may be a strong indication of miR-568's possible involvement in mechanisms associated with cell proliferation in HCC. Apoptosis was not affected by either treatment, indicating that miR-568 is not involved in regulation of apoptotic events.

Expression data of miR-568 in liver tumours was not yet attainable but would be interesting to analyse. If the expression is downregulated in tumour vs. normal liver tissue, it would support the notion of tumour suppressor role in inhibiting proliferation. Indeed, overall survival analysis did support a tumour suppressor role as patients with high miR-568 expression had a 2-fold higher overall survival compared to patients with low expression. How this corresponds with *F5* regulation in HCC is harder to elucidate. Knockdown of *F5* expression in the liver cancer cell lines HepG2 and Huh7 reduced migration and induced apoptosis (McCoig, 2018(unpublished)), hence, miR-568 regulation of *F5* expression fits well with the former but not with the latter. Additionally, high *F5* expression is associated with good prognosis in liver cancer, which does not conform with the low survival rate associated with low miR-568 expression.

A tumour suppressor role was also suggested by Li, W. *et al.* (2014), who found that miR-568 inhibited metastasis in breast cancer cells and inhibited the activation and function of CD4(+) T-cell and T-regulatory cells by targeting and downregulating Nuclear factor of Activated T-cells 5 (*NFAT5*) mRNA expression.

In summary, our findings indicated that miR-568 is a strong tumour suppressor, by inhibiting proliferation through, at least in part, its targeting and downregulation of *F5* expression in liver cancer.

5.3.4 miR-643 is a regulator of *F5* expression in HCC

In this study, the prediction algorithms TargetScan, miRAW, miRSearch and miRDB predicted that miR-643 could target the 3'UTR of *F5*. The luciferase reporter system was first used to confirm that miR-643 directly targets the 3'UTR of *F5*. Next, we confirmed

that miR-643 inhibits endogen *F5* expression at both the mRNA and protein levels in HepG2 cells. Furthermore, overexpression of miR-643 significantly impaired cell proliferation, but had no effect on apoptosis. Inhibition of miR-643 was not tested in this thesis. However, it would be interesting to study how inhibition would change proliferation and to further verify the specificity of the miRNA. This could further elucidate the miRNAs regulatory ability and functional effects. Downregulation of *F5* may explain some of the reduced proliferation observed, as knock-down of *F5* expression promoted apoptosis and inhibited migration in HepG2 cells (McCoig, 2018(unpublished)). Clinical analysis revealed that low miR-643 expression was associated with poor prognosis which contrasts with the positive prognosis associated with high *F5* expression in liver cancer. Thus, miR-643's regulation of *F5* expression cannot explain the genes effect on survival.

Articles on miR-643 role in liver cancer was not attainable, however, there were two studies of the miRNA's role in osteosarcoma and GEM cells. Wang *et al.* (2017) found that overexpression impaired the growth and invasiveness of osteosarcoma cell lines by targeting Zinc finger E-box-binding homeobox 1 (ZEB1). miR-643 was downregulated in osteosarcoma cells and cell lines, and they concluded that this downregulation might be a mechanism underlying the development of osteosarcoma (Wang *et al.*, 2017). Shen *et al.* (2015) reported that by targeting HMGB1 and SRSF2 miR-643 may be promoting the Gemcitabine resistance occurring in SW1990 cell lines after gemcitabine treatment.

In summary, miR-643 may have a tumour suppressor role in liver cancer, at least in part, by direct regulation *F5* expression. Although this notion is not supported by the clinical results for high *F5* expression which indicated a tumour suppressor role for *F5*, it does conform with the functional effect of downregulation of *F5* observed *in vitro*.

5.3.5 miR-651-3p is a regulator of *F5* expression in HCC

In this study, the prediction algorithms TargetScan and miRAW predicted that miR-651-3p could target the 3'UTR of *F5*. The luciferase reporter system was first used to confirm that miR-651-3p directly targets the 3'UTR of *F5*. Next, we confirmed that miR-651-3p inhibits endogen *F5* expression at both the mRNA and protein levels in HepG2 cells. Moreover, overexpression of miR-651-3p impeded proliferation but did not affect apoptosis in liver cancer.

Interestingly, miR-651-3p was found to be downregulated in liver cancer cells compared to healthy liver tissue, even though this was not significant it may still imply that expression of the miRNA is unfavourable for tumorigenesis. Additionally, low miR-651-3p expression was associated with poor prognosis. The high *F5* expression observed in liver cancer correlates well with low miR-651-3p expression, supporting our findings that miR-651-3p is a novel regulator of *F5*. However, the overall survival rates associated with low miRNA and high *F5* do not correspond since high *F5* expression is associated with good prognosis compared to low expression in patients with liver cancer. Thus, regulation of *F5* expression in HepG2 by miR-651-3p cannot yet explain the effect of *F5* observed in liver cancer on survival.

This thesis demonstrates the first regulatory mechanism by miR-651-3p. The sole article mentioning miR-651-3p in general is (Pu *et al.*, 2013). They found only a single nucleotide polymorphism (SNP) prevalent in non-small cell lung cancer cells that created a functional binding site for miR-651-3p. This was in the Fas cell surface death receptor (*FAS*) gene. However, they have yet to publish functional proof (Pu *et al.*, 2013).

In summary, overexpression of miR-651-3p inhibited growth of HepG2 cells, high miR-651-3p expression was associated with good prognosis in patients with HCC and endogen miR-651-3p expression in liver cancer was reduced compared to normal cells. Together, these findings indicate that miR-651-3p has a tumour suppressor role in HCC.

5.3.6 miR-1236-3p is a regulator of *F5* expression in HCC

In this study, the prediction algorithms TargetScan, MiRSearch and miRDB predicted that miR-1236-3p could target the 3'UTR of *F5*. The luciferase reporter system was first used to confirm that miR-1236-3p directly targets the 3'UTR of *F5*. Next, we confirmed that miR-1236-3p inhibits endogenous *F5* expression at both the mRNA and protein levels. Furthermore, overexpression of miR-1236-3p inhibited growth and induced apoptosis in HCC. McCoig (2018) (unpublished) showed that knockdown of *F5* expression in liver cancer cell lines HepG2 and Huh7 also inhibited migration and induced apoptosis. Hence, these functional effects of miR-1236-3p may, at least partially, be caused by the miRNAs ability to downregulate *F5*. The same result of miR-1236-3p on growth and apoptosis was also reported by Gao *et al.* (2015) who, in addition, showed that overexpression of miR-1236-3p suppressed migration and invasion, while inhibition of miR-1236-3p promoted

both. Additionally, they reported that miR-1236-3p was downregulated in both HCC tissue compared to adjacent healthy liver tissue and four cell lines, including HepG2, compared to an immortalized healthy liver cell line (Gao *et al.*, 2015). Hence, low levels of miR-1236-3p in HCC may explain, at least partially, the high *F5* expression observed in HCC.

Clinical analysis showed that low miR-1236-3p expression was associated with poor prognosis compared to that of patients with high expression. However, this does not fit the increased overall survival seen in patients with high *F5* expression. Thus, the effect *F5* has on survival cannot be explained by its regulation by miR-1236-3p and is still in need of study.

In addition to miR-1236-3p effect in HCC (Gao *et al.*, 2015; Li *et al.*, 2018), overexpression of miR-1236-3p inhibited cell proliferation, induced apoptosis and was found to be downregulated in a broad range of other malignancies, such as lung cancer (Bian *et al.*, 2017; Li, C. C. *et al.*, 2017; Wang *et al.*, 2019), glioma (Duan *et al.*, 2018), gastric cancer (An *et al.*, 2018), bladder cancer (Wang *et al.*, 2014; Zhang *et al.*, 2018), and renal cell carcinoma (Wang, C. H. *et al.*, 2016). Furthermore, one mechanism of miR-1236-3p effect has been shown to be induction of p21 activation, thereby inhibiting growth in several malignancies, including bladder cancer (Wang *et al.*, 2014; Zhang *et al.*, 2018), non-small cell lung carcinoma (Li, C. C. *et al.*, 2017), and renal cell carcinoma (Wang, C. H. *et al.*, 2016).

In summary, miR-1236-3p ability to promote apoptosis and inhibit proliferation by, in part, downregulating *F5* expression, is a strong indication of a tumour suppressor role in HCC. The finding that high miR-1236-3p expression is associated with good prognosis, coupled with its low expression levels in HCC (Gao *et al.*, 2015), further supports the tumour suppressor role in HCC.

5.3.7 miR-1278 is a regulator of *F5* expression in HCC

In this study, the prediction algorithm miRAW predicted that miR-1278 could target the 3'UTR of *F5*. The luciferase reporter system was first used to confirm that miR-1278 directly targets the 3'UTR of *F5*. Next, we confirmed that miR-1278 inhibits endogenous *F5* expression at both the mRNA and protein levels, while inhibition of miR-1278 removed its effect on *F5* expression. Moreover, miR-1278 inhibited proliferation in HCC cells, while

its inhibition increased proliferation. Clinical analysis revealed that high miR-1278 expression was associated with good prognosis, which contrasts with the positive prognosis associated with high *F5* expression in liver cancer. Thus, regulation of *F5* expression by miR-1278 cannot explain the survival rates associated with high *F5* in liver cancer patients.

To our knowledge, this thesis is the first to report a regulatory mechanism attributed to miR-1278 since its discovery in 2008 (Morin *et al.*, 2008).

In summary, our *in vitro* analysis of miR-1278 indicated a tumour suppressor role in liver cancer by inhibiting its growth, which may partially be through downregulation of the *F5* expression.

6 Conclusion

This thesis aimed to identify novel miRNAs regulating coagulation FV and TFPI, and to study the miRNAs functional effect on liver cancer progression. Twelve candidate miRNAs were selected using a combination of five miRNA target prediction algorithms. All candidate miRNAs were predicted to target *F5*, while eight of these were predicted to target *TFPIα/β*. In addition, seven miRNAs used in a pilot study by our group were added to the study as potential regulators of *F5* and *TFPIα/β*. The latter miRNAs were also predicted to target both genes before further validation.

To validate the predicted miRNAs as regulators of *F5* or *TFPI* expression, the miRNAs were tested for their ability to target *F5* 3'UTR, regulate endogenous *F5* and *TFPIα/β* mRNA expression, and regulate endogenous FV and TFPIα protein levels in HepG2 cells. As an additional validation step, the specificity of three of the miRNAs on regulation of *F5* and *TFPI* were tested using miRNA inhibitors.

We identified and validated six miRNAs as regulators of *F5* expression in liver cancer: miR-323a-3p, -568, -643, -651-3p, -1236-3p and -1278. These are the first miRNAs found to target *F5*. Additionally, we identified miR-7-5p as a novel regulator of *TFPIα*. These findings provide further evidence for miRNA as regulators of coagulation factors and provide insight into novel mechanisms of the miRNAs. It would also be interesting to study how the miRNAs regulation of FV and TFPI affect the blood coagulation cascade. All six miRNAs regulating *F5* were candidates from the initial *in silico* target prediction step. Thus, prediction of miRNAs to target our genes of interest proved to be both an efficient and successful strategy.

Functional analysis of the miRNAs indicated that all seven had a potential tumour suppressor role in liver cancer. However, how these findings relate to each miRNAs ability to regulate *F5* and *TFPI* is unclear and will need further study. In addition, clinical analysis of miR-568, -643, -651-3p, -1236-3p and -1278 effects on overall survival of patients with HCC were in support of a tumour suppressor role. However, for miR-7-5p and -323a-3p the clinical analysis suggested an oncogene role. Thus, there is a need for further studies into the effect each individual miRNA has on *F5* or *TFPIα* expression in relation to both the procoagulant state induced by HCC cells and liver cancer progression.

7 References

©KMPlotter.com. *Kaplan-Meier Plotter*. Available at: http://kmplot.com/analysis/index.php?p=service&cancer=liver_mirna (accessed: 05.04.2019).

Agarwal, V., Bell, G. W., Nam, J. W. & Bartel, D. P. (2015). Predicting effective microRNA target sites in mammalian mRNAs. *Elife*, 4. doi: 10.7554/eLife.05005.

Alberts, B., Johnson, A., Lewis, J., Morgan, D., Raff, M., Roberts, K. & Walter, P. (2015). *Molecular biology of the cell*. 6th ed. Molecular biology of the cell 771 Third Avenue, New York, NY 10017, US: Garland Science, Tylor & Francis Group, LLC.

Ali, H. O., Arroyo, A. B., Gonzalez-Conejero, R., Stavik, B., Iversen, N., Sandset, P. M., Martinez, C. & Skretting, G. (2016). The role of microRNA-27a/b and microRNA-494 in estrogen-mediated downregulation of tissue factor pathway inhibitor. *Journal of Thrombosis and Haemostasis*, 14 (6): 1226-1237. doi: 10.1111/jth.13321.

Amirkhosravi, A., Meyer, T., Chang, J. Y., Amaya, M., Siddiqui, F., Desai, H. & Francis, J. L. (2002). Tissue factor pathway inhibitor reduces experimental lung metastasis of B16 melanoma. *Thrombosis and Haemostasis*, 87 (6): 930-936.

An, J. X., Ma, M. H., Zhang, C. D., Shao, S., Zhou, N. M. & Dai, D. Q. (2018). miR-1236-3p inhibits invasion and metastasis in gastric cancer by targeting MTA2. *Cancer Cell International*, 18. doi: ARTN 66 10.1186/s12935-018-0560-9.

Arroyo, A. B., Salloum-Asfar, S., Perez-Sanchez, C., Teruel-Montoya, R., Navarro, S., Garcia-Barbera, N., Luengo-Gil, G., Roldan, V., Hansen, J. B., Lopez-Pedrera, C., et al. (2017). Regulation of TFPI alpha expression by miR-27a/b-3p in human endothelial cells under normal conditions and in response to androgens. *Scientific Reports*, 7. doi: ARTN 43500 10.1038/srep43500.

Asselta, R., Tenchini, M. L. & Duga, S. (2006). Inherited defects of coagulation factor V: the hemorrhagic side. *Journal of Thrombosis and Haemostasis*, 4 (1): 26-34. doi: DOI 10.1111/j.1538-7836.2005.01590.x.

Ay, C., Pabinger, I. & Cohen, A. T. (2017). Cancer-associated venous thromboembolism: Burden, mechanisms, and management. *Thromb Haemost*, 117 (2): 219-230. doi: 10.1160/TH16-08-0615.

Baek, D., Villen, J., Shin, C., Camargo, F. D., Gygi, S. P. & Bartel, D. P. (2008). The impact of microRNAs on protein output. *Nature*, 455 (7209): 64-U38. doi: 10.1038/nature07242.

Bartel, D. P. (2009). MicroRNAs: Target Recognition and Regulatory Functions. *Cell*, 136 (2): 215-233. doi: 10.1016/j.cell.2009.01.002.

Baugh, R. J., Broze, G. J. & Krishnaswamy, S. (1998). Regulation of extrinsic pathway factor Xa formation by tissue factor pathway inhibitor. *Journal of Biological Chemistry*, 273 (8): 4378-4386. doi: DOI 10.1074/jbc.273.8.4378.

Bernuau, J., Rueff, B. & Benhamou, J. P. (1986). Fulminant and subfulminant liver failure: definitions and causes. *Semin Liver Dis*, 6 (2): 97-106. doi: 10.1055/s-2008-1040593.

Bian, T. T., Jiang, D. S., Liu, J., Yuan, X. P., Feng, J., Li, Q., Zhang, Q., Li, X. L., Liu, Y. F. & Zhang, J. G. (2017). miR-1236-3p suppresses the migration and

invasion by targeting KLF8 in lung adenocarcinoma A549 cells. *Biochemical and Biophysical Research Communications*, 492 (3): 461-467. doi: 10.1016/j.bbrc.2017.08.074.

Bittar, L. F., Paula, E. V. D., Barnabé, A., Mazetto, B. M., Zapponi, K. C. S., Montalvão, S. A. L., Colella, M. P., Orsi, F. A. & Annichino-Bizzacchi, J. M. (2015). Plasma Factor VIII Levels as a Biomarker for Venous Thromboembolism. In Patel, V. B. & Preedy, V. R. (eds) *Biomarkers in Cardiovascular Disease*, pp. 1-19: Springer, Dordrecht.

Bohnsack, M. T., Czaplinski, K. & Gorlich, D. (2004). Exportin 5 is a RanGTP-dependent dsRNA-binding protein that mediates nuclear export of pre-miRNAs. *Rna-a Publication of the Rna Society*, 10 (2): 185-191. doi: 10.1261/rna.5167604.

Borchert, G. M., Lanier, W. & Davidson, B. L. (2006). RNA polymerase III transcribes human microRNAs. *Nat Struct Mol Biol*, 13 (12): 1097-101. doi: 10.1038/nsmb1167.

Brock, M., Trenkmann, M., Gay, R. E., Gay, S., Speich, R. & Huber, L. C. (2011). MicroRNA-18a Enhances the Interleukin-6-mediated Production of the Acute-phase Proteins Fibrinogen and Haptoglobin in Human Hepatocytes. *Journal of Biological Chemistry*, 286 (46): 40142-40150. doi: 10.1074/jbc.M111.251793.

Broze, G. J. & Miletich, J. P. (1987). Isolation of the Tissue Factor Inhibitor Produced by Hepg2 Hepatoma-Cells. *Proceedings of the National Academy of Sciences of the United States of America*, 84 (7): 1886-1890. doi: DOI 10.1073/pnas.84.7.1886.

Broze, G. J. J. & Girard, T. J. (2013). Tissue Factor Pathway Inhibitor: Structure-Function. *Front Biosci.* (17): 262-280.

Cai, X., Hagedorn, C. H. & Cullen, B. R. (2004). Human microRNAs are processed from capped, polyadenylated transcripts that can also function as mRNAs. *Rna*, 10 (12): 1957-66. doi: 10.1261/rna.7135204.

Catalanotto, C., Cogoni, C. & Zardo, G. (2016). MicroRNA in Control of Gene Expression: An Overview of Nuclear Functions. *Int J Mol Sci*, 17 (10). doi: 10.3390/ijms17101712.

Chang, S. Z., Chen, B. H., Wang, X. Y., Wu, K. Q. & Sun, Y. Q. (2017). Long non-coding RNA XIST regulates PTEN expression by sponging miR-181a and promotes hepatocellular carcinoma progression. *Bmc Cancer*, 17. doi: ARTN 248 10.1186/s12885-017-3216-6.

Chen, H. W., Gao, S. M. & Cheng, C. (2018). MiR-323a-3p suppressed the glycolysis of osteosarcoma via targeting LDHA. *Human Cell*, 31 (4): 300-309. doi: 10.1007/s13577-018-0215-0.

Chendrimada, T. P., Gregory, R. I., Kumaraswamy, E., Norman, J., Cooch, N., Nishikura, K. & Shiekhattar, R. (2005). TRBP recruits the Dicer complex to Ago2 for microRNA processing and gene silencing. *Nature*, 436 (7051): 740-4. doi: 10.1038/nature03868.

Chuang, K. H., Whitney-Miller, C. L., Chu, C. Y., Zhou, Z. R., Dokus, M. K., Schmit, S. & Barry, C. T. (2015). MicroRNA-494 is a master epigenetic regulator of multiple invasion-suppressor microRNAs by targeting ten eleven translocation 1 in invasive human hepatocellular carcinoma tumors. *Hepatology*, 62 (2): 466-480. doi: 10.1002/hep.27816.

Chuang, T. D., Luo, X. P., Panda, H. & Chegini, N. (2012). miR-93/106b and Their Host Gene, MCM7, Are Differentially Expressed in Leiomyomas and

Functionally Target F3 and IL-8. *Molecular Endocrinology*, 26 (6): 1028-1042. doi: 10.1210/me.2012-1075.

Dahlback, B., Vincent, L. M., Tran, S., Bensend, T. A. T., Milewicz, D. M. & Dahlback, B. (2013). Alternatively spliced factor V isoform in the east Texas bleeding disorder inhibits coagulation by binding and increasing tissue factor pathway inhibitor alpha (TFPIa) plasma levels. *Journal of Thrombosis and Haemostasis*, 11: 54-54.

Dahlback, B. (2016). Pro- and anticoagulant properties of factor V in pathogenesis of thrombosis and bleeding disorders. *Int J Lab Hematol*, 38 Suppl 1: 4-11. doi: 10.1111/ijlh.12508.

Davie, E. W. & Ratnoff, O. D. (1964). Waterfall Sequence for Intrinsic Blood Clotting. *Science*, 145 (3638): 1310-2.

Di, Y., Liu, Z. G., Tian, J., Zong, Y. Q., Yang, P. & Qu, S. (2010). TFPI or uPA-PAI-1 complex affect cell function through expression variation of type II very low density lipoprotein receptor. *Febs Letters*, 584 (15): 3469-3473. doi: 10.1016/j.febslet.2010.07.005.

Dong, Z., Qi, R. Z., Guo, X. D., Zhao, X., Li, Y. Y., Zeng, Z., Bai, W. L., Chang, X. J., Hao, L. Y., Chen, Y., et al. (2017). MiR-223 modulates hepatocellular carcinoma cell proliferation through promoting apoptosis via the Rab1-mediated mTOR activation. *Biochemical and Biophysical Research Communications*, 483 (1): 630-637. doi: 10.1016/j.bbrc.2016.12.091.

Donnellan, E. & Khorana, A. A. (2017). Cancer and Venous Thromboembolic Disease: A Review. *Oncologist*, 22 (2): 199-207. doi: 10.1634/theoncologist.2016-0214.

Du, C. L., Lv, Z., Cao, L. P., Ding, C. F., Gyabaah, O. A. K., Xie, H. Y., Zhou, L., Wu, J. & Zheng, S. S. (2014). MiR-126-3p suppresses tumor metastasis and angiogenesis of hepatocellular carcinoma by targeting LRP6 and PIK3R2. *Journal of Translational Medicine*, 12. doi: ARTN 259 10.1186/s12967-014-0259-1.

Duan, X. B., Liu, D. L., Wang, Y. & Chen, Z. Q. (2018). Circular RNA hsa_circ_0074362 Promotes Glioma Cell Proliferation, Migration, and Invasion by Attenuating the Inhibition of miR-1236-3p on HOXB7 Expression. *DNA and Cell Biology*, 37 (11): 917-924. doi: 10.1089/dna.2018.4311.

Duckers, C., Simioni, P., Spiezia, L., Radu, C., Gavasso, S., Rosing, J. & Castoldi, E. (2008). Low plasma levels of tissue factor pathway inhibitor in patients with congenital factor V deficiency. *Blood*, 112 (9): 3615-3623. doi: 10.1182/blood-2008-06-162453.

Elgheznawy, A., Shi, L., Hu, J., Wittig, I., Laban, H., Pircher, J., Mann, A., Provost, P., Randriamboavonjy, V. & Fleming, I. (2015). Dicer Cleavage by Calpain Determines Platelet microRNA Levels and Function in Diabetes. *Circulation Research*, 117 (2): 157-165. doi: 10.1161/Circresaha.117.305784.

Falanga, A., Panova-Noeva, M. & Russo, L. (2009). Procoagulant mechanisms in tumour cells. *Best Pract Res Clin Haematol*, 22 (1): 49-60. doi: 10.1016/j.beha.2008.12.009.

Falanga, A., Marchetti, M. & Vignoli, A. (2013). Coagulation and cancer: biological and clinical aspects. *J Thromb Haemost*, 11 (2): 223-33. doi: 10.1111/jth.12075.

Fang, J. H., Zhou, H. C., Zeng, C. X., Yang, J., Liu, Y. L., Huang, X. Z., Zhang, J. P., Guan, X. Y. & Zhuang, S. M. (2011). MicroRNA-29b Suppresses Tumor Angiogenesis, Invasion, and Metastasis by Regulating Matrix

Metalloproteinase 2 Expression. *Hepatology*, 54 (5): 1729-1740. doi: 10.1002/hep.24577.

Fang, Y., Xue, J. L., Shen, Q., Chen, J. & Tian, L. (2012). MicroRNA-7 inhibits tumor growth and metastasis by targeting the phosphoinositide 3-kinase/Akt pathway in hepatocellular carcinoma. *Hepatology*, 55 (6): 1852-62. doi: 10.1002/hep.25576.

Fort, A., Borel, C., Migliavacca, E., Antonarakis, S. E., Fish, R. J. & Neerman-Arbez, M. (2010). Regulation of fibrinogen production by microRNAs. *Blood*, 116 (14): 2608-2615. doi: 10.1182/blood-2010-02-268011.

Friedman, J. M. & Jones, P. A. (2009). MicroRNAs: critical mediators of differentiation, development and disease. *Swiss Medical Weekly*, 139 (33-34): 466-472.

Fuller, G. M. & Zhang, Z. X. (2001). Transcriptional control mechanism of fibrinogen gene expression. *Fibrinogen*, 936: 469-479.

Gao, R., Cai, C. L., Gan, J. C., Yang, X., Shuang, Z. Y., Liu, M., Li, S. P. & Tang, H. (2015). miR-1236 down-regulates alpha-fetoprotein, thus causing PTEN accumulation, which inhibits the PI3K/Akt pathway and malignant phenotype in hepatoma cells. *Oncotarget*, 6 (8): 6014-6028. doi: DOI 10.18632/oncotarget.3338.

Garcia, D. M., Baek, D., Shin, C., Bell, G. W., Grimson, A. & Bartel, D. P. (2011). Weak seed-pairing stability and high target-site abundance decrease the proficiency of lsy-6 and other microRNAs. *Nature Structural & Molecular Biology*, 18 (10): 1139-U75. doi: 10.1038/nsmb.2115.

Girard, T. J., Tuley, E. & Broze, G. J. (2012). TFPI beta is the GPI-anchored TFPI isoform on human endothelial cells and placental microsomes. *Blood*, 119 (5): 1256-1262. doi: 10.1182/blood-2011-10-388512.

Gregory, R. I., Yan, K. P., Amuthan, G., Chendrimada, T., Doratotaj, B., Cooch, N. & Shiekhattar, R. (2004). The Microprocessor complex mediates the genesis of microRNAs. *Nature*, 432 (7014): 235-40. doi: 10.1038/nature03120.

Gregory, R. I., Chendrimada, T. P., Cooch, N. & Shiekhattar, R. (2005). Human RISC couples microRNA biogenesis and posttranscriptional gene silencing. *Cell*, 123 (4): 631-40. doi: 10.1016/j.cell.2005.10.022.

Griffiths-Jones, S. (2004). The microRNA Registry. *Nucleic Acids Res*, 32 (Database issue): D109-11. doi: 10.1093/nar/gkh023.

Griffiths-Jones, S., Grocock, R. J., van Dongen, S., Bateman, A. & Enright, A. J. (2006). miRBase: microRNA sequences, targets and gene nomenclature. *Nucleic Acids Res*, 34 (Database issue): D140-4. doi: 10.1093/nar/gkj112.

Han, J., Lee, Y., Yeom, K. H., Kim, Y. K., Jin, H. & Kim, V. N. (2004). The Drosha-DGCR8 complex in primary microRNA processing. *Genes Dev*, 18 (24): 3016-27. doi: 10.1101/gad.1262504.

Hembrough, T. A., Swartz, G. M., Papathanassiu, A., Vlasuk, G. P., Rote, W. E., Green, S. J. & Pribluda, V. S. (2003). Tissue factor/factor VIIa inhibitors block angiogenesis and tumor growth through a nonhemostatic mechanism. *Cancer Research*, 63 (11): 2997-3000.

Hembrough, T. A., Ruiz, J. F., Swerdlow, B. M., Swartz, G. M., Hammers, H. J., Zhang, L., Plum, S. M., Williams, M. S., Strickland, D. K. & Pribluda, V. S. (2004). Identification and characterization of a very low density lipoprotein receptor-binding peptide from tissue factor pathway inhibitor that has antitumor and antiangiogenic activity. *Blood*, 103 (9): 3374-3380. doi: 10.1182/blood-2003-07-2234.

Hoffman, M. & Monroe, D. M., 3rd. (2001). A cell-based model of hemostasis. *Thromb Haemost*, 85 (6): 958-65.

Hoffman, M. (2003). A cell-based model of coagulation and the role of factor VIIa. *Blood Rev*, 17 Suppl 1: S1-5.

Holly, J. M. P., Biernacka, K. & Perks, C. M. (2019). Systemic Metabolism, Its Regulators, and Cancer: Past Mistakes and Future Potential. *Front Endocrinol (Lausanne)*, 10: 65. doi: 10.3389/fendo.2019.00065.

Hung, C. L., Yen, C. S., Tsai, H. W., Su, Y. C. & Yen, C. J. (2015). Upregulation of MicroRNA-19b predicts good prognosis in patients with hepatocellular carcinoma presenting with vascular invasion or multifocal disease. *Bmc Cancer*, 15. doi: ARTN 665 10.1186/s12885-015-1671-5.

Haase, A. D., Jaskiewicz, L., Zhang, H., Laine, S., Sack, R., Gatignol, A. & Filipowicz, W. (2005). TRBP, a regulator of cellular PKR and HIV-1 virus expression, interacts with Dicer and functions in RNA silencing. *EMBO Rep*, 6 (10): 961-7. doi: 10.1038/sj.embor.7400509.

Imura, S., Yamada, S., Saito, Y., Iwahashi, S., Arakawa, Y., Ikemoto, T., Morine, Y., Utsunomiya, T. & Shimada, M. (2017). miR-223 and Stathmin-1 Expression in Non-tumor Liver Tissue of Patients with Hepatocellular Carcinoma. *Anticancer Research*, 37 (10): 5877-5883. doi: 10.21873/anticanres.12033.

Iversen, N., Lindahl, A. K. & Abildgaard, U. (1998). Elevated TFPI in malignant disease: Relation to cancer type and hypercoagulation. *British Journal of Haematology*, 102 (4): 889-895. doi: DOI 10.1046/j.1365-2141.1998.00875.x.

Izumi, S., Langley, P. G., Wendon, J., Ellis, A. J., Pernambuco, R. B., Hughes, R. D. & Williams, R. (1996). Coagulation factor V levels as a prognostic indicator in fulminant hepatic failure. *Hepatology*, 23 (6): 1507-11. doi: 10.1002/hep.510230630.

Ketting, R. F., Fischer, S. E., Bernstein, E., Sijen, T., Hannon, G. J. & Plasterk, R. H. (2001). Dicer functions in RNA interference and in synthesis of small RNA involved in developmental timing in C. elegans. *Genes Dev*, 15 (20): 2654-9. doi: 10.1101/gad.927801.

Khalil, J., Bensaid, B., Elkacemi, H., Afif, M., Bensaid, Y., Kebdani, T. & Benjaafar, N. (2015). Venous thromboembolism in cancer patients: an underestimated major health problem. *World J Surg Oncol*, 13: 204. doi: 10.1186/s12957-015-0592-8.

Khorana, A. A., Francis, C. W., Culakova, E., Kuderer, N. M. & Lyman, G. H. (2007). Thromboembolism is a leading cause of death in cancer patients receiving outpatient chemotherapy. *J Thromb Haemost*, 5 (3): 632-4. doi: 10.1111/j.1538-7836.2007.02374.x.

Khorana, A. A., Francis, C. W., Blumberg, N., Culakova, E., Refaai, M. A. & Lyman, G. H. (2008). Blood transfusions, thrombosis, and mortality in hospitalized patients with cancer. *Arch Intern Med*, 168 (21): 2377-81. doi: 10.1001/archinte.168.21.2377.

Khvorova, A., Reynolds, A. & Jayasena, S. D. (2003). Functional siRNAs and miRNAs exhibit strand bias. *Cell*, 115 (2): 209-16.

Knöbl, P. & Lechner, K. (1998). Acquired factor V inhibitors. *Baillieres Clin Haematol*, 11 (2): 305-18.

Kozomara, A. & Griffiths-Jones, S. (2011). miRBase: integrating microRNA annotation and deep-sequencing data. *Nucleic Acids Res*, 39 (Database issue): D152-7. doi: 10.1093/nar/gkq1027.

Kozomara, A. & Griffiths-Jones, S. (2014). miRBase: annotating high confidence microRNAs using deep sequencing data. *Nucleic Acids Res*, 42 (Database issue): D68-73. doi: 10.1093/nar/gkt1181.

Kuang, S. Q., Hasham, S., Phillips, M. D., Wolf, D., Wan, Y., Thiagarajan, P. & Milewicz, D. M. (2001). Characterization of a novel autosomal dominant bleeding disorder in a large kindred from east Texas. *Blood*, 97 (6): 1549-1554. doi: DOI 10.1182/blood.V97.6.1549.

Kurer, M. A. (2007). Protein and mRNA expression of tissue factor pathway inhibitor-1 (TFPI-1) in breast, pancreatic and colorectal cancer cells. *Molecular Biology Reports*, 34 (4): 221-224. doi: 10.1007/s11033-006-9036-4.

Law, P. T. Y., Ching, A. K. K., Chan, A. W. H., Wong, Q. W. L., Wong, C. K., To, K. F. & Wong, N. (2012). MiR-145 modulates multiple components of the insulin-like growth factor pathway in hepatocellular carcinoma. *Carcinogenesis*, 33 (6): 1134-1141. doi: 10.1093/carcin/bgs130.

Lee, R. C., Feinbaum, R. L. & Ambros, V. (1993). The C. elegans heterochronic gene lin-4 encodes small RNAs with antisense complementarity to lin-14. *Cell*, 75 (5): 843-54.

Lee, Y., Ahn, C., Han, J., Choi, H., Kim, J., Yim, J., Lee, J., Provost, P., Radmark, O., Kim, S., et al. (2003). The nuclear RNase III Drosha initiates microRNA processing. *Nature*, 425 (6956): 415-9. doi: 10.1038/nature01957.

Lee, Y., Kim, M., Han, J., Yeom, K. H., Lee, S., Baek, S. H. & Kim, V. N. (2004). MicroRNA genes are transcribed by RNA polymerase II. *EMBO J*, 23 (20): 4051-60. doi: 10.1038/sj.emboj.7600385.

Lee, Y., Hur, I., Park, S. Y., Kim, Y. K., Suh, M. R. & Kim, V. N. (2006). The role of PACT in the RNA silencing pathway. *EMBO J*, 25 (3): 522-32. doi: 10.1038/sj.emboj.7600942.

Lewis, B. P., Shih, I. H., Jones-Rhoades, M. W., Bartel, D. P. & Burge, C. B. (2003). Prediction of mammalian microRNA targets. *Cell*, 115 (7): 787-798. doi: Doi 10.1016/S0092-8674(03)01018-3.

Lewis, B. P., Burge, C. B. & Bartel, D. P. (2005). Conserved seed pairing, often flanked by adenosines, indicates that thousands of human genes are microRNA targets. *Cell*, 120 (1): 15-20. doi: 10.1016/j.cell.2004.12.035.

Li, B. G., Mao, R., Liu, C. F., Zhang, W. H., Tang, Y. & Guo, Z. (2018). LncRNA FAL1 promotes cell proliferation and migration by acting as a CeRNA of miR-1236 in hepatocellular carcinoma cells. *Life Sciences*, 197: 122-129. doi: 10.1016/j.lfs.2018.02.006.

Li, C. C., Ge, Q. Q., Liu, J. X., Zhang, Q. S., Wang, C. H., Cui, K. & Chen, Z. (2017). Effects of miR-1236-3p and miR-370-5p on activation of p21 in various tumors and its inhibition on the growth of lung cancer cells. *Tumor Biology*, 39 (6). doi: Artn 710824 10.1177/1010428317710824.

Li, J. F., Xu, X., Meng, S., Liang, Z., Wang, X., Xu, M. J., Wang, S., Li, S. Q., Zhu, Y., Xie, B., et al. (2017). MET/SMAD3/SNAIL circuit mediated by miR-323a-3p is involved in regulating epithelial-mesenchymal transition progression in bladder cancer. *Cell Death & Disease*, 8. doi: ARTN e3010 10.1038/cddis.2017.331.

Li, S. F., Chen, H., Ren, J. Y., Geng, Q., Song, J. X., Lee, C. Y., Cao, C. F., Zhang, J. & Xu, N. (2014). MicroRNA-223 inhibits tissue factor expression in vascular

endothelial cells. *Atherosclerosis*, 237 (2): 514-520. doi: 10.1016/j.atherosclerosis.2014.09.033.

Li, W., Kong, L. B., Li, J. T., Guo, Z. Y., Xue, Q., Yang, T., Meng, Y. L., Jin, B. Q., Wen, W. H. & Yang, A. G. (2014). MiR-568 inhibits the activation and function of CD4(+) T cells and T-reg cells by targeting NFAT5. *International Immunology*, 26 (5): 269-281. doi: 10.1093/intimm/dxt065.

Liang, H. P., Kerschen, E. J., Basu, S., Hernandez, I., Zogg, M., Jia, S., Hessner, M. J., Toso, R., Rezaie, A. R., Fernandez, J. A., et al. (2015). Coagulation factor V mediates inhibition of tissue factor signaling by activated protein C in mice. *Blood*, 126 (21): 2415-23. doi: 10.1182/blood-2015-05-644401.

Lim, L., Balakrishnan, A., Huskey, N., Jones, K. D., Jodari, M., Ng, R., Song, G., Riordan, J., Anderton, B., Cheung, S. T., et al. (2014). MicroRNA-494 Within an Oncogenic MicroRNA Megacluster Regulates G(1)/S Transition in Liver Tumorigenesis Through Suppression of Mutated in Colorectal Cancer. *Hepatology*, 59 (1): 202-215. doi: 10.1002/hep.26662.

Lima, L. G. & Monteiro, R. Q. (2013). Activation of blood coagulation in cancer: implications for tumour progression. *Biosci Rep*, 33 (5). doi: 10.1042/BSR20130057.

Lin, C.-C., Lin, C.-W., Tsai, M.-C., Huang, K.-T., Chen, C.-L. & Chen, K.-D. (2016). Authophagy and Coagulation in Liver Cancer and Disorders. In *Autophagy in Current Trends in Cellular Physiology and Pathology*: IntechOpen.

Lindahl, A. K., Sandset, P. M., Abildgaard, U., Andersson, T. R. & Harbitz, T. B. (1989). High Plasma-Levels of Extrinsic Pathway Inhibitor and Low-Levels of Other Coagulation Inhibitors in Advanced Cancer. *Acta Chirurgica Scandinavica*, 155 (8): 389-393.

Lindahl, A. K., Odegaard, O. R., Sandset, P. M. & Harbitz, T. B. (1992). Coagulation Inhibition and Activation in Pancreatic-Cancer - Changes during Progress of Disease. *Cancer*, 70 (8): 2067-2072. doi: Doi 10.1002/1097-0142(19921015)70:8<2067::Aid-Cncr2820700809>3.0.Co;2-A.

Liu, L., Cai, X., Liu, E. Q., Tian, X. & Tian, C. (2017). MicroRNA-18a promotes proliferation and metastasis in hepatocellular carcinoma via targeting KLF4. *Oncotarget*, 8 (40): 68263-68269.

Llovet, J. M., Bru, C. & Bruix, J. (1999). Prognosis of hepatocellular carcinoma: the BCLC staging classification. *Semin Liver Dis*, 19 (3): 329-38. doi: 10.1055/s-2007-1007122.

Llovet, J. M., Zucman-Rossi, J., Pikarsky, E., Sangro, B., Schwartz, M., Sherman, M. & Gores, G. (2016). Hepatocellular carcinoma. *Nat Rev Dis Primers*, 2: 16018. doi: 10.1038/nrdp.2016.18.

Llovet, J. M., Montal, R., Sia, D. & Finn, R. S. (2018). Molecular therapies and precision medicine for hepatocellular carcinoma. *Nat Rev Clin Oncol*, 15 (10): 599-616. doi: 10.1038/s41571-018-0073-4.

Long, D., Lee, R., Williams, P., Chan, C. Y., Ambros, V. & Ding, Y. (2007). Potent effect of target structure on microRNA function. *Nature Structural & Molecular Biology*, 14 (4): 287-294. doi: 10.1038/nsmb1226.

Lu, G., Broze, G. J., Jr. & Krishnaswamy, S. (2004). Formation of factors IXa and Xa by the extrinsic pathway: differential regulation by tissue factor pathway inhibitor and antithrombin III. *J Biol Chem*, 279 (17): 17241-9. doi: 10.1074/jbc.M312827200.

Lund, E., Guttinger, S., Calado, A., Dahlberg, J. E. & Kutay, U. (2004). Nuclear export of microRNA precursors. *Science*, 303 (5654): 95-8. doi: 10.1126/science.1090599.

Lupu, C., Goodwin, C. A., Westmuckett, A. D., Emeis, J. J., Scully, M. F., Kakkar, V. V. & Lupu, F. (1997). Tissue factor pathway inhibitor in endothelial cells colocalizes with glycolipid microdomains/caveolae - Regulatory mechanism(s) of the anticoagulant properties of the endothelium. *Arteriosclerosis Thrombosis and Vascular Biology*, 17 (11): 2964-2974. doi: Doi 10.1161/01.Atv.17.11.2964.

Lupu, C., Hu, X. H. & Lupu, F. (2005). Caveolin-1 enhances tissue factor pathway inhibitor exposure and function on the cell surface. *Journal of Biological Chemistry*, 280 (23): 22308-22317. doi: 10.1074/jbc.M503333200.

Ma, C. Q., Qi, Y., Shao, L. P., Liu, M., Li, X. & Tang, H. (2013). Downregulation of miR-7 Upregulates Cullin 5 (CUL5) to Facilitate G1/S Transition in Human Hepatocellular Carcinoma Cells. *Iubmb Life*, 65 (12): 1026-1034. doi: 10.1002/iub.1231.

Macfarlane, R. G. (1964). An Enzyme Cascade in the Blood Clotting Mechanism, and Its Function as a Biochemical Amplifier. *Nature*, 202: 498-9.

MacRae, I. J., Ma, E., Zhou, M., Robinson, C. V. & Doudna, J. A. (2008). In vitro reconstitution of the human RISC-loading complex. *Proc Natl Acad Sci U S A*, 105 (2): 512-7. doi: 10.1073/pnas.0710869105.

Mann, K. G., Krishnaswamy, S. & Lawson, J. H. (1992). Surface-dependent hemostasis. *Semin Hematol*, 29 (3): 213-26.

Mann, K. G. & Kalafatis, M. (2003). Factor V: a combination of Dr Jekyll and Mr Hyde. *Blood*, 101 (1): 20-30. doi: 10.1182/blood-2002-01-0290.

Marchand, A., Proust, C., Morange, P. E., Lompre, A. M. & Tregouet, D. A. (2012). miR-421 and miR-30c Inhibit SERPINE 1 Gene Expression in Human Endothelial Cells. *Plos One*, 7 (8). doi: ARTN e44532 10.1371/journal.pone.0044532.

Maroney, S. A., Ellery, P. E. & Mast, A. E. (2010). Alternatively spliced isoforms of tissue factor pathway inhibitor. *Thromb Res*, 125 Suppl 1: S52-6. doi: 10.1016/j.thromres.2010.01.038.

Martinelli, I., Bottasso, B., Duca, F., Faioni, E. & Mannucci, P. M. (1996). Heightened thrombin generation in individuals with resistance to activated protein C. *Thromb Haemost*, 75 (5): 703-5.

McCoig, C. (2018). *The functional role of coagulation factor V in liver cancer*. Master thesis: Norwegian University of Life Sciences.

McMichael, M. (2012). New models of hemostasis. *Top Companion Anim Med*, 27 (2): 40-5. doi: 10.1053/j.tcam.2012.07.005.

Meister, G., Landthaler, M., Patkaniowska, A., Dorsett, Y., Teng, G. & Tuschl, T. (2004). Human Argonaute2 mediates RNA cleavage targeted by miRNAs and siRNAs. *Mol Cell*, 15 (2): 185-97. doi: 10.1016/j.molcel.2004.07.007.

Morin, R. D., O'Connor, M. D., Griffith, M., Kuchenbauer, F., Delaney, A., Prabhu, A. L., Zhao, Y., McDonald, H., Zeng, T., Hirst, M., et al. (2008). Application of massively parallel sequencing to microRNA profiling and discovery in human embryonic stem cells. *Genome Research*, 18 (4): 610-621. doi: 10.1101/gr.7179508.

Nagy, A., Lanczky, A., Menyhart, O. & Gyorffy, B. (2018). Validation of miRNA prognostic power in hepatocellular carcinoma using expression data of

independent datasets. *Sci Rep*, 8 (1): 9227. doi: 10.1038/s41598-018-27521-y.

Nesheim, M. E., Taswell, J. B. & Mann, K. G. (1979). The contribution of bovine Factor V and Factor Va to the activity of prothrombinase. *J Biol Chem*, 254 (21): 10952-62.

Nicolaes, G. A. & Dahlback, B. (2002). Factor V and thrombotic disease: description of a janus-faced protein. *Arterioscler Thromb Vasc Biol*, 22 (4): 530-8.

Nishida, N., Arizumi, T., Hagiwara, S., Ida, H., Sakurai, T. & Kudo, M. (2017). MicroRNAs for the Prediction of Early Response to Sorafenib Treatment in human Hepatocellular Carcinoma. *Liver Cancer*, 6 (2): 113-125. doi: 10.1159/000449475.

Okamura, K., Hagen, J. W., Duan, H., Tyler, D. M. & Lai, E. C. (2007). The mirtron pathway generates microRNA-class regulatory RNAs in Drosophila. *Cell*, 130 (1): 89-100. doi: 10.1016/j.cell.2007.06.028.

Otsuka, M., Kishikawa, T., Yoshikawa, T., Yamagami, M., Ohno, M., Takata, A., Shibata, C., Ishibashi, R. & Koike, K. (2017). MicroRNAs and liver disease. *Journal of Human Genetics*, 62 (1): 75-80. doi: 10.1038/jhg.2016.53.

Palta, S., Saroa, R. & Palta, A. (2014). Overview of the coagulation system. *Indian J Anaesth*, 58 (5): 515-23. doi: 10.4103/0019-5049.144643.

Paraskevopoulou, M. D., Georgakilas, G., Kostoulas, N., Vlachos, I. S., Vergoulis, T., Reczko, M., Filippidis, C., Dalamagas, T. & Hatzigeorgiou, A. G. (2013). DIANA-microT web server v5.0: service integration into miRNA functional analysis workflows. *Nucleic Acids Res*, 41 (Web Server issue): W169-73. doi: 10.1093/nar/gkt393.

Patel, N., Tahara, S. M., Malik, P. & Kalra, V. K. (2011). Involvement of miR-30c and miR-301a in immediate induction of plasminogen activator inhibitor-1 by placental growth factor in human pulmonary endothelial cells. *Biochemical Journal*, 434: 473-482. doi: 10.1042/Bj20101585.

Peterson, S. M., Thompson, J. A., Ufkin, M. L., Sathyanarayana, P., Liaw, L. & Congdon, C. B. (2014). Common features of microRNA target prediction tools. *Frontiers in Genetics*, 5. doi: ARTN 23 10.3389/fgene.2014.00023.

Pillai, R. S., Artus, C. G. & Filipowicz, W. (2004). Tethering of human Ago proteins to mRNA mimics the miRNA-mediated repression of protein synthesis. *RNA*, 10 (10): 1518-25. doi: 10.1261/rna.7131604.

Pla, A., Zhong, X. & Rayner, S. (2018). miRAW: A deep learning-based approach to predict microRNA targets by analyzing whole microRNA transcripts. *PLoS Comput Biol*, 14 (7): e1006185. doi: 10.1371/journal.pcbi.1006185.

Prandoni, P., Falanga, A. & Piccioli, A. (2005). Cancer and venous thromboembolism. *Lancet Oncol*, 6 (6): 401-10. doi: 10.1016/S1470-2045(05)70207-2.

Pu, X., Roth, J. A., Hildebrandt, M. A. T., Ye, Y. Q., Wei, H., Minna, J. D., Lippman, S. M. & Wu, X. F. (2013). MicroRNA-Related Genetic Variants Associated with Clinical Outcomes in Early-Stage Non-Small Cell Lung Cancer Patients. *Cancer Research*, 73 (6): 1867-1875. doi: 10.1158/0008-5472.Can-12-0873.

Reczko, M., Maragkakis, M., Alexiou, P., Grosse, I. & Hatzigeorgiou, A. G. (2012). Functional microRNA targets in protein coding sequences. *Bioinformatics*, 28 (6): 771-6. doi: 10.1093/bioinformatics/bts043.

Reinhart, B. J., Slack, F. J., Basson, M., Pasquinelli, A. E., Bettinger, J. C., Rougvie, A. E., Horvitz, H. R. & Ruvkun, G. (2000). The 21-nucleotide let-7 RNA regulates

developmental timing in Caenorhabditis elegans. *Nature*, 403 (6772): 901-6. doi: 10.1038/35002607.

Research, G. H. (2019). *Factor V Leiden thrombophilia*. Available at: https://ghr.nlm.nih.gov/condition/factor-v-leiden-thrombophilia (accessed: 16.04.2019).

Research, W. C. R. F. A. I. f. C. (2018). *Diet, nutrition, physical activity and liver cancer*. Continuous Update Project Expert Report 2018.

Ruby, J. G., Jan, C. H. & Bartel, D. P. (2007). Intronic microRNA precursors that bypass Drosha processing. *Nature*, 448 (7149): 83-6. doi: 10.1038/nature05983.

Sahu, A., Jha, P. K., Prabhakar, A., Singh, H. D., Gupta, N., Chatterjee, T., Tyagi, T., Sharma, S., Kumari, B., Singh, S., et al. (2017). MicroRNA-145 Impedes Thrombus Formation via Targeting Tissue Factor in Venous Thrombosis. *EBioMedicine*, 26: 175-186. doi: 10.1016/j.ebiom.2017.11.022.

Saini, H. K., Griffiths-Jones, S. & Enright, A. J. (2007). Genomic analysis of human microRNA transcripts. *Proc Natl Acad Sci U S A*, 104 (45): 17719-24. doi: 10.1073/pnas.0703890104.

Salgame, P., Varadhachary, A. S., Primiano, L. L., Fincke, J. E., Muller, S. & Monestier, M. (1997). An ELISA for detection of apoptosis. *Nucleic Acids Res*, 25 (3): 680-1.

Salloum-Asfar, S., Teruel-Montoya, R., Arroyo, A. B., Garcia-Barbera, N., Chaudhry, A., Schuetz, E., Luengo-Gil, G., Vicente, V., Gonzalez-Conejero, R. & Martinez, C. (2014). Regulation of Coagulation Factor XI Expression by MicroRNAs in the Human Liver. *Plos One*, 9 (11). doi: ARTN e111713 10.1371/journal.pone.0111713.

Schwarz, D. S., Hutvagner, G., Du, T., Xu, Z., Aronin, N. & Zamore, P. D. (2003). Asymmetry in the assembly of the RNAi enzyme complex. *Cell*, 115 (2): 199-208.

Sennblad, B., Basu, S., Mazur, J., Suchon, P., Martinez-Perez, A., van Hylckama Vlieg, A., Truong, V., Li, Y., Gadin, J. R., Tang, W., et al. (2017). Genome-wide association study with additional genetic and post-transcriptional analyses reveals novel regulators of plasma factor XI levels. *Hum Mol Genet*, 26 (3): 637-649. doi: 10.1093/hmg/ddw401.

Shen, Y. H., Pan, Y., Xu, L. T., Chen, L. Y., Liu, L. M., Chen, H., Chen, Z. & Meng, Z. Q. (2015). Identifying microRNA-mRNA regulatory network in gemcitabine-resistant cells derived from human pancreatic cancer cells. *Tumor Biology*, 36 (6): 4525-4534. doi: 10.1007/s13277-015-3097-8.

Sierko, E., Wojtukiewicz, M. Z., Zimnoch, L. & Kisiel, W. (2010). Expression of tissue factor pathway inhibitor (TFPI) in human breast and colon cancer tissue. *Thrombosis and Haemostasis*, 103 (1): 198-204. doi: 10.1160/Th09-06-0416.

Smith, S. A. (2009). The cell-based model of coagulation. *J Vet Emerg Crit Care (San Antonio)*, 19 (1): 3-10. doi: 10.1111/j.1476-4431.2009.00389.x.

Sorensen, H. T., Mellemkjaer, L., Olsen, J. H. & Baron, J. A. (2000). Prognosis of cancers associated with venous thromboembolism. *N Engl J Med*, 343 (25): 1846-50. doi: 10.1056/NEJM200012213432504.

Stavik, B., Skretting, G., Sletten, M., Sandset, P. M. & Iversen, N. (2010). Stable overexpression and knockdown of TFPI in breast cancer cells suggest antitumor properties of TFPI. *Thrombosis Research*, 125: S187-S187. doi: Doi 10.1016/S0049-3848(10)70129-8.

Stavik, B., Skretting, G., Aasheim, H. C., Tinholt, M., Zernichow, L., Sletten, M., Sandset, P. M. & Iversen, N. (2011). Downregulation of TFPI in breast cancer cells induces tyrosine phosphorylation signaling and increases metastatic growth by stimulating cell motility. *Bmc Cancer*, 11. doi: Artn 357 10.1186/1471-2407-11-357.

Stavik, B., Skretting, G., Olstad, O. K., Sletten, M., Vigeland, M. D., Sandset, P. M. & Iversen, N. (2012). TFPI Alpha and Beta Regulate mRNAs and microRNAs Involved in Cancer Biology and in the Immune System in Breast Cancer Cells. *Plos One*, 7 (10). doi: ARTN e47184 10.1371/journal.pone.0047184.

Stenvang, J., Petri, A., Lindow, M., Obad, S. & Kauppinen, S. (2012). Inhibition of microRNA function by antimiR oligonucleotides. *Silence*, 3 (1): 1. doi: 10.1186/1758-907X-3-1.

Tang, Z., Li, C., Kang, B., Gao, G., Li, C. & Zhang, Z. (2017). GEPIA: a web server for cancer and normal gene expression profiling and interactive analyses. *Nucleic Acids Res*, 45 (W1): W98-W102. doi: 10.1093/nar/gkx247.

Tay, J., Romeo, G., Hughes, Q. & Baker, R. (2013). Downregulation of protein S by oestrogens and miR-494. *Journal of Thrombosis and Haemostasis*, 11: 253-253.

Tay, J., Tiao, J., Hughes, Q., Gilmore, G. & Baker, R. (2016). Therapeutic Potential of miR-494 in Thrombosis and Other Diseases: A Review. *Australian Journal of Chemistry*, 69 (10): 1078-1093. doi: 10.1071/Ch16020.

Tay, J., Tiao, J., Hughes, Q., Jorritsma, J., Gilmore, G. & Baker, R. (2018). Circulating MicroRNA as Thrombosis Sentinels: Caveats and Considerations. *Semin Thromb Hemost*, 44 (3): 206-215. doi: 10.1055/s-0037-1606568.

Teruel, R., Corral, J., Perez-Andreu, V., Martinez-Martinez, I., Vicente, V. & Martinez, C. (2011a). Potential Role of miRNAs in Developmental Haemostasis. *Plos One*, 6 (3). doi: ARTN e17648 10.1371/journal.pone.0017648.

Teruel, R., Perez-Sanchez, C., Corral, J., Herranz, M. T., Perez-Andreu, V., Saiz, E., Garcia-Barbera, N., Martinez-Martinez, I., Roldan, V., Vicente, V., et al. (2011b). Identification of miRNAs as potential modulators of tissue factor expression in patients with systemic lupus erythematosus and antiphospholipid syndrome. *Journal of Thrombosis and Haemostasis*, 9 (10): 1985-1992. doi: 10.1111/j.1538-7836.2011.04451.x.

ThermoFisher-Scientific. *How cationic mediated transfection works* Available at: https://www.thermofisher.com/no/en/home/references/gibco-cell-culture-basics/transfection-basics/gene-delivery-technologies/cationic-lipid-mediated-delivery/how-cationic-lipid-mediated-transfection-works.html (accessed: 14.02.19).

Thorelli, E., Kaufman, R. J. & Dahlback, B. (1999). Cleavage of factor V at Arg 506 by activated protein C and the expression of anticoagulant activity of factor V. *Blood*, 93 (8): 2552-8.

Tinholt, M., Viken, M. K., Dahm, A. E., Vollan, H. K., Sahlberg, K. K., Garred, O., Borresen-Dale, A. L., Jacobsen, A. F., Kristensen, V., Bukholm, I., et al. (2014). Increased coagulation activity and genetic polymorphisms in the F5, F10 and EPCR genes are associated with breast cancer: a case-control study. *BMC Cancer*, 14: 845. doi: 10.1186/1471-2407-14-845.

Tinholt, M., Garred, O., Borgen, E., Beraki, E., Schlichting, E., Kristensen, V., Sahlberg, K. K. & Iversen, N. (2018). Subtype-specific clinical and prognostic relevance of tumor-expressed F5 and regulatory F5 variants in breast

cancer: the CoCaV study. *J Thromb Haemost*, 16 (7): 1347-1356. doi: 10.1111/jth.14151.

VanDeWater, L., Tracy, P. B., Aronson, D., Mann, K. G. & Dvorak, H. F. (1985). Tumor-Cell Generation of Thrombin Via Functional Prothrombinase Assembly. *Cancer Research*, 45 (11): 5521-5525.

Vincent, L. M., Tran, S., Livaja, R., Bensend, T. A., Milewicz, D. M. & Dahlback, B. (2013). Coagulation factor V-A2440G causes east Texas bleeding disorder via TFPI alpha. *Journal of Clinical Investigation*, 123 (9): 3777-3787. doi: 10.1172/Jci69091.

Vossen, C. Y., Hoffmeister, M., Chang-Claude, J. C., Rosendaal, F. R. & Brenner, H. (2011). Clotting Factor Gene Polymorphisms and Colorectal Cancer Risk. *Journal of Clinical Oncology*, 29 (13): 1722-1727. doi: 10.1200/Jco.2010.31.8873.

Wang, C. H., Chen, Z., Ge, Q. Q., Hu, J. H., Li, F., Hu, J., Xu, H., Ye, Z. Q. & Li, L. C. (2014). Up-regulation of p21(WAF1/CIP1) by miRNAs and its implications in bladder cancer cells. *Febs Letters*, 588 (24): 4654-4664. doi: 10.1016/j.febslet.2014.10.037.

Wang, C. H., Tang, K., Li, Z., Chen, Z., Xu, H. & Ye, Z. Q. (2016). Targeted p21(WAF1/CIP1) activation by miR-1236 inhibits cell proliferation and correlates with favorable survival in renal cell carcinoma. *Urologic Oncology-Seminars and Original Investigations*, 34 (2). doi: ARTN 59.e23 10.1016/j.urolonc.2015.08.014.

Wang, F. R., Qiang, Y., Zhu, L. R., Jiang, Y. S., Wang, Y. D., Shao, X., Yin, L., Chen, J. H. & Chen, Z. (2016). MicroRNA-7 downregulates the oncogene VDAC1 to influence hepatocellular carcinoma proliferation and metastasis. *Tumor Biology*, 37 (8): 10235-10246. doi: 10.1007/s13277-016-4836-1.

Wang, H., Xing, D. M., Ren, D., Feng, W., Chen, Y., Zhao, Z. M., Xiao, Z. H. & Peng, Z. R. (2017). MicroRNA-643 regulates the expression of ZEB1 and inhibits tumorigenesis in osteosarcoma. *Molecular Medicine Reports*, 16 (4): 5157-5164. doi: 10.3892/mmr.2017.7273.

Wang, Z. G., Liu, L. M., Guo, X. F., Guo, C. M. & Wang, W. X. (2019). microRNA-1236-3p regulates DDP resistance in lung cancer cells. *Open Medicine*, 14 (1): 41-51. doi: 10.1515/med-2019-0007.

Warn-Cramer, B. J., Rao, L. V. M., Maki, S. L. & Rapaport, S. I. (1988). Modifications of Extrinsic Pathway Inhibitor (Epi) and Factor-Xa That Affect Their Ability to Interact and to Inhibit Factor-Viia Tissue Factor - Evidence for a 2-Step Model of Inhibition. *Thrombosis and Haemostasis*, 60 (3): 453-456.

Wightman, B., Ha, I. & Ruvkun, G. (1993). Posttranscriptional regulation of the heterochronic gene lin-14 by lin-4 mediates temporal pattern formation in C. elegans. *Cell*, 75 (5): 855-62.

Winter, J., Jung, S., Keller, S., Gregory, R. I. & Diederichs, S. (2009). Many roads to maturity: microRNA biogenesis pathways and their regulation. *Nat Cell Biol*, 11 (3): 228-34. doi: 10.1038/ncb0309-228.

Witkowski, M., Weithauser, A., Tabaraie, T., Steffens, D., Krankel, N., Witkowski, M., Stratmann, B., Tschoepe, D., Landmesser, U. & Rauch-Kroehnert, U. (2016). Micro-RNA-126 Reduces the Blood Thrombogenicity in Diabetes Mellitus via Targeting of Tissue Factor. *Arterioscler Thromb Vasc Biol*, 36 (6): 1263-71. doi: 10.1161/ATVBAHA.115.306094.

Wojtukiewicz, M. Z., Zacharski, L. R., Memoli, V. A., Kisiel, W., Kudryk, B. J., Rousseau, S. M. & Stump, D. C. (1989). Indirect Activation of Blood-Coagulation in Colon Cancer. *Thrombosis and Haemostasis*, 62 (4): 1062-1066.

Wong, N. & Wang, X. (2015). miRDB: an online resource for microRNA target prediction and functional annotations. *Nucleic Acids Res*, 43 (Database issue): D146-52. doi: 10.1093/nar/gku1104.

Wood, J. P., Ellery, P. E., Maroney, S. A. & Mast, A. E. (2014). Biology of tissue factor pathway inhibitor. *Blood*, 123 (19): 2934-43. doi: 10.1182/blood-2013-11-512764.

Yi, R., Qin, Y., Macara, I. G. & Cullen, B. R. (2003). Exportin-5 mediates the nuclear export of pre-microRNAs and short hairpin RNAs. *Genes Dev*, 17 (24): 3011-6. doi: 10.1101/gad.1158803.

Yu, G., Li, H., Wang, X., Wu, T., Zhu, J., Huang, S. J., Wan, Y. L. & Tang, J. Q. (2013). MicroRNA-19a targets tissue factor to inhibit colon cancer cells migration and invasion. *Molecular and Cellular Biochemistry*, 380 (1-2): 239-247. doi: 10.1007/s11010-013-1679-6.

Yue, D., Liu, H. & Huang, Y. F. (2009). Survey of Computational Algorithms for MicroRNA Target Prediction. *Current Genomics*, 10 (7): 478-492. doi: Doi 10.2174/138920209789208219.

Zanetto, A., Campello, E., Spiezia, L., Burra, P., Simioni, P. & Russo, F. P. (2018). Cancer-Associated Thrombosis in Cirrhotic Patients with Hepatocellular Carcinoma. *Cancers (Basel)*, 10 (11). doi: 10.3390/cancers10110450.

Zhang, Q. S., Miao, S., Li, C. C., Cui, K., Ge, Q. Q. & Chen, Z. (2018). S-phase kinase-associated protein 2 impairs the inhibitory effects of miR-1236-3p on bladder tumors. *American Journal of Translational Research*, 10 (3): 731-+.

Zhang, X., Hu, S. J., Zhang, X., Wang, L., Zhang, X. F., Yan, B., Zhao, J., Yang, A. G. & Zhang, R. (2014). MicroRNA-7 arrests cell cycle in G1 phase by directly targeting CCNE1 in human hepatocellular carcinoma cells. *Biochemical and Biophysical Research Communications*, 443 (3): 1078-1084. doi: 10.1016/j.bbrc.2013.12.095.

Zhang, X. X., Yu, H. J., Lou, J. R., Zheng, J., Zhu, H., Popescu, N. I., Lupu, F., Lind, S. E. & Ding, W. Q. (2011). MicroRNA-19 (miR-19) Regulates Tissue Factor Expression in Breast Cancer Cells. *Journal of Biological Chemistry*, 286 (2): 1429-1435. doi: 10.1074/jbc.M110.146530.

Zhang, Y. Q., Guo, X. D., Li, Z. W., Li, B. A., Li, Z. Y., Li, R. S., Guo, Q. Y., Xiong, L., Yu, L. X., Zhao, J. M., et al. (2015). A systematic investigation based on microRNA-mediated gene regulatory network reveals that dysregulation of microRNA-19a/Cyclin D1 axis confers an oncogenic potential and a worse prognosis in human hepatocellular carcinoma. *Rna Biology*, 12 (6): 643-657. doi: 10.1080/15476286.2015.1022702.

Zhou, Q., Huang, T., Wang, Y. F., Zhou, X. B., Liang, L. J. & Peng, B. G. (2011). Role of tissue factor in hepatocellular carcinoma genesis, invasion and metastasis. *Chin Med J (Engl)*, 124 (22): 3746-51.

Zoller, B., Holm, J., Svensson, P. & Dahlback, B. (1996). Elevated levels of prothrombin activation fragment 1 + 2 in plasma from patients with heterozygous Arg506 to Gln mutation in the factor V gene (APC-resistance) and/or inherited protein S deficiency. *Thromb Haemost*, 75 (2): 270-4.

Appendix

Appendix A: Test of endogen control genes

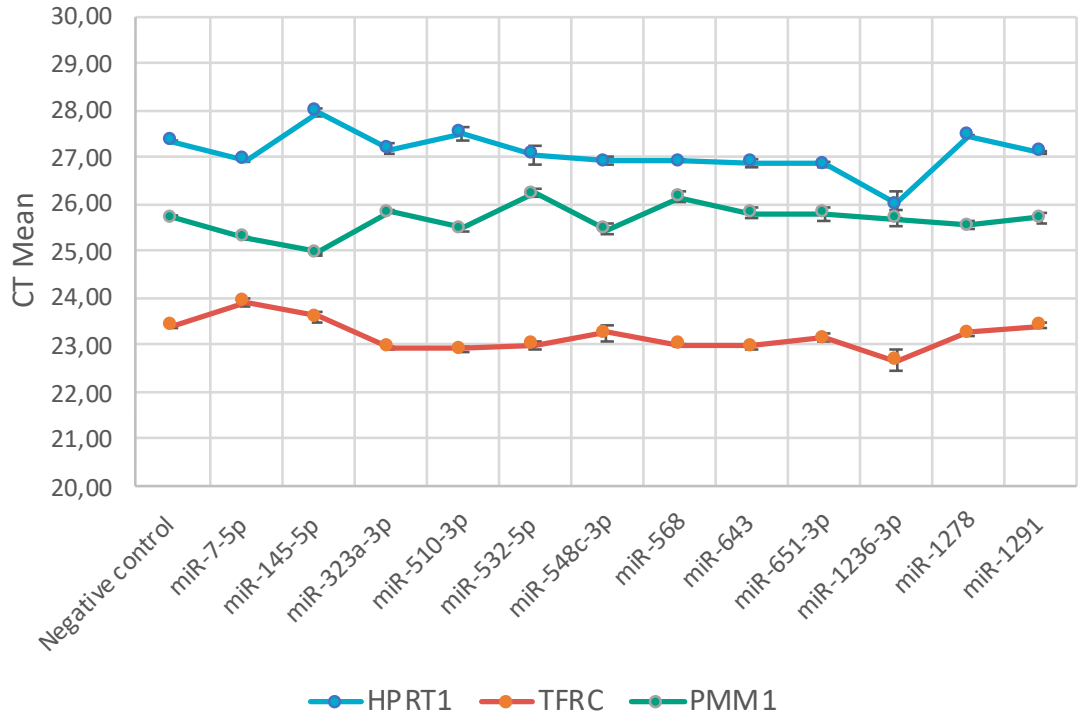

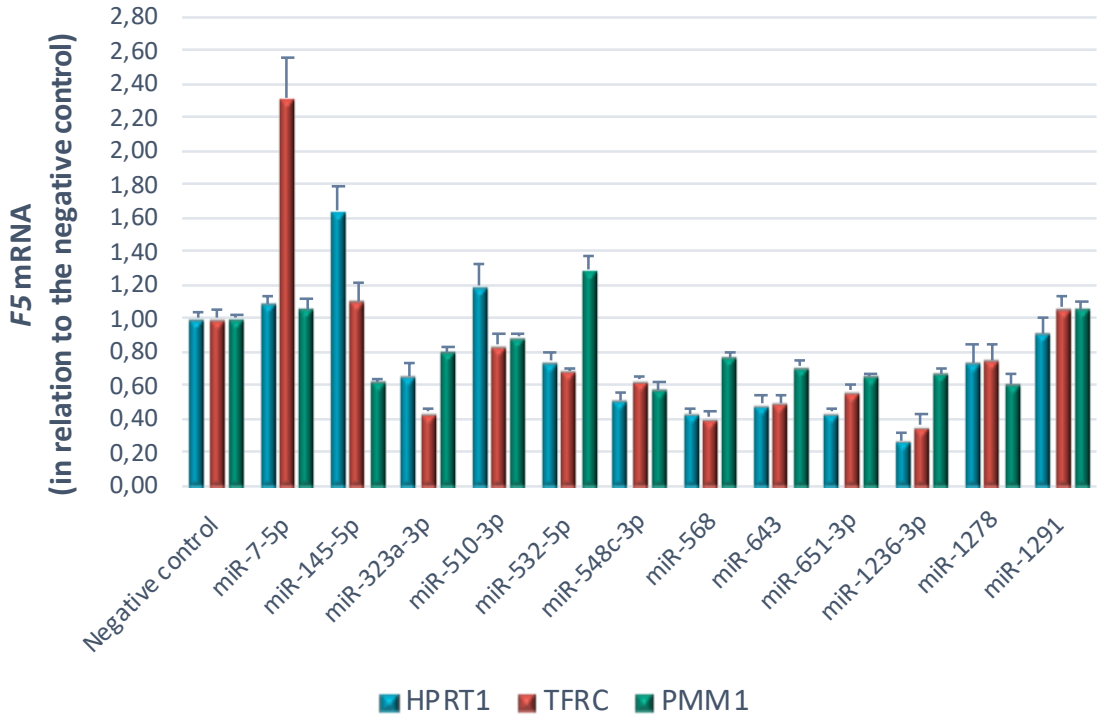

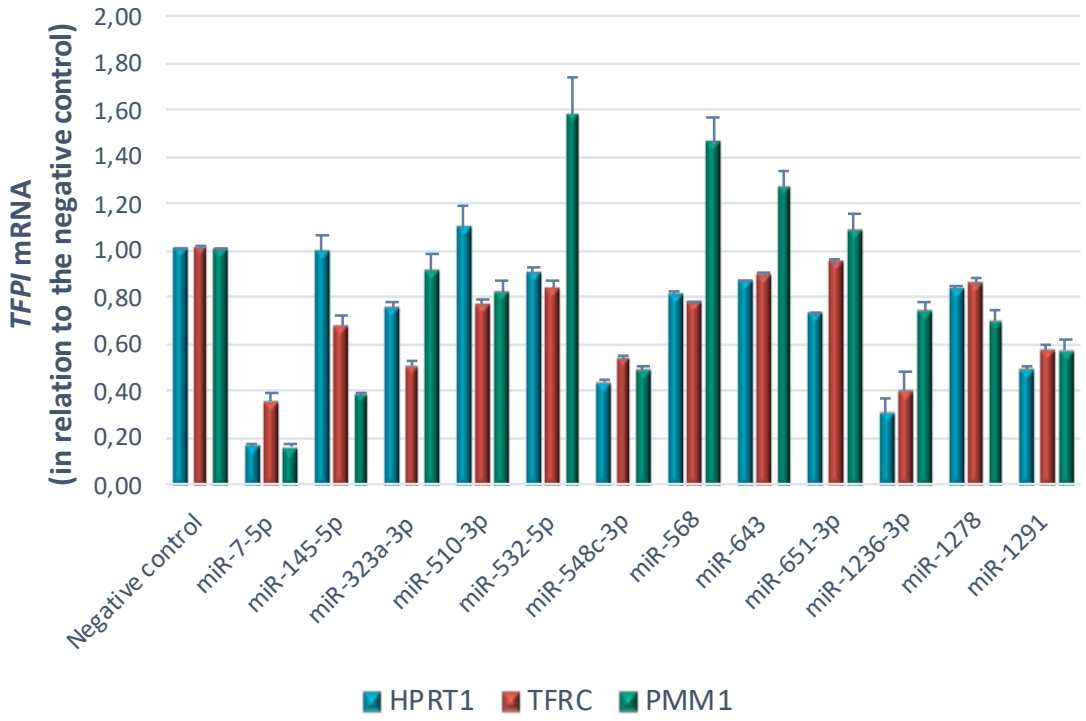
TFPI mRNA
(in relation to the negative control)
2,00
1,80
1,60
1,40
1,20
1,00
0,80
0,60
0,40
0,20
0,00
Negative control
miR-7-5p
miR-145-5p
miR-323a-3p
miR-510-3p
miR-532-5p
miR-548c-3p
miR-568
miR-643
miR-651-3p
miR-1236-3p
miR-1278
miR-1291
HPRT1
TFRC
PMM1

Appendix B: instruments, software, kits, reagents and disposables

Table S1 Instruments and suppliers

Instrument	Supplier
Applied Biosystems™ QuantStudio™ 12K Flex Real-Time System	Thermo Scientific
Forma™ 370 Steri-Cycle™ CO_2 Incubator	Thermo Scientific
NanoDrop® ND-1000	Thermo Scientific
Nikon Eclipse TE 300	Nikon
Nikon Eclipse Ts2-FL	Nikon
NucleoCounter® NC-100™	ChemoMetec A/S
Synergy H1 Microplate Reader	BioTek Instruments, Inc.
Steri-Cycle CO_2 Incubator	Thermo Electron Corporation
Veriti™ 96 well Thermal Cycler	Applied Biosystems
VersaMax™ Microplate Reader	Molecular Devices
QuantaStudio 12k Flex	Thermo Fisher

Table S2: Software and suppliers

Software	Supplier
Gen5 micorplate Reader and Imager Software	BioTek Instruments, Inc.
ImageQuant™ TL 1D v8.1	GE Healthcare Life Sciences
SoftMax® Pro 6.4	Molecular Devices

Table S3: Disposables and suppliers.

Disposables	Supplier
Nunc™ Cell Culture treated flask (T25, T75 and T175)	ThermoFisher Scientific
Microplate, 96 well, half area, µclear®, white, med. Binding	Greiner bio-one GmbH
NuncTM Cell Culture Treated Multidishes (96, 12, and 6-well)	Thermo Scientific
NucleoCassetteTM	ChemoMetec A/S

Table S4: Kits, suppliers and catalogue numbers.

Kit	Supplier	Catalogue number
Cell Death Detection ELISA^{PLUS} Kit	Roche Applied Science, IN, USA	11774425001
Dual-Luciferase® Reporter Assay System	Promega, Madison, Wi, USA	E1960
Luc-Pair™ Duo-Luciferase Assay Kit 2.0	GeneCopoeia, MD, USA	LF006
High Capacity cDNA Reverse Transcription Kit, 1000 reactions	Applied Biosystems®	4368813
MycoAlert^{TM} Mycoplasma Detection Kit	Lonza, Walkersville, Inc., Verviers, Belgium	LT07
Pierce^{TM} BCA Protein Assay Kit	Thermo Fisher Scientific, Waltham, MA, USA	23225
Monarch® Total RNA Miniprep Kit	New England Biolabs® Inc., Ipswich, MA, USA	T2010S
ZymoPURE^{TM} Plasmid Maxiprep Kit	Zymo Research, Irvine, CA, USA	D4203
Factor V Human ELISA Kit	Abcam®, Cambridge, UK	Ab137976
Asserachrom® Total TFPI kit	Diagnistica Stago, Asneries, France	00261

Table S5: Chemicals, reagents, suppliers and catalogue numbers.

Chemicals	Supplier	Catalogue number
Ampicillin, Sodium Salt	Calbiochem®	171254
Bovine Serum Albumin	Sigma-Aldrich®	A7906-100G
Dulbecco's phosphate-buffered Saline (DPBS)	Thermo Fisher Scientific	A7906-100G
Dulbecco's Modified Eagle Medium (DMEM)	Lonza, Verviers, Belgium	12-604F

Fetal Bovine Serum Gold (FBS)	PAA, Pasching, Austria	A15-151
GelRed Nucleic Acid Gel Stain	VWR, Oslo, Norway	730-2958
GeneRuler DNA Ladder Mix, ready to use	Thermo Fisher Scientific, Waltham, MA, USA	SM0333
HaltTM Protease & Phosphatase Inhibitor cocktail (100x)	Thermo Fisher Scientific	1861281
Lipofectamine®RNAiMAX	Invitrogen Carlsbad, CA, USA	13778150
Lipofectamine®3000	Invitrogen Carlsbad, CA, USA	LR3000015
OPTI-MEM®	Gibco by Life Technologies	31985-062
P3000™ Enhancer Reagent	Invitrogen Carlsbad, CA, USA	LR3000015
Reagent A100 Lysis buffer	Chemometec, Allerød, Denmark	910-0003
Reagent B Stabilizing buffer	Chemometec, Allerød, Denmark	910-0002
RIPA Buffer	Sigma-Aldrich, St. Louis, USA	R0278
Seakem® LE Agarose	Lonza, Rockland, USA	50004
S.O.C Medium	Invitrogen, Carlsbad, CA, USA	1749148
2X Taqman® Gene Expression Master Mix	Applied Biosystems, Foster City, USA	4369016
TBE Electrophoresis buffer (10X)	Fermentas, Vilnius, Lithuania	#5B2
Trypsin-EDTA (0.05%)	Thermo Fisher Scientific	25300054

Appendix C: Primers, miRNA sequences and plasmids

Table S6: qRT PCR assays

Assay	Name	20X assay concentration	Sequence (5'→3')
PMM1	PMM1 Forward Primer	18 µM	CCGGCTCGCCAGAAAATT
	PMM1 Reverse primer	18 µM	CGATCTGCACTCTACTTCGTAGCT
	PMM1 Probe	5 µM	ACCCTGAGGTGGCCGCCTTCC
Total TFPI	Total TFPI Forward primer	18 µM	ACACACAATTATCACAGATACGGAGTT
	Total TFPI Reverse primer	18 µM	GCCATCATCCGCCTTGAA
	Total TFPI Probe	5µM	CCACCACTGAAACTTATGCATTCATTTTGTGC
FV 250rx	TaqMan Gene Expression assay Hs00914120_m1	-	-

Table S7: Selected miRNA and their corresponding order-number in Dharmacon

miRNA	MiRiDian Dharmacon
hsa-miR-127-5p	C-301062-01-0005
hsa-miR-134-3p	C-303279-00-0005
hsa-miR-323a-3p	C-300698-05-0005
hsa-miR-369-3p	C-300675-03-0005
hsa-miR-510-3p	C-303030-00-0005
hsa-miR-532-5p	C-300867-01-0005
hsa-miR-543	C-301248-01-0005
hsa-miR-548c-3p	C-300942-01-0005
hsa-miR-568	C-300886-01-0005
hsa-miR-643	C-300970-01-0005
hsa-miR-651-3p	C-303252-00-0005
hsa-miR-1236-3p	C-301292-01-0005
hsa-miR-1278	C-301417-00-0005
hsa-miR-1291	C-301345-00-0005
hsa-miR-4495	C-302099-00-0005
Negative Control #2	CN-002000-01-05

Table S8: miTarget™ miRNA 3'UTR Target Clone

Insert	Vector	Catalogue No.:	Supplier
F5-3'UTR	pEZX-MT06	HmiT005058-MT06	GeneCopoeia, Inc., Rockvile, MD, USA

Appendix C: Cell lines

Cell line	Producer
HepG2 [HepG2] (ATCC® HB8065™)	American Type Culture Collection (ATCC), Manassas, VA, USA
HEK293T [293T] (ATCC® CRL-3216™)	American Type Culture Collection (ATCC), Manassas, VA, USA

Appendix E: recipes for solutions and medium

Lysogeny broth (LB) medium

10 g tryptone

10 g NaCl

5 g yeast extract

900 mL MQ-H_2O

pH adjusted to 7.0 with 12 M HCl

Volume adjusted to 1 L using MQ-H_2O and autoclaved

1% Agarose Gel

0.75 g Seakem® LE Agarose

50 mL 1X TBE Electrophoresis buffer

Boil for 30 sec, then add 5 ul GelRed Nucleic Acid Gel Stain

Appendix F: R-printout with results from ANOVA and Dunnett's test.

```
> fit.FV.full <- aov(RQ~miRNA, data=FV.full)
> summary(fit.FV.full)
             Df Sum Sq Mean Sq F value Pr(>F)
miRNA        12  6.461  0.5384   43.17 <2e-16 ***
Residuals   140  1.746  0.0125
---
Signif. codes:  0 '***' 0.001 '**' 0.01 '*' 0.05 '.' 0.1 ' ' 1
> Dunnet.FV <- glht(fit.FV.full, linfct=mcp(miRNA="Dunnett"))
> summary(Dunnet.FV)

         Simultaneous Tests for General Linear Hypotheses

Multiple Comparisons of Means: Dunnett Contrasts


Fit: aov(formula = RQ ~ miRNA, data = FV.full)

Linear Hypotheses:
                                      Estimate Std. Error t value Pr(>|t|)
miR-1236-3p - A Negative control  == 0  -0.26278    0.04559  -5.764  < 1e-04 ***
miR-1278 - A Negative control  == 0      -0.33056    0.03722  -8.880  < 1e-04 ***
miR-1291  - A Negative control  == 0     -0.14944    0.04559  -3.278  0.01415 *
miR-145-5p  - A Negative control  == 0   -0.36589    0.04404  -8.307  < 1e-04 ***
miR-323a-3p  - A Negative control  == 0  -0.20056    0.03722  -5.388  < 1e-04 ***
miR-510-3p - A Negative control  == 0     0.02389    0.04559   0.524  0.99991
miR-532-5p  - A Negative control  == 0    0.44611    0.04559   9.785  < 1e-04 ***
miR-548c-3p - A Negative control  == 0   -0.31944    0.04559  -7.007  < 1e-04 ***
miR-568 - A Negative control  == 0       -0.28507    0.03777  -7.548  < 1e-04 ***
miR-643  - A Negative control  == 0      -0.19944    0.04559  -4.375  0.00027 ***
miR-651-3p - A Negative control  == 0    -0.29611    0.04559  -6.495  < 1e-04 ***
miR-7-5p  - A Negative control  == 0      0.10722    0.04559   2.352  0.17268
---
Signif. codes:  0 '***' 0.001 '**' 0.01 '*' 0.05 '.' 0.1 ' ' 1
(Adjusted p values reported -- single-step method)
```

Figure S1: qRT-PCR results for *F5* mRNA test, with ANOVA and Dunnett's test.

```
> fit.FV.prot.u.total <- aov(ratio~miRNA, data=FV.prot.u.total)
> summary(fit.FV.prot.u.total)
             Df Sum Sq Mean Sq F value   Pr(>F)
miRNA        12  2.311 0.19254   6.175 3.88e-07 ***
Residuals    66  2.058 0.03118
---
Signif. codes:  0 '***' 0.001 '**' 0.01 '*' 0.05 '.' 0.1 ' ' 1
1 observation deleted due to missingness
> Dunnet.FV.prot.u.total <- glht(fit.FV.prot.u.total, linfct=mcp(miRNA="Dunnett"))
> summary(Dunnet.FV.prot.u.total)

         Simultaneous Tests for General Linear Hypotheses

Multiple Comparisons of Means: Dunnett Contrasts


Fit: aov(formula = ratio ~ miRNA, data = FV.prot.u.total)

Linear Hypotheses:
                                       Estimate Std. Error t value Pr(>|t|)
miR-1236-3p - A Negative control == 0 -0.564545   0.135734  -4.159  0.00109 **
miR-1278 - A Negative control == 0     -0.049091   0.075292  -0.652  0.99937
miR-1291 - A Negative control == 0     -0.209545   0.135734  -1.544  0.71936
miR-145-5p - A Negative control == 0   -0.003434   0.079365  -0.043  1.00000
miR-323a-3p - A Negative control == 0 -0.432727   0.075292  -5.747  < 0.001 ***
miR-510-3p - A Negative control == 0    0.155455   0.135734   1.145  0.93955
miR-532-5p - A Negative control == 0   -0.009545   0.135734  -0.070  1.00000
miR-548c-3p - A Negative control == 0   0.050455   0.135734   0.372  1.00000
miR-568 - A Negative control == 0      -0.131818   0.075292  -1.751  0.56364
miR-643 - A Negative control == 0      -0.126768   0.079365  -1.597  0.67996
miR-651 - A Negative control == 0      -0.314545   0.135734  -2.317  0.20989
miR-7-5p - A Negative control == 0      0.067455   0.095238   0.708  0.99862
---
Signif. codes:  0 '***' 0.001 '**' 0.01 '*' 0.05 '.' 0.1 ' ' 1
(Adjusted p values reported -- single-step method)
```

Figure S2: Statistical test (ANOVA and Dunnett's) of FV protein level change compared with negative control without correction for total protein within each sample.

```
> fit.FV.prot.m.total <- aov(ratio~miRNA, data=FV.prot.m.total)
> summary(fit.FV.prot.m.total)
            Df Sum Sq Mean Sq F value   Pr(>F)
miRNA        9 1.7684 0.19649    12.5 1.52e-09 ***
Residuals   44 0.6917 0.01572
---
Signif. codes:  0 '***' 0.001 '**' 0.01 '*' 0.05 '.' 0.1 ' ' 1
1 observation deleted due to missingness
> Dunnet.FV.prot.m.total <- glht(fit.FV.prot.m.total, linfct=mcp(miRNA="Dunnett"))
> summary(Dunnet.FV.prot.m.total)

         Simultaneous Tests for General Linear Hypotheses

Multiple Comparisons of Means: Dunnett Contrasts


Fit: aov(formula = ratio ~ miRNA, data = FV.prot.m.total)

Linear Hypotheses:
                                       Estimate Std. Error t value Pr(>|t|)
miR-1236-3p - A Negative control == 0 -0.38000    0.08359  -4.546   <0.001 ***
miR-1278 - A Negative control == 0    -0.12556    0.05911  -2.124   0.2523
miR-1291 - A Negative control == 0    -0.06333    0.08359  -0.758   0.9888
miR-145-5p - A Negative control == 0  -0.22333    0.08359  -2.672   0.0784 .
miR-323a-3p - A Negative control == 0 -0.52111    0.05911  -8.816   <0.001 ***
miR-568 - A Negative control == 0     -0.35444    0.05911  -5.997   <0.001 ***
miR-643 - A Negative control == 0     -0.39667    0.08359  -4.745   <0.001 ***
miR-651 - A Negative control == 0     -0.25000    0.08359  -2.991   0.0357 *
miR-7-5p - A Negative control == 0    -0.08000    0.08359  -0.957   0.9527
---
Signif. codes:  0 '***' 0.001 '**' 0.01 '*' 0.05 '.' 0.1 ' ' 1
(Adjusted p values reported -- single-step method)
```

Figure S3: Statistical test (ANOVA and Dunnett's) of FV protein level change compared with negative control with correction for total protein within each sample.

```
> fit.TFPI.full <- aov(RQ~miRNA, data=TFPI.full)
> summary(fit.TFPI.full)
             Df Sum Sq Mean Sq F value Pr(>F)
miRNA        12 14.309  1.1924   28.26 <2e-16 ***
Residuals   140  5.907  0.0422
---
Signif. codes:  0 '***' 0.001 '**' 0.01 '*' 0.05 '.' 0.1 ' ' 1
1 observation deleted due to missingness
>
> Dunnet.full <- glht(fit.TFPI.full, linfct=mcp(miRNA="Dunnett"))
> summary(Dunnet.full)

         Simultaneous Tests for General Linear Hypotheses

Multiple Comparisons of Means: Dunnett Contrasts


Fit: aov(formula = RQ ~ miRNA, data = TFPI.full)

Linear Hypotheses:
                                        Estimate Std. Error t value Pr(>|t|)
miR-1236-3p - A Negative control  == 0  -0.35111    0.08386  -4.187  < 0.001 ***
miR-1278 - A Negative control  == 0     -0.35833    0.06847  -5.233  < 0.001 ***
miR-1291  - A Negative control  == 0    -0.26667    0.08386  -3.180  0.01913 *
miR-145-5p  - A Negative control  == 0  -0.61211    0.08102  -7.556  < 0.001 ***
miR-323a-3p  - A Negative control  == 0 -0.23111    0.06847  -3.375  0.01038 *
miR-510-3p - A Negative control  == 0   -0.29778    0.08386  -3.551  0.00578 **
miR-532-5p  - A Negative control  == 0   0.39444    0.08386   4.704  < 0.001 ***
miR-548c-3p - A Negative control  == 0  -0.25889    0.08386  -3.087  0.02546 *
miR-568 - A Negative control  == 0       0.21242    0.06947   3.058  0.02784 *
miR-643  - A Negative control  == 0      0.05333    0.08386   0.636  0.99937
miR-651-3p - A Negative control  == 0    0.07556    0.08386   0.901  0.98648
miR-7-5p  - A Negative control  == 0    -0.85222    0.08386 -10.163  < 0.001 ***
---
Signif. codes:  0 '***' 0.001 '**' 0.01 '*' 0.05 '.' 0.1 ' ' 1
(Adjusted p values reported -- single-step method)
```

Figure S4: qRT-PCR results for *TFPI* mRNA test, with ANOVA and Dunnett's test.

```
> fit.TFPI.prot.u.total <- aov(ratio~miRNA, data=TFPI.prot.u.total)
> summary(fit.TFPI.prot.u.total)
            Df Sum Sq Mean Sq F value   Pr(>F)
miRNA        8 2.9094  0.3637   27.58 2.66e-16 ***
Residuals   53 0.6989  0.0132
---
Signif. codes:  0 '***' 0.001 '**' 0.01 '*' 0.05 '.' 0.1 ' ' 1
> Dunnet.TFPI.prot.u.total <- glht(fit.TFPI.prot.u.total, linfct=mcp(miRNA="Dunnett"))
> summary(Dunnet.TFPI.prot.u.total)

         Simultaneous Tests for General Linear Hypotheses

Multiple Comparisons of Means: Dunnett Contrasts


Fit: aov(formula = ratio ~ miRNA, data = TFPI.prot.u.total)

Linear Hypotheses:
                                      Estimate Std. Error t value Pr(>|t|)
miR-1236-3p - A Negative control == 0 -0.02714    0.06138  -0.442   0.9991
miR-1278 - A Negative control == 0     0.03000    0.06138   0.489   0.9981
miR-1291 - A Negative control == 0    -0.17286    0.06138  -2.816   0.0421 *
miR-145-5p - A Negative control == 0  -0.12000    0.06138  -1.955   0.2698
miR-323a-3p - A Negative control == 0  0.06143    0.06138   1.001   0.8845
miR-510-3p - A Negative control == 0   0.09310    0.06389   1.457   0.5805
miR-651 - A Negative control == 0      0.19143    0.06138   3.119   0.0192 *
miR-7-5p - A Negative control == 0    -0.59714    0.06138  -9.729   <0.001 ***
---
Signif. codes:  0 '***' 0.001 '**' 0.01 '*' 0.05 '.' 0.1 ' ' 1
(Adjusted p values reported -- single-step method)
```

Figure S5: Statistical test (ANOVA and Dunnett's) of TFPI protein level change compared with negative control without correction for total protein within each sample.

```
> fit.TFPI.prot.m.total <- aov(ratio~miRNA, data=TFPI.prot.m.total)
> summary(fit.TFPI.prot.m.total)
            Df Sum Sq Mean Sq F value   Pr(>F)
miRNA        7 0.8670 0.12386   18.57 1.43e-06 ***
Residuals   16 0.1067 0.00667
---
Signif. codes:  0 '***' 0.001 '**' 0.01 '*' 0.05 '.' 0.1 ' ' 1
>
> Dunnet.TFPI.prot.m.total <- glht(fit.TFPI.prot.m.total, linfct=mcp(miRNA="Dunnett"))
> summary(Dunnet.TFPI.prot.m.total)

         Simultaneous Tests for General Linear Hypotheses

Multiple Comparisons of Means: Dunnett Contrasts


Fit: aov(formula = ratio ~ miRNA, data = TFPI.prot.m.total)

Linear Hypotheses:
                                      Estimate Std. Error t value Pr(>|t|)
miR-1236-3p - A Negative control == 0  0.02667    0.06669   0.400    0.999
miR-1278 - A Negative control == 0     0.10333    0.06669   1.550    0.499
miR-1291 - A Negative control == 0    -0.03000    0.06669  -0.450    0.997
miR-145-5p - A Negative control == 0  -0.03333    0.06669  -0.500    0.995
miR-323a-3p - A Negative control == 0  0.07000    0.06669   1.050    0.824
miR-651-3p - A Negative control == 0   0.04333    0.06669   0.650    0.978
miR-7-5p - A Negative control == 0    -0.53333    0.06669  -7.998   <0.001 ***
---
Signif. codes:  0 '***' 0.001 '**' 0.01 '*' 0.05 '.' 0.1 ' ' 1
(Adjusted p values reported -- single-step method)
```

Figure S6: Statistical test (ANOVA and Dunnett's) of TFPI protein level change compared with negative control with correction for total protein within each sample.

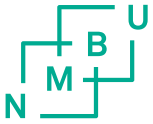

Norges miljø- og biovitenskapelige universitet
Noregs miljø- og biovitskapelege universitet
Norwegian University of Life Sciences

Postboks 5003
NO-1432 Ås
Norway